DISCOVERY AND CHARACTERIZATION OF THE POLYCOMB

REPRESSIVE COMPLEX 1 OF *C. ELEGANS*

APPROVED BY SUPERVISORY COMMITTEE

Mentor: Scott Cameron, M.D. Ph.D.

Committee Chairman: Leon Avery, Ph.D.

Committee Member: James Chen, Ph.D.

Committee Member: Jane Johnson, Ph.D.

DISCOVERY AND CHARACTERIZATION OF THE POLYCOMB REPRESSIVE COMPLEX 1 OF *C. ELEGANS*

by

ÖZGÜR KARAKUZU

DISSERTATION

Presented to the Faculty of the Graduate School of Biomedical Sciences

The University of Texas Southwestern Medical Center at Dallas

In Partial Fulfillment of the Requirements

For the Degree of

DOCTOR OF PHILOSOPHY

The University of Texas Southwestern Medical Center at Dallas

Dallas, Texas

Decemeber, 2008

Acknowledgements

I would like to thank everybody that supported me during my graduate school years. First of all, I give my gratitude to Scott Cameron for his great mentorship, patient guidance, and the friendly environment he created in the lab. I thank my thesis committee members Leon Avery, James Chen, and Jane Johnson for their helpful criticism, advice and precious time. Past and present members of the Cameron Lab, Tamara Strauss, Malia Potts, Audra Heinze, David Wang, Jennie Winn, Robert Pollok, Vera Paulson, and others were great fellows, and I thank them for their contributions to my work and for their friendship. Especially, I would like to mention David Wang and thank him for his experimental contributions, and Brinda Prasad, who first identified MIG-32 and shared that information with us. I greatly appreciate the Avery, Lin, and Horvitz labs for sharing their knowledge and resources. I also thank Yuji Kohara for cDNAs, the Mitani laboratory, the Horvitz lab and the CGC for many nematode strains used in this work (the CGC is funded by the NIH National Center for Research Resources). Finally I want to express my gratitude to family for their life-time support and patience.

DISCOVERY AND CHARACTERIZATION OF THE POLYCOMB REPRESSIVE COMPLEX 1 OF *C. ELEGANS*

Publication No. _____

Özgür Karakuzu, M.S.

The University of Texas Southwestern Medical Center at Dallas, 2008

Supervising Professor: John Scott Cameron, M.D., Ph.D.

unc-3 encodes the *C. elegans* homolog of the Olf-1/Early B cell factor family of transcription factors, which in vertebrates regulate development and differentiation of B lymphocytes, adipocytes, and cells of the nervous system. In the first chapter I analyze the role of *unc-3* in determining the fates of neurons in ventral nerve cord (VNC). *unc-3* mutants are uncoordinated in locomotion. I show that *unc-3* represses a VC-like motor

neuron program in the VA and VB motor neurons, which in wild-type animals control backwards and forwards locomotion, respectively. Our lab identified a physical interaction between UNC-3 and the C2H2 zinc finger transcription factor PAG-3, the mammalian homologs of which are coexpressed in olfactory epithelium and hematopoietic cells. Our data explain the locomotory defects of *unc-3* mutants and suggest that interactions between *unc-3* and *pag-3* homologs in other species may be functionally important.

The second chapter of the thesis is about the analysis of MIG-32 a RING protein similar to some Polycomb proteins that were identified in a yeast two hybrid screen with UNC-3 as bait. The Polycomb repression complex 2 (PRC2) methylates histone H3 lysine 27 at target genes to modify gene expression, and this mark is recognized by PRC1, which ubiquitylates histone H2A. In *Caenorhabditis elegans*, a complex of the MES-2, MES-3, and MES-6 proteins is functionally analogous to the PRC2 complex, but the functional analog of PRC1, and indeed whether *C. elegans* has such a complex, has been unclear. I describe here that MIG-32 is a homolog of BMI-1, a core component of PRC1. I also identify SPAT-3A as a homolog of Ring1B, a partner protein of BMI-1 in the PRC1 core complex. *mig-32* and *spat-3* mutants have some defects that overlap with those of *mes* mutants. However, unlike the mes mutants, *mig-32 and spat-3* mutants are fertile, despite lacking apparent H2A ubiquitylation. Migration and axon guidance of specific neurons were defective in *mig-32* and *spat-3* mutants. Our data suggest that *mig-32* and *spat-3* encode core components of a PRC1-like complex in *C. elegans.*

Prior Publications

Karakuzu O, Wang DP, Cameron S. MIG-32 is a PRC1-like component and BMI-1 homolog in *Caenorhabditis elegans*. S*ubmitted.*

Prasad B, **Karakuzu O,** Reed RR, Cameron S. *unc-3*-dependent repression of specific motor neuron fates in *Caenorhabditis elegans.* Dev Biol. 2008 Sep 9. [Epub ahead of print] .

Erbel PJ, Card PB, **Karakuzu O**, Bruick RK, Gardner KH. Structural basis for PAS domain heterodimerization in the basic helix-loop-helix-PAS transcription factor hypoxia-inducible factor. Proc Natl Acad Sci U S A. 2003 Dec 23;100(26):15504-9

Table of Contents

List of Figures

List of Tables

List of Abbreviations

A-P - Antero-Posterior

BSA - Bovine serum albumin

C.e. - *Caenorhabditis elegans*

ChIP - Chromoatin immunoprecipitation

DAPI - 4',6-Diamidino-2-phenylindole

DIC - Differential interference contrast

D-V - Dorso-Ventral

GEF - Guanine exchange factor

GFP- Green fluorescent frotein

H2A-Ub - Histone H2A ubiquitylated at lysine 119

H2B-Ub - Histone H2B ubiquitylated at lysine 123

H3K20 - Histone H3 Lysine 20

H3K27-3Me - Hisone H3 trimethylated at lysine 27

H3K4 – Histone H3 lysine 4

H3K9 - Histone H3 lysine 9

HSN - Hermaphrodite specific neuron

L1 - Larval stage 1

L2 - Larval stage 2

L3 - Larval stage 3

L4 - Larval stage 4

LG - Linkage Group

mes - maternal effect sterility

Muv - Multi-vulva

NIB - Nuclear isolation buffer

NGM - Nematode Growth Medium

PcG - Polycomb

PRC1 - Polycomb repressive complex 1

PRC2 - Polycomb repressive complex 2

PRE - Polycomb responsive element

RNAi - interfering double stranded RNA

SDS-PAGE - SDS Polyacrylamide gel electrophoresis

SL - Splice leader

SynMuv - Synthetic multi-vulva

TAP - Tandem affinity purification

TCA - Trichloro acetic acid

TRE - Trithorax responsive element

txrG - Trithorax

VNC - Ventral nerve cord

VPC - Vulval precursor cell

Vul - Vulvaless

Preface

Transcriptional regulation is a key process in biology, as it is a mechanism that results in precise temporal and spatial control of gene expression. For many genes, their activity is restricted to certain cells and certain times. This control can be achieved by transcriptional regulators including transcription factors, nucleosome modeling factors, and chromatin modifier enzymes. There are many factors identified that activate or repress a target gene. Usually the chromatin modifying factors work in complexes. In this thesis, I provide data about the identity of three proteins that regulate transcription in *C. elegans*. I show in this thesis that UNC-3 is a variant bHLH transcription factor that is required for establishment of motor neuron fates in ventral nerve cord. I also identify MIG-32, a RING domain protein similar to mammalian Polycomb protein BMI-1, and SPAT-3A as components of a PRC1-like complex in *C. elegans.*

In the first chapter I provide evidence that unc-3 is involved in establishing cell fates of a subset of ventral nerve cord neurons, the VA, VB, and VC neurons, and their embryonic equivalents. Most of the work in this chapter was done by Brinda Prasad and Scott Cameron. I summarized the data collected by Scott and Brinda in part "1.2. Summary of previous studies about *unc-3* done in Cameron Lab"

The second chapter describes my analysis of *mig-32 and spat-3,* which together encode components of a PRC1-like Polycomb complex *in C. elegans*. I describe the role of this complex in nervous system development.

In the third chapter I seek more information about how *mig-32* modifies chromatin to regulate target genes. I did most of the work in second and third chapters, with help from Scott Cameron and David Wang.

The last chapter summarizes the studies I have done and includes future perspectives that might help us understand better how *mig-32* and its mammalian homologs function.

CHAPTER 1

unc-3-dependent repression of specific motor neuron fates in *Caenorhabditis elegans*

1.1. Introduction

The known and essentially invariant cell lineage of *Caenorhabditis elegans* provides a basis for examining the mechanisms that establish cell fates with single cell resolution (Sternberg and Horvitz, 1984). The characterization of *C. elegans* mutants that move in an uncoordinated fashion has revealed genes that together generate the proper numbers and types of motor neurons, including genes that encode transcription factors. Among these genes is *unc-3*, originally identified by Brenner in the initial description of *C. elegans* as an organism with tractable genetics (Brenner, 1974). *unc-3* encodes a 511 amino acid variant HLH protein that is highly conserved in other species (Dubois and Vincent, 2001; Prasad et al., 1998). Vertebrate homologs of *unc-3* include four Olf-1/Early B cell factor genes of mice (Garel et al., 1997; Hagman et al., 1993; Wang and Reed, 1993; Wang et al., 2002; Wang et al., 1997). Genetic analyses of O/E genes indicates that they have overlapping expression patterns and functions in the central nervous system, including directing projection of neuronal axons to the olfactory bulb and through the thalamus (Davis and Reed, 1996; Garel et al., 1999; Garel et al., 2002; Wang et al., 2004d; Wang et al., 1997). In *C. elegans*, *unc-3* is expressed in the two ASI

chemosensory neurons and in motor neurons of the ventral nerve cord (Prasad et al., 1998). In the ASI neurons, *unc-3* prevents transcription of genes characteristic of other types of neurons; in some cases these genes are direct targets of the UNC-3 protein (Kim et al., 2005).

unc-3 mutants are also profoundly defective in locomotion (Brenner, 1974). The ventral nerve cord motor neurons of *unc-3* mutants have axon fasciculation defects, neuromuscular junctions at ectopic sites and make inappropriate synapses with interneurons (Prasad et al., 1998). In wild-type newly hatched larvae, the ventral nerve cord and associated ganglia contain 22 motor neurons of three classes (White et al., 1976). Ablation of individual classes of motor neurons in newly hatched animals resulted in a model for locomotion in which the A and B class motor neurons mediate muscle contraction for backward and forward movement, respectively (Chalfie et al., 1985). An additional 53 neurons are added to the ventral nerve cord during postembryonic development. With specific exceptions, the fates adopted by these neurons are strikingly correlated with their lineage histories (Sulston, 1976; Sulston and Horvitz, 1977). For example, the motor neurons generated as the most anterior descendant in the P cell lineages adopt a VA motor neuron fate (Pflugrad et al., 1997; Sulston and Horvitz, 1977; White et al., 1976). The embryonic DA and postembryonic VA motor neurons share features, including anteriorly-directed axonal processes, similar synaptic inputs from interneurons, and mediation of backwards movement (Miller and Niemeyer, 1995;

Pflugrad et al., 1997; White et al., 1976). Comparable similarities exist for the embryonic and postembryonic B and D class motor neurons (White et al., 1976).

Here we establish a role for *unc-3* in specifying a portion of this precise pattern of motor neuron development. We describe the expression pattern of *unc-3* in the postembryonic motor neurons and changes in the pattern of motor neuron fates in *unc-3* mutants. Using a laser to ablate specific cells in the P cell lineages of *unc-3* mutants, we demonstrate that *unc-3* represses a VC-like motor neuron fate in the VA and VB motor neurons. \

1.2. Summary of previous studies about *unc-3* done in Cameron Lab

The gene *lin-11* is expressed in the six VC motor neurons of the ventral nerve cord. In a genetic screen of descendants of mutagenized hermaphrodites carrying a $P_{lin\text{-}11}gfp$ reporter (Cameron et al., 2002) *n3412*, *n3413* and *n3366* alleles (Figure 1-1) of *unc-3* were identified as mutants with approximately four extra fluorescent neurons in the ventral nerve cord of adults as compared to wild-type animals (Table 1-1) (Prasad et al., 2008).

Table 1: Numbers of VA and VC-like cells in *unc-3* mutants

Genotype	Number of fluorescent nuclei	n
nIs106 ($P_{lin\text{-}11}gfp$)	4.3 ± 0.4	50
nIs106 unc-3(e151)	8.1 ± 0.1	36
nIs106 unc-3(n3412)	8.3 ± 0.3	35
nIs106 unc-3(n3435)	8.5 ± 0.3	46

Table 1-1: Numbers of VA and VC-like cells in *unc-3* mutants (Adopted from Prasad et al. 2008)
The number of $P_{lin\text{-}11}gfp$-expressing nuclei in the ventral nerve cords of adult hermaphrodites is shown. Values are means ± s.e.m. Two VC neurons, VC4 and VC5, are often obscured by vulval fluorescence and were not scored.

The expression in *unc-3* mutants of two other VC markers, *ida-1 (Zahn et al., 2001)* and the neuropeptide FMRFamide (Schinkmann and Li, 1992) was examined. Using a $P_{ida\text{-}1}gfp$ reporter construct, *unc-3* mutants had about three extra neurons that express the reporter. Using an antiserum against FMRFamide, extra FMRFamide-expressing neurons were identified (Prasad et al., 2008).

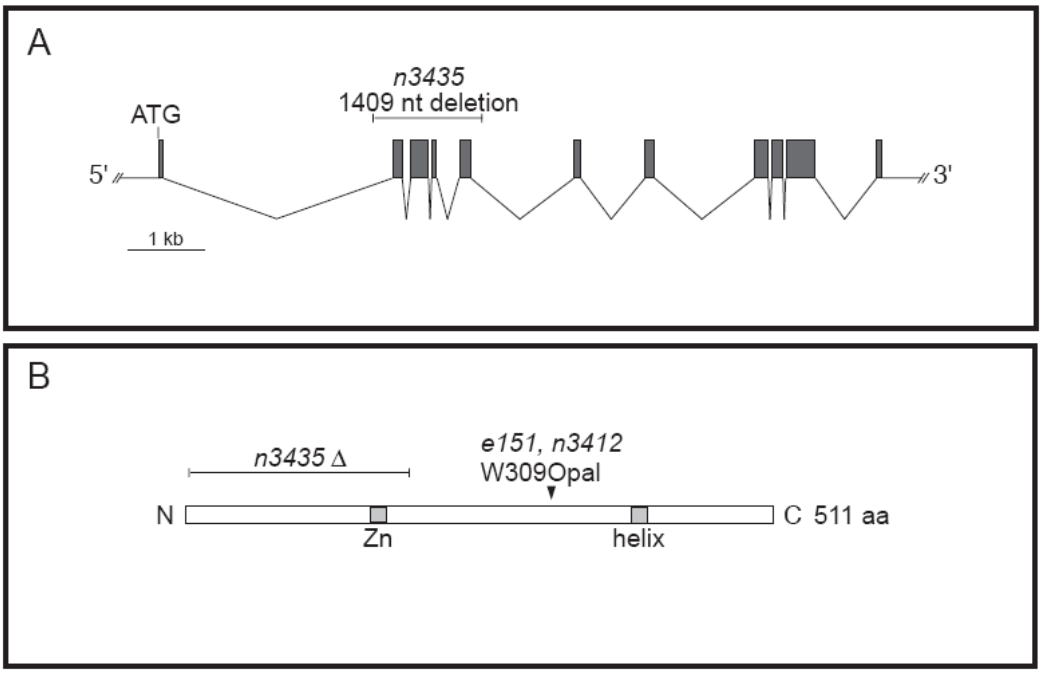

Figure 1-1: Diagram of the *unc-3* locus and alleles.
(A) *unc-3* exons are indicated as shaded boxes. The *n3435* deletion is indicated above exons 2, 3, 4 and 5. (B) The UNC-3 protein is represented with an indication of the location of the protein sequences altered in the *e151*, *n3412*, and *n3435* alleles. Shaded boxes indicate the zinc finger and helix domains.

Lineage analysis of P cell descendants in *unc-3* mutants showed that the pattern and timing of divisions were normal. To explore further which neurons might be transformed to a VC-like fate in *unc-3* mutants as defined by expression of $P_{lin\text{-}11}gfp$, P cell lineages were followed in *unc-3* mutants carrying the VC-specific $P_{lin\text{-}11}gfp$ reporter and specific cells were ablated using a laser microbeam. This led to the identification of those cell(s) that when ablated restored a wild-type pattern of $P_{lin\text{-}11}gfp$ reporter expression; such cells would be either directly or indirectly responsible for generation of the extra $P_{lin\text{-}11}gfp$-expressing cells. In summary, it was shown that Pn.aaaa and Pn.aaap (VA and VC

neurons respectively) were responsible for generation of the extra VC-like cells in *unc-3* mutants. This suggests that *unc-3* represses a VC-like program of development in some VA and VB motor neurons (Prasad et al., 2008).

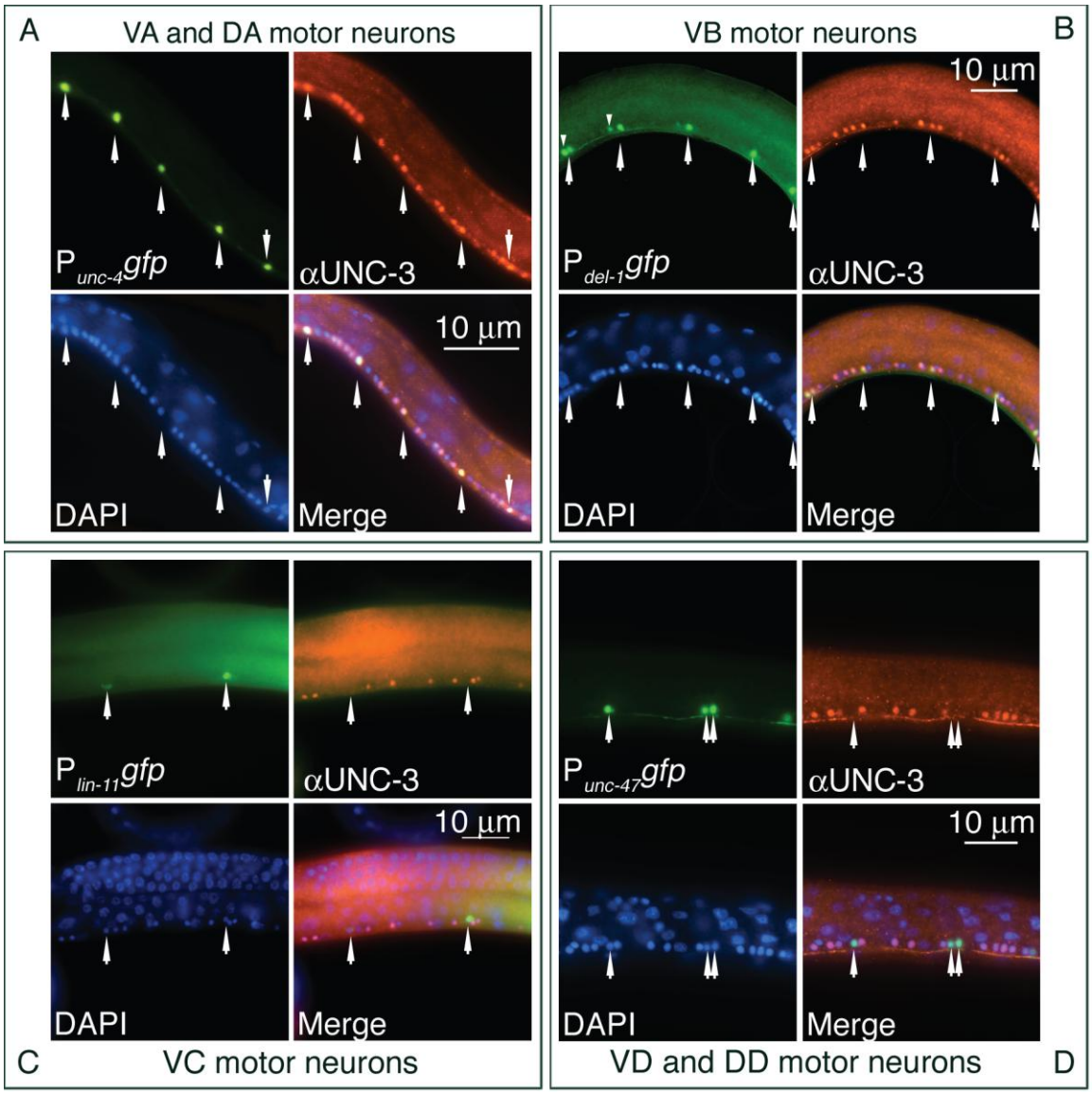
A
VA and DA motor neurons
P unc-4 gfp
αUNC-3
DAPI
Merge
10 μm
B
VB motor neurons
P del-1 gfp
αUNC-3
DAPI
Merge
10 μm
C
VC motor neurons
P lin-11 gfp
αUNC-3
DAPI
Merge
10 μm
D
VD and DD motor neurons
P unc-47 gfp
αUNC-3
DAPI
Merge
10 μm

Figure 1-2: *unc-3* is expressed postembryonically in the VA and VB but not the VC or VD motor neurons (Adopted from Prasad et al. 2008).
Each set of four panels displays images of neurons showing (i) *gfp* from a motor neuron type-specific promoter, (ii) UNC-3 protein detected with UNC-3 antiserum (anti-UNC-3), (iii) DAPI, (iv) a merged image. Each set of four panels assesses expression of *unc-3* in the indicated class(es) of motor neurons. Residual fluorescence from GFP after fixation was used to detect specific classes of motor neurons. (A) *unc-3* is expressed in the class A motor neurons. Images are from animals carrying the $P_{unc-4}gfp$ reporter, which is expressed in DA, VA and VC motor neurons (17, 39). *unc-3* is not expressed in the VC neurons (see panel C). (B) *unc-3* is expressed in the class B motor neurons. Images are from animals carrying the $P_{del-1}gfp$ reporter, which is expressed in the VB motor neurons. In L3 animals the $P_{del-1}gfp$ reporter is visible in some VA neurons at the anterior end of the ventral nerve cord (19). The more anterior nucleus of each pair of fluorescent nuclei in the anterior half of this image is a VA motor neuron and is marked by a small arrowhead above the nucleus. (C) *unc-3* is not expressed in the VC motor neurons. Images are from animals carrying the $P_{lin-11}gfp$ reporter, which is expressed in the VC motor neurons (13). (D) *unc-3* is not expressed in the VD motor neurons. Images are from animals carrying the $P_{unc-47}gfp$ reporter, which is expressed in the DD and VD motor neurons (40). Anterior, leftwards; ventral, downwards. Arrowheads indicate specific motor neurons identified by *gfp* expression. L3 animals were examined except for $P_{lin-11}gfp$, for which young adults were examined.

unc-3 expression pattern was analyzed by using UNC-3 antiserum (Prasad et al., 1998) to stain transgenic animals carrying *gfp* reporters expressed in specific classes of motor neurons. L1 animals shortly after hatching showed expression of *unc-3* in the embryonic DA and DB motor neurons; no staining of the DD neurons was detected. L2 and L3 animals showed bright staining of the VA and VB motor neurons but not of the precursor cell that generated them. VC, VD or DD motor neurons did not have any UNC-3 expression. In summary, UNC-3 was detected in the class A and B motor neurons (Figure 1-2) (Prasad et al., 2008).

Biochemical analysis of UNC-3 protein using immunoprecipitation from transfected mammalian cells showed that UNC-3 can form homodimers similar to its mammalian homologs O/E proteins (Hagman et al., 1995; Wang et al., 1997). This

homomeric interaction of UNC-3 protein was confirmed independently using a yeast 2-hybrid assay (Prasad et al., 2008).

pag-3 that encodes a predicted 337 amino acid transcription factor with five C2H2 zinc fingers (Jia et al., 1997) might function with *unc-3* to regulate neuronal fates in VNC. *pag-3* mutants displayed extra VC-like cells similar to *unc-3* mutants. However, the extra VC-like cells *in pag-3* mutants are caused by reiteration of Pn.aa fate (Cameron et al., 2002). PAG-3 antiserum detects protein in the Pn.aa neuroblasts and their descendants, the VA, VB and VC neurons (Cameron et al., 2002); that protein becomes undetectable very shortly after the VA, VB and VC neurons are generated. PAG-3 is not present in the ASI neurons (data not shown), which express UNC-3 (Prasad et al., 1998). PAG-3 and UNC-3 are therefore coexpressed in the VA and VB motor neurons during a very brief period immediately after these neurons are generated. As *unc-3* is expressed in only the ASI neurons and ventral nerve cord motor neurons, the VA and VB motor neurons are likely to be the only cells of the postembryonic larva or adult in which *pag-3* and *unc-3* are coexpressed.

The mammalian homologs of UNC-3, the O/E proteins, physically interact with OAZ, a protein with 30 predicted C2H2 zinc fingers (Tsai and Reed, 1998). Similarly, coimmunoprecipitation analysis of tagged proteins in mammalian cells suggested that UNC-3 and PAG-3 might physically interact in differentiating VA and VB motor neurons. If *unc-3* and *pag-3* act together to repress the VC fate in the VA and VB neurons, *unc-3 pag-3* double mutants might be expected to have a number of VC neurons

similar to that of single mutants. Indeed, *unc-3 pag-3* mutants had the same number of VC-like neurons as *pag-3* mutants. To address the possibility that *unc-3* expression may depend upon *pag-3* function in a manner analogous to that of *unc-86* and *mec-3* (Xue et al., 1992; Xue et al., 1993), expression pattern of *unc-3* in *pag-3* mutants were examined by whole-mount staining with UNC-3 antiserum. Many motor neurons in the ventral nerve cord of *pag-3* mutants expressed UNC-3 protein, ruling out the possibility that *pag-3* is required for *unc-3* expression by all motor neurons (Prasad et al., 2008).

1.3. Materials and Methods

1.3.1. Strains and alleles

Strains were maintained at 20ºC as described by Brenner (Brenner, 1974). Unless otherwise indicated, strains were obtained from the MIT/Horvitz laboratory collection or were provided by the *Caenorhabditis* Genetic Center, which is funded by the NIH National Center for Research Resources.

Mutations used were:

LGII. *wdIs4*, an integrated $P_{unc\text{-}4}gfp$ transgene, *wdIs6*, an integrated $P_{del\text{-}1}gfp$ transgene (both provided by David Miller), *juIs76*, an integrated $P_{unc\text{-}25}gfp$ transgene, *inIs179*, an integrated $P_{ida\text{-}1}gfp$ transgene.

LGX. *oxIs12*, an integrated P_{unc-47}*gfp* transgene, *nIs106*, an integrated P_{lin-11}*gfp* transgene (Cameron et al., 2002), *pag-3(n3098) (Cameron et al., 2002)*, *wdEx75*, an extrachromosomal P_{acr-5}*gfp* array (provided by David Miller).

1.3.2. Cell-lineage studies

Cell lineages were observed as described (Sulston and Horvitz, 1977).

1.4. Results

1.4.1. The A and B class motor neurons are abnormal or absent in *unc-3* mutants

unc-3 mutants are severely defective in forwards and backwards movement, suggesting that the class A (DA and VA) and B (DB and VB) neurons, which mediate locomotion (Chalfie et al., 1985), could be defective. At hatching, L1 animals have nine DA, seven DB and six DD neurons in the ventral nerve cord and associated ganglia (Sulston and Horvitz, 1977). Beginning late during L1, a series of divisions by the W and P blast cells generates postembryonic neurons, adding 12 VA, 11 VB, six VC and 13 VD neurons as well as additional cells to the ventral nerve cord; these divisions are completed during the early L2 (Sulston and Horvitz, 1977). UNC-3 was detected in the class A and B motor neurons by antibody staining (Prasad et al., 2008). To assess the role of *unc-3* in establishing this precise pattern of motor neuron types, I surveyed specific classes of

motor neurons using *gfp* reporters. For most neuronal classes I counted the number of neurons expressing each reporter in L3 larvae, which have differentiated embryonic and postembryonic class A, B and D motor neurons. To estimate the number of postembryonic neurons, I subtracted the number of neurons expressing each reporter in L1 animals, which have only the embryonic motor neurons, from the number in L3 animals. The VC neuron reporters are not expressed until the late L3 or L4 (Table 1-2 and data not shown), and these reporters were scored in young adults. Using these data I estimated the number of reporter-expressing embryonic and postembryonic neurons in *unc-3* mutants. Our results are presented in Table 1-2.

The embryonic DA and postembryonic VA and VC motor neurons express the P_{unc-4}*gfp* reporter (Lickteig et al., 2001; Miller and Niemeyer, 1995). In L1 *unc-3* mutants, the number of embryonic DA motor neurons is reduced to 1.3 ± 0.2 P_{unc-4}*gfp* -expressing neurons compared to 2.8 ± 0.3 in otherwise wild-type animals ($P<0.0001$, unpaired two-tailed t-test) (Table 1-1). The ventral nerve cord of *unc-3* mutants has a normal number of neuronal nuclei (data not shown) suggesting that the DA neurons are not missing and instead develop abnormally in *unc-3* mutants. In contrast to the decreased number of embryonic P_{unc-4}*gfp* -expressing neurons, L3 *unc-3* mutants have an increased number of P_{unc-4}*gfp* -expressing neurons compared to wild-type animals; 15.1 ± 0.4 neurons express P*unc-4gfp* in *unc-3* mutants compared to 10.9 ± 0.3 in the wild-type ($P<0.0001$, unpaired two-tailed t-test) (Table 1-2). Previous work had suggested that the levels of P_{unc-4}*gfp* expression in *unc-3* mutants are not markedly different from wild-type

(Prasad et al., 1998). On re-examining the effects of *unc-3* on the numbers of neurons that express *unc-4*, I discovered stage-dependent and opposite effects in the embryonic and postembryonic ventral nerve cord, likely accounting for why this difference had not been observed earlier. I observed that expression of $P_{unc\text{-}4}gfp$ in L3 *unc-3* mutants occurred in pairs of adjacent nuclei along the ventral nerve cord with the exception of the posterior nerve cord, where single fluorescent nuclei were present. This observation suggested that the additional $P_{unc\text{-}4}gfp$ -expressing neurons might normally be the VB motor neurons, which are generally immediately posterior to the VA motor neuron nuclei and absent from the P11 and P12 lineages in the posterior, where the lineal homologs of the VB neurons undergo programmed cell death (Sulston and Horvitz, 1977). I confirmed that the VB neurons of *unc-3* mutants express $P_{unc\text{-}4}gfp$ by directly observing partial cell lineages of the P9 and P10 blast cells of six *unc-3* mutants carrying the $P_{unc\text{-}4}gfp$ transgene. Each P9 and P10 cell lineage of wild-type animals generates one VA and one VB neuron as daughter cells of the neuroblasts P9.aaa and P10.aaa (Pn.aaa, the anterior daughter of the anterior daughter of the anterior daughter of any P blast cell) (Sulston and Horvitz, 1977). I observed that all of the VA neurons of *unc-3* mutants expressed *gfp* within an hour after the division that generated them; expression in the VB neurons became apparent two to three hours later in seven of 12 VB neurons generated by the two P cell lineages in the six animals. Most but not all VB neurons of *unc-3* mutants express $P_{unc\text{-}4}gfp$. 33 of 50 VB neurons scored at random from the P9 and P10 descendants of 25 L3 *unc-3* mutants expressed *gfp*, compared to none of 50 neurons in wild-type animals (data not shown). I

considered the possibility that the *unc-4* gene might mediate essential aspects of the *unc-3* mutant phenotype; if so, the movement defects of an *unc-4; unc-3* double mutant might be more similar to *unc-4* than to *unc-3*. I constructed *unc-4; unc-3* double mutants and confirmed the genotype by DNA sequencing. The movement defect of the double mutant was indistinguishable from an *unc-3* mutant, suggesting that *unc-4* is one of multiple target genes of *unc-3* in ventral nerve cord motor neurons.

Consistent with the VB motor neurons being abnormal in *unc-3* mutants, B class motor neuron markers were often not expressed in *unc-3* mutants. As assessed using the $P_{acr\text{-}5}gfp$ reporter, which is expressed in DB and VB motor neurons (Winnier et al., 1999), the number of embryonic DB motor neurons of L1 *unc-3* mutants was reduced from 5.4 ± 0.1 in the wild type to 1.5 ± 0.1 in *unc-3* mutants ($P<0.0001$, unpaired two-tailed t-test) (Table 1-2). As determined by expression of $P_{acr\text{-}5}gfp$ and a second marker, $P_{del\text{-}1}gfp$, which is expressed specifically by VB motor neurons (Winnier et al., 1999), two-thirds of the VB motor neurons of *unc-3* mutants also failed to develop normally (Table 1-2). These defects in the class B motor neurons, which are required for forward movement (Chalfie et al., 1985), likely account for the severe abnormality in forward movement of *unc-3* mutants. By contrast, expression of two class D-specific markers, $P_{unc\text{-}47}gfp$ and $P_{unc\text{-}25}gfp$, was normal in the embryonic DD and postembryonic VD motor neurons of *unc-3* mutants (Table 1-2). In summary, *unc-3* is essential for normal differentiation of DA, DB and VB motor neurons but apparently dispensable for differentiation of class D neurons. *unc-3* represses the VA and VC-specific gene *unc-4* in

the VB motor neurons, suggesting that these neurons are transformed to a VA or VC-like fate.

Table 1-2: Expression of motor neuron markers in *unc-3* mutants

Stage	VA and/or DA[a]		VB and/or DB				VD and/or DD			
	$P_{unc-4}gfp$	$P_{unc-4}gfp$; *unc-3*	[b]$P_{acr-5}gfp$	$P_{acr-5}gfp$; *unc-3*	[c]$P_{del-1}gfp$	[c]$P_{del-1}gfp$; *unc-3*	$P_{unc-25}gfp$	$P_{unc-25}gfp$; *unc-3*	$P_{unc-47}gfp$	$P_{unc-47}gfp$; *unc-3*
L3	10.9±0.3	15.1±0.4	13.3±0.3	4.1±0.4	9.0±0.0	2.5±0.3	17.6±0.4	18.4±0.2	18.7±0.1	18.6±0.1
L1	2.8±0.3	1.3±0.2	5.4±0.1	1.5±0.1	0.0±0.0	0.0±0.0	6.0±0.0	6.0±0.0	6.0±0.0	6.0±0.0
L3-L1	8.1±0.6	14.0±0.6	7.9±0.4	2.6±0.5	9.0±0.0	2.5±0.3	11.6±0.4	12.4±0.0	12.7±0.1	12.6±0.1
	VC									
	[d]$P_{lin-11}gfp$	$P_{lin-11}gfp$; *unc-3*	[d]$P_{ida-1}gfp$	$P_{ida-1}gfp$; *unc-3*						
Adult	4.2±0.1	8.5±0.3	6.0±0.0	9.0±0.3						
L3	0.0±0.0	0.0±0.0	0.0±0.0	0.0±0.0						
L1	0.0±0.0	0.0±0.0	0.0 ±0.0	0.0±0.0						

The numbers of fluorescent nuclei in the ventral nerve cords of otherwise wild-type and *unc-3* mutant transgenic animals are shown. n=30–50 in all cases. Numbers represent mean±s.e.m. For $P_{unc-4}gfp$ we scored the P3 P11 region; for $P_{acr-5}gfp$ and $P_{del-1}gfp$ we scored the P2–P10 region; these regions were chosen to avoid scoring additional fluorescent nuclei present in the ganglia in the anterior and posterior nerve cord.

[a] The $P_{unc-4}gfp$ reporter detects DA and VA neurons in L3 animals (1, 2). The VC neurons of wild-type animals do not express $P_{unc-4}gfp$ until late L3 or L4 (3).

[b] The $P_{acr-5}gfp$ reporter is an extrachromosomal array and can be lost mitotically in some cells, which may account for the small difference in the estimate of VB motor neuron number when compared to the integrated $P_{del-1}gfp$ reporter.

[c] The $P_{del-1}gfp$ reporter is expressed in the VA neurons in the anterior portion of the ventral nerve cords of late L3 animals (4). Initial VA expression is dimmer than in the VB neurons. The numbers for L3 animals do not include these VA nuclei.

[d] The $P_{lin-11}gfp$ and $P_{ida-1}gfp$ reporters are first expressed in L4 animals; young adults were scored. $P_{lin-11}gfp$ is expressed in vulval muscle and hypodermal cells, typically obscuring the VC4 and VC5 nuclei, which flank the vulva. $P_{ida-1}gfp$ is not expressed in the vulva. The VC4 and VC5 neurons are visible in animals carrying $P_{ida-1}gfp$, accounting for the two additional VC neurons in otherwise wild-type animals.

1.4. Discussion

Prior studies of *unc-3* established its role in regulating transcription in the ASI chemosensory neurons (Kim et al., 2005). In the ASI neurons, *unc-3* directly represses the transcription of genes normally expressed in other neuron types and is required for transcription of *daf-7*, a gene that regulates entry in the dauer larva stage, an alternative developmental program adapted for survival under unfavorable environmental conditions. Together, these findings suggest that *unc-3* mutants have defects in dauer entry at least in part because the transcriptional program associated with the ASI fate is defective. Our findings concerning the role of *unc-3* in the motor neurons of the ventral nerve cord suggest a similar explanation for the defects in locomotion of *unc-3* mutants.

Using motor neuron-specific markers, the A and B class motor neurons are abnormal in *unc-3* mutants. The laser-ablation data indicate that some VA and VB motor neurons of *unc-3* mutants express $P_{lin\text{-}11}gfp$, a marker that is normally restricted to VC neurons (Ref). Some VB neurons of *unc-3* mutants also express the VA and VC-specific marker $P_{unc\text{-}4}gfp$. The timing of this expression, which begins shortly after the cells are generated, is characteristic of VA motor neurons and our data suggest that more VB neurons express $P_{unc\text{-}4}gfp$ than $P_{lin\text{-}11}gfp$ or $P_{ida\text{-}1}gfp$, specific markers of the VC fate. These data suggest that in *unc-3* mutants the VB motor neurons are transformed to a mixed VA and VC-like fate similar to that of the VA neurons of *unc-3* mutants. I therefore propose that *unc-3* represses a VC-like program in the VA and VB neurons, and a VA-like program in the VB neurons. As the A and B class motor neurons are required for backwards and forwards locomotion (Chalfie et al., 1985), respectively, these abnormalities are probably responsible for the profound defect in locomotion of *unc-3* mutants. Previous studies of *unc-3* mutants had described inappropriate synaptic neural connections and a disorganized ventral nerve cord with defasciculated axons (Durbin, 1987; Prasad et al., 1998), including FMRFamide-positive axons on the wrong side of the nerve cord (Wightman et al., 1997) Some of these defects might reflect on the abnormal motor neuron fates I observed rather than a primary role for *unc-3* in controlling fasciculation or connectivity.

The vertebrate *O/E* genes are expressed in postmitotic neurons of the developing CNS (Davis and Reed, 1996). Electroporation into chick embryos of a dominant-negative

form of the O/E protein Ebf1 blocks neuronal differentiation without interfering with cell cycle exit (Garcia-Dominguez et al., 2003). Analysis of mutant *C. elegans* completely lacking *unc-3* function revealed that the timing of neuroblast cell divisions was similar to that in wild-type animals, and additional rounds of neuroblast divisions were not observed (Prasad et al., 2008), as might be expected if *unc-3* were required for cell cycle exit. In mice, mutations in members of the *O/E* gene family result in abnormal neuronal migration and axon pathfinding in several systems (Garel et al., 2000; Garel et al., 1999; Wang et al., 2004d). Migrating facial branchiomotor neurons respond to their changing environment by altering gene expression; this process is defective in *O/E-1* mutants (Garel et al., 2000). In the olfactory system, disruption of the *O/E-2* or *O/E-3* genes leads to defects in axonal projection to the olfactory bulb (Wang et al., 2004d). In spite of the overlapping expression of all four *O/E* family members in these sensory neurons, loss of both alleles of a single member (or even single alleles of *O/E-2* and *O/E-3* in double heterozygous animals) is sufficient to produce widespread defects in neuronal organization. These experiments further suggested that defects in axon pathfinding might be a consequence of reduced odorant receptor expression in migrating axons, suggesting that they are cell autonomous defects rather than a result of an inappropriate response to environmental cues during migration. Our data from *C. elegans*, in which we have precisely described defects in cell fates established by differentiating neurons in their normal locations, strongly support the proposal that the neurons are intrinsically defective (Garel et al., 1997; Wang et al., 2004d). *unc-3* is expressed in chemosensory neurons and

in several different classes of motor neurons, suggesting that the UNC-3 protein cooperates with other factors to determine cell fates. PAG-3, GFI-1 homolog in *C. elegans* might be an interacting partner for UNC-3 as reported in Prasad et al. 2008. Authors describe there that *pag-3* expression immediately precedes expression of *unc-3* that *pag-3* and *unc-3* are briefly coexpressed, and that *pag-3* is repressed as *unc-3* expression is established. A similar pattern exists for *pag-3* and *unc-3* homologs as hematopoietic stem cells (HSCs) commit to lymphoid lineages. *Gfi-1* is expressed in HSCs and controls their proliferation, then is partially repressed as the HSCs generate committed progenitors including common lymphoid progenitors, in which *O/E-1* expression is first detected (Akashi et al., 2003; Dias et al., 2005; Hock et al., 2003; Krivtsov et al., 2006). These data suggest that Gfi and O/E proteins might physically interact to specify aspects of cell lineage and cell fate in vertebrates, as their homologs do in *C. elegans* (Prasad et al., 2008).

CHAPTER 2

MIG-32 is a PRC1-like component and BMI-1 homolog in *Caenorhabditis elegans*

2.1. Introduction

Development of a multicellular organism needs a well-orchestrated spatial and temporal regulation of gene activity. This regulation involves the ability to partition the genome into active and quiescent regions. This partitioning of genes is maintained through many cell divisions, indicating the presence of a cellular memory. The Polycomb (PcG) and Trithorax (txrG) proteins are key regulators of this cellular memory (Schwartz and Pirrotta, 2007). The PcG group genes encode components of chromatin-modifying complexes, and were initially identified in *Drosophila* as modifiers of *Hox* gene expression that antagonize the action of txrG group genes (Kennison and Tamkun, 1988; Lewis, 1978; Nusslein-Volhard et al., 1985; Simon et al., 1992). *Hox* genes specify the identity of cells along the anteroposterior (A-P) axis in segmented animals. Transient expression of segmentation genes determines the initial expression domains of *Hox*. However, PcG and txrG proteins are required to maintain the pre-set transcriptional status. PcG proteins are responsible for maintenance of the repressed state. Studies in Drosophila identified DNA elements called PcG and txrG response elements (PREs and

TREs) that recruit PcG and trxG proteins. These elements mediate the inheritance of active and inactive state of genes through cell divisions (Chan et al., 1994; Fauvarque and Dura, 1993; Kassis, 1994). PcG genes are also identified in plants and animals. PcG genes are implicated in many processes like cell proliferation, stem cell identity, cancer, X-chromosome inactivation, and genomic imprinting (Delaval and Feil, 2004; Guitton and Berger, 2005; Heard, 2005; Martinez and Cavalli, 2006; Sparmann and van Lohuizen, 2006).

2.1.1. Polycomb Complexes

Biochemical and molecular analyses have defined at least three protein complexes, termed Polycomb Repressive Complex 2 (PRC2), PhoRC and PRC1. The SET domain protein Enhancer of zeste (E(Z)) is the key component of PRC2 and is a histone methyltransferase that methylates Histone 3 lysine 27 (H3K27). E(Z) is responsible for all mono-, di-, and tri-methylation of K3K27 *in vivo* in the *Drosophila melanogaster* genome. Tri-methylation of H3K27 is associated with silenced states of genes and 5-10 percent of all Histone H3 is tri-methylated. Mono- and di-methylation of H3K27 is a more wide-spread mark present on more than 50 percent of Histone H3, however the significance of these marks is not well understood. Other components of PRC2 include Extra sex combs (ESC), Suppressor of Zeste (Su(z)12) and Nurf-55 (Cao et al., 2002; Czermin et al., 2002; Kuzmichev et al., 2002; Muller et al., 2002). E(Z) has its methyl transferase activity only when it is in this comoplex. Su(z)12 is a Zinc-finger

protein. ESC and Nurf-55 are WD-40 Domain proteins that bind histones and remodeling complexes (Polo and Almouzni, 2006; Taylor-Harding et al., 2004). Two major PRC2 complexes were identified from flies, a 600 KD and a 1 MD. The 600 KD complex is considered to be the universal PRC2 complex. The 1 MD complex has another PcG protein, Polycomb-like (PCL), that is required for Polycomb silencing in flies (Tie et al., 2003). In mammals there are PRC2, PRC3 and PRC4 complexes characterized by different isoforms of EED, the homologue of fly ESC, present in each complex (Kuzmichev et al., 2004; Kuzmichev et al., 2005).

The H3K27me3 histone mark is in turn recognized by the PRC1 complex (Cao et al., 2002; Czermin et al., 2002; Kuzmichev et al., 2002; Saurin et al., 2001), which has as core components in flies dRING, Posterior Sex Combs (PSC), Polycomb (PC), and Polyhomeotic (PH), and lower amounts of Sex comb on midleg (SCM) (Saurin et al., 2001; Shao et al., 1999). Many additional factors are also involved in this complex (Saurin et al., 2001). The human PRC1 complex was purified from HeLa cells and includes HPC(1, 2, 3), HPH(1, 2, 3), RING1A, RING1B, BMI-1, and MEL-18 (Levine et al., 2002; Wang et al., 2004b; Wang et al., 2004c). These are homologous to fly PC, PH, dRING, and PSC, respectively. PRC1 is recruited to sites tri-methylated by PRC2 as a result of the affinity of the chromodomain of the HPC component to H3K27-3Me mark. In turn, the Ring1A/Ring1B proteins of PRC1 monoubiquitylate H2A at lysine 119 (Wang et al., 2004a; Wang et al., 2004b). In this complex, BMI-1 enhances the stability and enzymatic activity of Ring2/Ring1B (Cao et al., 2005). A list of identified Polycomb

proteins is presented in Table 2-1.

Drosophila protein	Human homologues	*C. elegans* homologs	Complex	Protein domains	Biochemical activity
PC (Polycomb)	HPC1, HPC2, HPC3,	?	PRC1	Chromo domain	Binding to H3K27-3Me
PH (Polyhomeotic)	HPH1, HPH2, HPH3	?	PRC1	SAM	?
PSC (Posterior Sex Combs)	BMI-1, MEL-18	?	PRC1	RING	Cofactor for SCE
SCE (Sex Comb Extra) (dRING)	RING1A, RING1B	?	PRC1	RING	E3 Ubiquitin ligase for H2AK119
SCM (Sex Combs on Midleg)	SCMH1, SCML2	LIN-61?	PRC1	SAM, MBT, Zn-Finger	?
E(Z) Enhancer of Zeste	EZH2, EZH1	MES-2	PRC2	SET	Methyl transferase for H3K9, H3K27
ESC (Extra Sex combs)	EED	MES-6	PRC2	WD40	Cofactor for E(Z)
NURF-55	P55	MES-6	PRC2	WD40	Cofactor for E(Z)
SU(Z)12 (Suppressor of Zeste 12)	SUZ12	-	PRC2	Zn-finger	?
PCL	PHF19, MTF2	-	PRC2	PHD, Tudor	?
PHO (Pleiohomeotic)	YY1, YY2	-	PhoRC	Zn-finger	DNA Binding
PHOL	YY1, YY2	-	PhoRC	Zn-Finger	DNA Binding
SFMBT	L3MBTL2, MBTD1	LIN-61?	PhoRc	MBT-SAM	Binds to mono- and dimethyl H3K9, H4K20

Table 2-1: Polycomb complex components in flies, human, and *C. elegans*
Polycomb complex components in flies, human, and *C. elegans* together with their corresponding complexes, protein domains, and biochemical functions. (re-organized from (Schwartz and Pirrotta, 2007)).

PhoRC is the third PcG complex identified in flies. Pleiohomeotic (PHO), Pleiohomeotic-like (PHOL), and SFMBT are the main components of this complex. PHO and PHOL are homologues of mammalian Yin-Yang 1(YY1), which has both activating and repressing functions. In addition these are the only PcG proteins that can bind to DNA directly (Brown et al., 2003; Brown et al., 1998; Fritsch et al., 1999). PhoRC complex is also involved in transcriptional repression of homeotic genes and the SFMBT protein, which has four MBT domains, is required for silencing. MBT repeats can bind to mono- and dimethylated H3K9 and H4K20 (Klymenko et al., 2006). PHO and PHOL can also interact with PRC1 and PRC2 (Levine et al., 2002; Poux et al., 2001; Satijn et al., 2001; Wang et al., 2004b).

2.1.2. Recruitment of PcG Complexes to Their Targets

Several PRE elements were identified in flies from regulatory regions of different genes including *engrailed*, *Fab7*, and *bxd*. PRE s are stretches of hundreds of base pairs which do not have any consensus sequence but instead have combinations of sites for different transcription factors including PHO, PHOL, GAGA factor, Pipsqueak, BTP/POZ, SP1/KLF, and dorsal switch protein 1 (DSP1)(Brown et al., 2005; Hodgson et al., 2001; Horard et al., 2000). None of the single sites are sufficient to recruit the PcG

complexes to PREs or silence the reporter genes. This suggest that combinatorial action of different factors might be required for PcG recruitment to PREs

The chromodomain of PC binds specifically to methylated H3K27, suggesting a mechanism for PRC1 recruitment. Methylation of H3K27 by the PRC2 complex that is recruited to PRE elements by PRE binding proteins might precede the recruitment of PRC1 (Wang et al., 2004b). This idea is supported by inactivation of E(Z) by a temperature-sensitive mutation, which leads to loss of PRC1 binding from polytene chromosomes (Rastelli et al., 1993). In addition, incubation of cells with H3K27-3Me peptides competed PC binding away from the polytene chromosomes (Ringrose et al., 2004). Contradictory to this model, ChIP on microarray experiments in flies showed that the H3K27-3Me mark is distributed over the entire transcription unit involving tens of kilobases. On the other hand, PRC1 and PRC2 complexes mapped to presumptive PREs and did not parallel the distribution of the H3K27-3Me mark (Kahn et al., 2006; Papp and Muller, 2006; Schwartz et al., 2006). This suggests that additional factors might specify the recruitment of PRC1 in addition to H3K27-3Me. Similar experiments in mammalian cells showed a better correlation between PRC1, PRC2 binding and H3K27-3Me distribution over broad regions. This also suggests that regulation of PcG recruitment in flies might be different from mammals. A recent report showed that PRC1 could bind to paternal chromosomes independent of PRC2 during mouse zygote development (Puschendorf et al., 2008).

In conclusion, PRE elements are sites where PcG recruitment is initiated but the

mechanism is not clear. PRC1 might be recruited both in PRC2 dependent and independent ways.

2.1.3. Polycomb target genes

PcG genes were classically defined as negative regulators of *Hox* genes in flies. However it is known that PcG proteins have many other targets. Individual reports showed that PcG proteins regulate genes involved in stem cell maintenance, differentiated cell identity, X-inactivation and cancer in vertebrates (Heard, 2005; Sparmann and van Lohuizen, 2006). In flies and plants, PcG target genes are the ones involved in proliferation and cell fate determination (Pires-daSilva and Sommer, 2003; Ringrose and Paro, 2004; Schubert et al., 2005). Recent advances in genome-wide profiling of target genes revealed that 1-5 percent of genes in mice, human and flies are targeted by PcG proteins. Using either ChIP or DamID profiling methods, six groups mapped binding sites for several PcG proteins in flies and vertebrates (Boyer et al., 2006; Bracken et al., 2006; Lee et al., 2006; Negre et al., 2006; Ringrose, 2007; Schwartz et al., 2006; Tolhuis et al., 2006). According to the most conservative estimate, 500-700 genes in vertebrates and 200 genes in flies are regulated by PcG proteins. There were differences in binding profiles of PcG proteins in different studies probably due to statistical discrepancies, choice of mapping method (ChIP or DamID), and true differences in PcG functions in different cell types and stages of development. On the other hand, several classes of genes were identified in common as PcG targets in all these

studies. These classes include transcription factors and genes involved in major morphogenetic pathways. The majority of the transcription factors mapped are regulators of cell fate specification, and half of them are homeodomain proteins.

Mapping of PcG targets in mouse and human ES cells together with some previous reports helps us to understand the role of PcG proteins in maintaining pluripotency of stem cells and differentiation (Boyer et al., 2006; Buszczak and Spradling, 2006; Lee et al., 2006; O'Carroll et al., 2001). The observations suggest that PcG proteins maintain pluripotency of ES cells by repressing genes that would activate differentiation. Consistent with this model, PcG proteins were displaced from their target sites during differentiation. Reactivation of PcG targets indicates that PcG silencing is not actually a stable and "locked in" state as described before, but highly dynamic during early stages of development (Ringrose, 2007).

One interesting outcome of these PcG protein target-mapping studies was that 10-20 percent of the mapped target sites are actively transcribed in ES cells and these genes were largely occupied by Polymerase II. It was suggested that PcG bound genes might be poised for either activation or silencing, and each mode of PcG regulation might require an additional signal upon differentiation (Bracken et al., 2007; Ringrose, 2007).

In conclusion, recent genome-wide methods of mapping helped us to understand how PcG proteins might execute their roles during development. Not only *Hox* genes but also many other transcription factors and genes are regulated by PcG proteins, and this regulation is highly dynamic during early development.

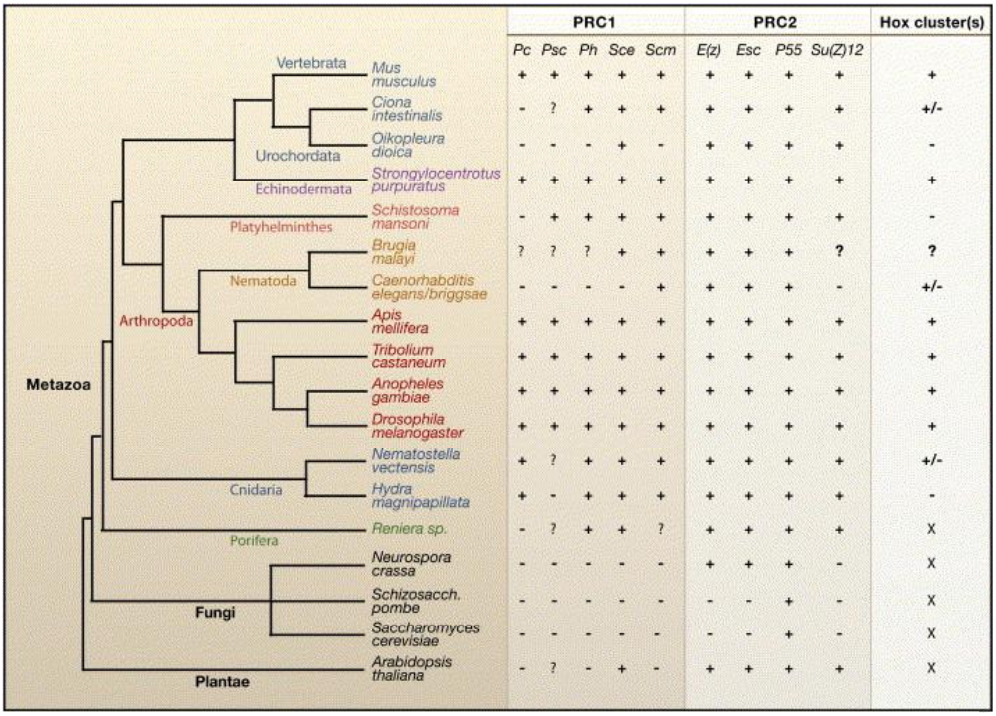

	PRC1					PRC2				Hox cluster(s)
	Pc	Psc	Ph	Sce	Scm	E(z)	Esc	P55	Su(Z)12	
Mus musculus	+	+	+	+	+	+	+	+	+	+
Ciona intestinalis	-	?	+	+	+	+	+	+	+	+/-
Oikopleura dioica	-	-	-	+	-	+	+	+	+	-
Strongylocentrotus purpuratus	+	+	+	+	+	+	+	+	+	+
Schistosoma mansoni	-	+	+	+	+	+	+	+	+	-
Brugia malayi	?	?	?	+	+	+	+	+	?	?
Caenorhabditis elegans/briggsae	-	-	-	-	+	+	+	+	-	+/-
Apis mellifera	+	+	+	+	+	+	+	+	+	+
Tribolium castaneum	+	+	+	+	+	+	+	+	+	+
Anopheles gambiae	+	+	+	+	+	+	+	+	+	+
Drosophila melanogaster	+	+	+	+	+	+	+	+	+	+
Nematostella vectensis	+	?	+	+	+	+	+	+	+	+/-
Hydra magnipapillata	+	-	+	+	+	+	+	+	+	-
Reniera sp.	-	?	+	+	?	+	+	+	+	X
Neurospora crassa	-	-	-	-	-	+	+	+	-	X
Schizosacch. pombe	-	-	-	-	-	-	-	+	-	X
Saccharomyces cerevisiae	-	-	-	-	-	-	-	+	-	X
Arabidopsis thaliana	-	?	-	+	-	+	+	+	+	X

Figure 2-1: Phylogenetic Distribution of the PRC1, PRC2, and *Hox* Gene clusters. For each species, + indicates the presence and - the absence of the proteins that constitute the PRC1 and PRC2 complexes. The existence of *Hox* gene clusters in the different species is also indicated. + indicates the presence of one or more "bona fide" *Hox* clusters, +/- indicates the existence of partial *Hox* clusters, – indicates that *Hox* genes exist, but are not clustered, and X indicates the absence of *Hox* genes. (Adapted from (Schuettengruber et al., 2007) with permission from Dr. Giacomo Cavalli)

2.1.4. Transcriptional Repression by Polycomb Proteins

The Polycomb proteins maintain inhibition of gene expression through mechanisms that are as yet not entirely clear but which may involve repressing the initiation of transcription, inhibiting nucleosome remodeling, regulating association of linker histone H1 and/or chromatin compaction (Francis et al., 2004; King et al., 2002; Levine et al., 2002; Shao et al., 1999; Zhu et al., 2007). Recent genome-wide identification of Polycomb target genes has also shown that some targets are transcribed

despite the presence of Polycomb proteins on the gene, suggesting that repression may not be a universal outcome at all loci (Boyer et al., 2006; Bracken et al., 2006; Lee et al., 2006; Tolhuis et al., 2006).

2.1.5 Polycomb Proteins in Different Species

The analysis of PcG proteins from an evolutionary perspective might help us to understand their roles. PRC2 complex components are present in plants, animals, and *N. crassa* but not in other fungi including *S. cerevisiae* and *S. pombe*, suggesting an ancient role in the regulation of global gene transcription (Figure 2-1) (Schuettengruber et al., 2007).

PRC1 components, on the other hand, show a more complicated story. For the animal kingdom, BLAST analysis of genomes of different species indicates that PRC1 genes might have originated early in animals. Some components are present in some members of Cnidaria, Porifera, and Urochordata. Several insect and vertebrate species have the complete set of PRC1 components. Nematodes and some urochordata look like they don't have the core components (Figure 2-1, Table 2-1). Finally plants and fungi do not have any component of PRC1 (Figure 2-1) (Schuettengruber et al., 2007; Springer et al., 2002). This information indicates that PRC1 components might have been lost during animal evolution. Presence of PRC2 but absence of PRC1 in some species also indicates that these two complexes might have independent functions.

2.1.6. *C. elegans* homologs of Polycomb proteins

C. elegans homologs of the PRC2 complex have been identified and well characterized. These include the products of the *mes-2, mes-3* and *mes-6* genes, mutations in which result in maternal effect sterility (Capowski et al., 1991). The MES proteins form a complex in which the SET domain of MES-2 mediates di- and tri-methylation of H3K27 (Bender et al., 2004; Holdeman et al., 1998). The H3K27me3 mark is concentrated on the X chromosome of wild-type animals, and transcription of X chromosome genes is normally silenced in the germline (Fong et al., 2002; Xu et al., 2001). In *mes-2*, *mes-3* and *mes-6* mutants chromatin marks associated with active chromatin are found on the X chromosome, and the current model is that inappropriate expression of X chromosome genes in the germline is responsible for the degeneration of germ cells and the sterility observed in *mes* mutants (Fong et al., 2002).

In addition to their role in the germ line, *mes* genes also act in somatic cells. *mes-2, mes-3* and *mes-6* mutants have weak but reproducible defects consistent with abnormal *Hox* gene activity, in agreement with the classical role of Polycomb group genes as repressors of *Hox* gene activity (Ross and Zarkower, 2003). The abnormalities include subtle defects in migration by specific neurons, expansion of the domains of *Hox* gene expression, and mislocalization of sensory rays in the male tail. The genetic screens that identified the *mes* genes did not identify genes homologous to PRC1 components, and the *C. elegans* genome does not encode obvious homologs of many of the components of PRC1. These data suggest that either *C. elegans* lacks a PRC1 complex, which would suggest that

PRC2 function could be uncoupled from PRC1 function, or that the function, composition or amino acid sequences of the proteins in a PRC1-like complex are sufficiently divergent to make recognizing them difficult.

Here I describe the gene *mig-32*, which encodes a homolog of the human PRC1 component BMI-1 and related proteins. Consistent with *mig-32* encoding a component of a PRC1-like complex, ubiquitylation of H2A is markedly reduced or absent in *mig-32* mutants. *mig-32* mutants have some defects in their nervous system that are similar those of *mes* mutants. Surprisingly, unlike *mes* mutants *mig-32* mutants are fertile, suggesting that *mig-32* is not required in the germline to recognize marks placed by the MES/PRC2 complex. Our data reveal novel roles in the nervous system for a chromatin-modifying protein that is functionally related to PRC1.

2.2. Materials and Methods

2.2.1 Alleles and Strains

All strains were maintained at 20°C as described by Brenner (Brenner, 1974). Mutations and mapped integrated transgenes used were: `

LGI, *mig-1(e1787), lin-59(n3192), lin-59(n3168), lin-59(n3425), unc-73(e936), mes-3(bn35), unc-40(e271), lin-35(n745), lin-61(n3809), lin-53(n833, ced-1(e1735).*

LGII, *lin-8(n111), dpl-1(n2994), unc-4(e120), mes-2(bn11), muIs32[*$P_{mec\text{-}7}$*gfp]* (Pujol et al., 2000), *muIs16[*$P_{mab\text{-}5}$*gfp]* (Hunter et al., 1999), *nIs128[*$P_{pkd\text{-}2}$*gfp]* (Yu et al., 2003).

LGIII, *pal-1(e2091), ced-4(n1162, lin-39(n1760, cec-1(ok1005); mig-10(ct41); lin-9(n112), unc-119(ed3).*

LGIV, *plx-1(nc37), ced-10(n1993), mes-6(bn38), dpy-20(e1282), mig-32(n4275)* (kindly provided by the Horvitz lab), *mig-32(tm1807), mig-32(tm1684)* (kindly provided by the Mitani lab), *unc-31(e928).*

LGV, *tam-1(cc567), him-5(e1490).*

LGX, *nIs106[P_{lin-11}gfp]* (Cameron et al., 2002), *kyIs4[P_{ceh-23}gfp]* (Zallen et al. 1998), *oxIs12[P_{unc-47}gfp]* (McIntire et al., 1997), *spat-3(gk22), unc-6(ev400), mig-2(mu28); slt-1(eh15), lin-15(n765ts), lin-15A(n767), lin-15B(n744)*

Integrated transgenes not mapped to a chromosome included:

kyIs39[P_{sra-6}gfp] (Troemel et al., 1995), *bxIs13[P_{egl-5}gfp]* (Zhang and Emmons, 2001); *mxIs23[P_{mig-32}mig-32:gfp]*.

Extra-chromosomal arrays included*:*

rtEx238 [P_{nlp-1}gfp] (kindly provided by Anne Hart), *mxEx53[P_{plx-1}mig-32:cfp]*

2.2.2. Isolation of *mig-32* alleles

The *mig-32(n4275)* allele was isolated in the Horvitz lab in an EMS screen for random mutations. *mig-32(tm1684)* and *mig-32(tm1807)* alleles were isolated in the Mitani lab using UV/Tmp mutagenesis. I confirmed the exact deletion borders by sequencing with nested primers after doing PCR flanking the deletion areas.

2.2.3. Brood size and egg counting

For brood size counting, single L4 worms were put on separate plates with bacteria. The mother worms were transferred to a new plate every day until stopped laying eggs. The progeny worms on each plate were counted.

Eggs inside adult worms were counted to learn how many eggs are deposited in different strains. For each strain 50-60 L4s were put on a fresh plate with bacteria. 24 hours later each worm was put in a separate well of a 96-well plate in 100µl of M9 buffer. In each well 100µl of 2X bleach solution (0.5M KOH, 4 percent hypochlorite) was added. After the worms disintegrated, the eggs were counted.

2.2.4. Imaging

Transgenic animals were imaged using a Zeiss Axiophot with Openlab software. To quantitate HSN and ALM migrations, the distance along the body axis between the rectum and the HSN or ALM nuclei was determined using Openlab software and compared to the distance to the vulva.

2.2.5. Construction and analysis of *mig-32/Df* animals

sDf62 unc-31(e169)/nT1(IV); +/nT1(V) hermaphrodites were mated with *him-5(e1490)* males, and cross-progeny males were mated with *mig-32(n4275) unc-31(e928)* hermaphrodites. Uncoordinated male cross progeny were collected at young adult stage and the position of Ray 1 determined by observation with Nomarski optics.

2.2.6. RNAi knockdown of target genes

All RNAi plasmids are derivatives of the L4440 backbone vector. They were either generated in our lab using standard cloning techniques or kindly provided by Rueyling Lin. The RNAi feeding procedure was followed as described in (Timmons et al., 2001). Worms on RNAi plates were incubated at 15ºC or 20ºC depending on the assay.

2.2.7. Plasmid constructs

To construct $P_{mig\text{-}32}$ *mig-32:gfp*, an 8065 bp *BamH*I/*Sph*I fragment of the F11A10 cosmid was cloned into a pUC19 vector. An *Xma*I fragment of pPD102.33 (kindly generated by Dr. Andy Fire) including the GFP coding sequences was cloned into the *Age*I site in the first exon of *mig-32*, which is located ten codons after the predicted initiating ATG. This construct was injected into *lin-15(765ts)* worms at 25 ng/µl concentration along with a *lin-15* rescuing plasmid (50 ng/µl). The resulting extrachromosomal array was transferred to the *mig-32(n4275); him-5(e1490)* background and integrated using gamma irradiation, followed by backcrossing 3 times with *mig-32(n4275); him-5(e1490).*

To construct $P_{plx\text{-}1}$*mig-32::cfp*, an *Eco*RI-*Xba*I fragment of the full length yk1321a11 *mig-32* cDNA was cloned into pUC19. CFP coding sequences were amplified by PCR and dropped into *mig-32* at the *Age*I site near the N-terminus. The *mig-32* start codon was converted into an *Nsi*I site using site-directed mutagenesis, and 2.6kb of the *plx-1* promoter (Dalpe et al., 2004) was PCR amplified and cloned into the *Nsi*I site.

Constructs were injected into *unc-119(ed3); mig-32(n4275); him-5(e1490)* worms at 10 ng/µl concentration along with 50 ng/µl of rescuing *unc-119* plasmid. All regions of all constructs subjected to PCR were fully sequenced. I used the position of Ray 1 as an assay for *mig-32* function. 28 ± 6 percent of transgenic *mig-32(n4275)* mutants carrying the P_{mig-32}*mig-32:gfp* reporter (n=50) had anterior Ray 1s, compared with 64 ± 5 percent of *mig-32* mutants (n=100).

2.2.8. Generation of synchronized worm populations

Gravid adult worms were collected from plates in M9 suspension. Worms were washed three times with M9 buffer to remove bacteria. 10X the volume of worm pellet of bleach solution was added (0.25M NaOH, 1 percent hypochlorite) to the worms and vortexed for five minutes until the worms were broken and eggs were released. Eggs were collected immediately by spinning and then washed three times with M9 buffer. Washed eggs were incubated in S medium (Stiernagel, 1999) overnight to allow synchronization of worms at L1 stage. L1 worms were put on plates with food and incubated until the desired stage was reached.

2.2.9. Core histone extraction and western blotting

0.5 ml of packed L1 stage worms were harvested from freshly-starved 6X peptone NGM agar plates (For 1 liter: 3 g NaCl, 17 g agar, and 15 g peptone, 1 ml 1 M $CaCl_2$, 1 ml 5 mg/ml cholesterol in ethanol, 1 ml 1 M $MgSO_4$ and 25 ml 1 M KPO_4 buffer). L1

staged worms were separated from others using gravity in M9 suspension. Worms were resuspended in 5 mls of NIB buffer (15mM PIPES (pH 6.8), 5 mM $MgCl_2$, 60 mM KCl, 0.25 M sucrose, 15 mM NaCl, 1 mM $CaCl_2$, 0.8 percent Triton, protease inhibitors) (Jackson et al., 2004) and sonicated 3-4 times until the cuticle was completely broken (30 second sonication with 3 minute intervals). The lysate was centrifuged at 10,000 g for 10 minutes. The pellet was resuspended in 2 mls of 0.4 N H_2SO_4 and incubated at 4°C for 1 hour to overnight. After spinning at 10,000 g for 10 minutes the supernatant was either dialyzed with PBS or precipitated with 20 percent TCA. TCA-precipitated histone extract was washed with cold acetone 3 times and the final pellet dried and dissolved in water. Acetone precipitates did not completely dissolve, so suspensions of histones were electrophoresed on a 15 percent SDS-PAGE gel together with BSA as a standard for protein amount and stained with Coomassie brilliant blue. The concentration of histone H2A was calculated roughly by comparing it to the BSA standard. 1-10μgs of histones were loaded per lane for western blots. Samples were electrophoresed by SDS-PAGE using a 15 percent discontinuous gel and transferred to PVDF membrane for 75 minutes at 100V. Histone H2A western blots were used to confirm equal loading. For detection of H2A, rabbit antiserum against histone H2A from Upstate (#07-146) was used at 1/1000 dilution. For detection of ubiquitylated histones, monoclonal anti-ubiquitin (clone P4D1) from Cell Signaling Technology was used at 1/1000 dilution.

2.3. Results

2.3.1 MIG-32 is a RING domain-containing protein similar to Polycomb family members

I identified MIG-32 as a protein most similar to a family of vertebrate proteins including BMI-1 (Figure 8), which is a core component of the PRC1 complex (Levine et al., 2002). As no PRC1-like complex has been described in *C. elegans* the genetic pathways in which *mig-32* might participate are unclear. I therefore identified mutations in *mig-32* to study its function, as described below.

I confirmed the gene structure predictions for *mig-32* by determining the DNA sequences of five full-length *mig-32* cDNAs, and found that all were identical in the predicted coding sequences and were SL2 spliced, consistent with genome database predictions that *mig-32* is the second gene in a three-gene operon (WormBase web site, http://www.wormbase.org, release WS193, July, 2008) (Spieth et al., 1993). *mig-32* is predicted to encode a 542 amino acid protein with no close homologs in the completely sequenced *C. elegans* genome identified using the BLAST algorithm (Altschul et al., 1990), and with a predicted RING domain as the only domain recognized by Pfam (Bateman et al., 2002). Using BLAST searches I identified MIG-32 homologs in vertebrate genomes, including six homologous proteins from humans (Figure 2-2). Included in this group are the BMI-1 protein, which is a core component of the PRC1 complex and well characterized as a modifier of gene expression that acts by altering

chromatin (Levine et al., 2002; Li et al., 2006; Shao et al., 1999; Wang et al., 2004b), and the related proteins MEL-18/RFP110, NSPc1/PcGRF1 and Pcgf5, which participate in related complexes (Alkema et al., 1997; Sanchez et al., 2007; Trimarchi et al., 2001).The *Drosophila melanogaster* genome contains two homologs: *Posterior sex combs*, a component of the *Drosophila* PRC1 complex (Saurin et al., 2001), and *Lethal (3) 73 Ah*, an essential gene (Belote et al., 1990; Irminger-Finger and Nothiger, 1995). I identified a single MIG-32 homolog in the genomic sequences of each of the nematodes *C. briggsae* and *C. remanei* (Figure 8). These data suggest that MIG-32 is a RING domain protein most similar to core components of human and *Drosophila* Polycomb complexes.

I identified three deletion alleles of *mig-32* by screening libraries of mutagenized *C. elegans* (see Materials and Methods). Each of the allele deletes *mig-32* genomic coding sequences but not coding sequences of the upstream or downstream genes, as outlined in Figure 2-3. The *n4275* allele deletes 460 nucleotides including 59 nt 5' of the ATG of *mig-32* and the codons for the first 134 amino acids. *mig-32(n4275)* mutants, and mutants carrying the *tm1684* and *tm1807* alleles, are homozygous viable and have defects in the male tail and other structures as outlined briefly here and in greater detail below.

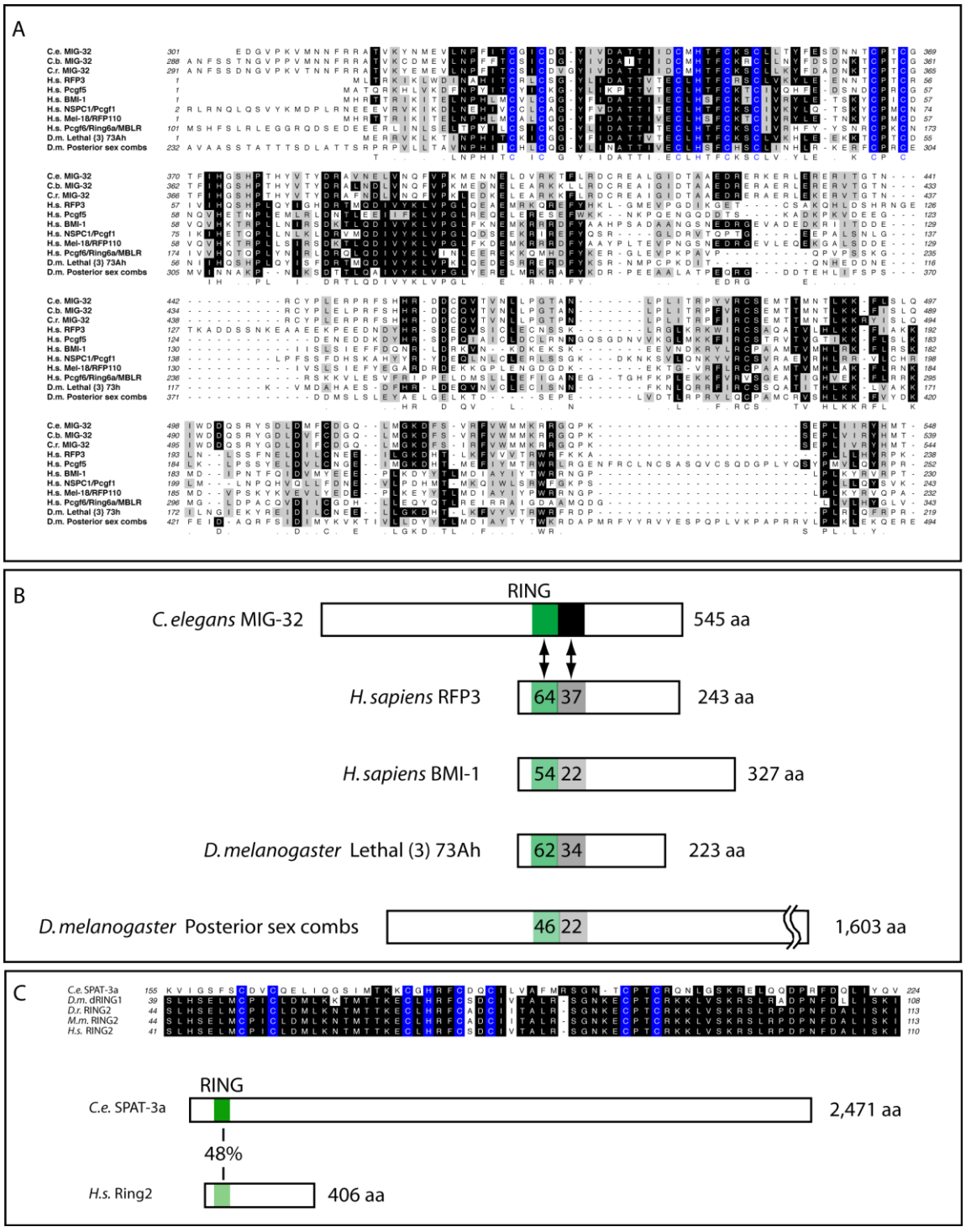
A
C.e. MIG-32
C.b. MIG-32
C.r. MIG-32
H.s. RFP3
H.s. Pcgf5
H.s. BMI-1
H.s. NSPC1/Pcgf1
H.s. Mel-18/RFP110
H.s. Pcgf6/Ring6a/MBLR
D.m. Lethal (3) 73Ah
D.m. Posterior sex combs
B
RING
C. elegans MIG-32
545 aa
H. sapiens RFP3
64 37
243 aa
H. sapiens BMI-1
54 22
327 aa
D. melanogaster Lethal (3) 73Ah
62 34
223 aa
D. melanogaster Posterior sex combs
46 22
1,603 aa
C
C.e. SPAT-3a
D.m. dRING1
D.r. RING2
M.m. RING2
H.s. RING2
RING
C.e. SPAT-3a
2,471 aa
48%
H.s. Ring2
406 aa

Figure 2-2: MIG-32 and SPAT-3a are RING domain proteins most closely related to Polycomb family members

(A) Amino acid sequence alignments of MIG-32 with related proteins from nematodes, humans and fruit flies. Colored amino acids highlight the RING domain. The extended N termini of MIG-32 and related proteins from nematodes have been removed for this alignment, as have the N terminus of NSPc1/PcGRF1 and the N and C termini of Posterior sex combs. The *mig-32* cDNA sequence is deposited in the EMBL/GenBank data library under accession number NM069892. Sequences of the predicted *C. briggsae* and *C. remanei* proteins were assembled from genomic DNA sequences using homology with the *C. elegans* protein and cDNAs to guide assembly. Black, grey, and blue highlights represent identical residues, similar residues and cysteines and histidines of RING domains respectively. (B) Schematic diagrams of MIG-32 from *C. elegans* and four related proteins from human and fruit fly. The green boxes indicate the RING domain. Grey boxes indicate a region conserved among Polycomb RING proteins, Percent amino acid sequence identities are indicated. (C) Amino acid sequence alignments of SPAT-3A with related proteins from flies and vertebrates.

The male tail has nine bilateral sensory ray structures (Emmons, 2005). I used the defect in the position of one of these rays to examine the consequences for *mig-32* function of the three deletion alleles. I found that all three alleles result in qualitatively and quantitatively similar defects in the position of Ray 1, with 60-80 percent of the mutant worms having an anterior Ray 1 (Figure 2-3); all three also result in similar defects in migration of the HSN neurons (see below). The alleles are recessive (Figure 2-3 and data not shown), and mutants of genotype *n4275/sDf62*, a chromosomal deficiency that deletes the *mig-32* region, have defects in Ray 1 position similar to those of *mig-32* homozygotes. The brood size of *mig-32(n4275)* mutants is 45 percent of the wild-type strain, N2, and that of *mig-32(tm1807)* is 64 percent of the wild-type, and eggs laid by *mig-32* mutants hatch at rates similar to those of wild-type animals. Three observations suggest that the deletions specifically affect *mig-32* function and not the function of *F11A10.8* or *F11A10.6*, the upstream and downstream genes in the operon, respectively.

F11A10.8 encodes a very well-conserved homolog of human CPSF4, a splicing factor (WormBase). Inactivation of *F11A10.8* by RNAi is lethal, as is a deletion mutation, *ok844*, which deletes parts of the F11A10.8 and *mig-32* coding regions (Figure 2-3) (WormBase), suggesting that the *mig-32(n4275), tm1684* and *tm1807* deletions do not severely impair *F11A10.8* function. Second, RNAi of *mig-32*, which primarily targets processed mRNA (Fire et al., 1998), results in an anterior position of Ray 1, as I observed in *mig-32* mutants (Figure 2-3). Last, expression using the *plx-1* promoter (Dalpe et al., 2004) of a *mig-32* cDNA in the male tail rescued the anterior Ray 1 defects of *mig-32(n4275)* mutants. Specifically, of 50 *mig-32(n4275)* mutants carrying a $P_{plx\text{-}1}$*mig-32:cfp* transgene, 12 ± 5 percent (standard error of the proportion) had an anterior Ray 1 compared with 64 ± 5 percent of 100 uninjected controls, and in contrast to *mig-32* mutant males the transgenic males mated efficiently (data not shown). These data suggest that the *n4275, tm1684* and *tm1807* alleles are strong loss-of-function or null alleles of *mig-32*. Unless otherwise indicated I used the *mig-32(n4275)* allele for the experiments described here.

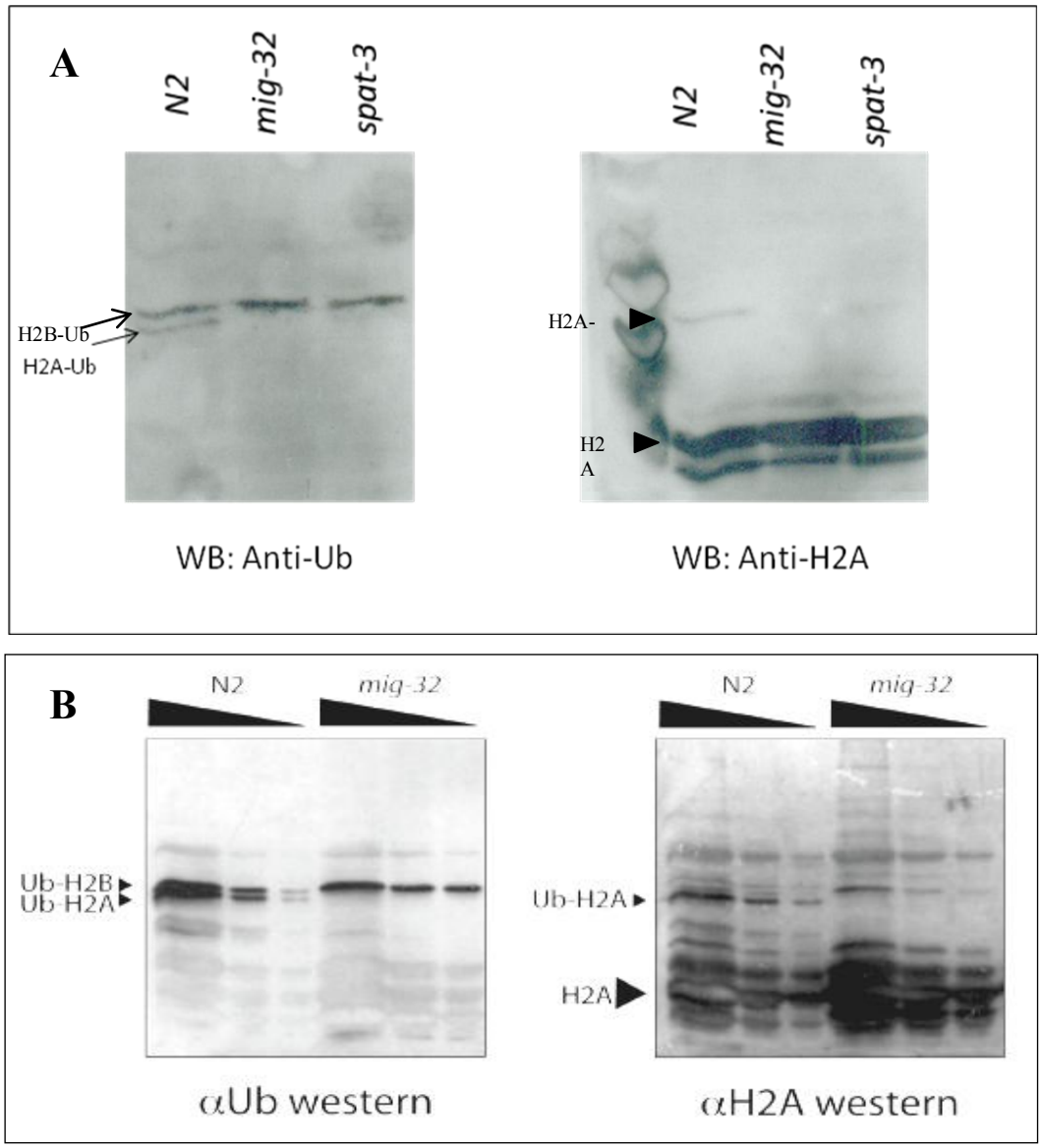

Figure 2-3: *mig-32* is required for ubiquitylation of histone H2A
(A)Western blot analysis of acid-extracted histones from wild-type, *mig-32*, and *spat-3* mutant *C. elegans*. The filter shown in the left panel was probed with anti-ubiquitin antibody. Arrows indicate ubiquitylated H2A and H2B. In the right panel, this blot was stripped and reprobed with anti-H2A antibody. Arrowheads indicate ubiquitylated H2A and unmodified H2A. (B) A second pair of western blots intentionally overloaded to enhance detection of modified H2A in *mig-32* mutants are shown.

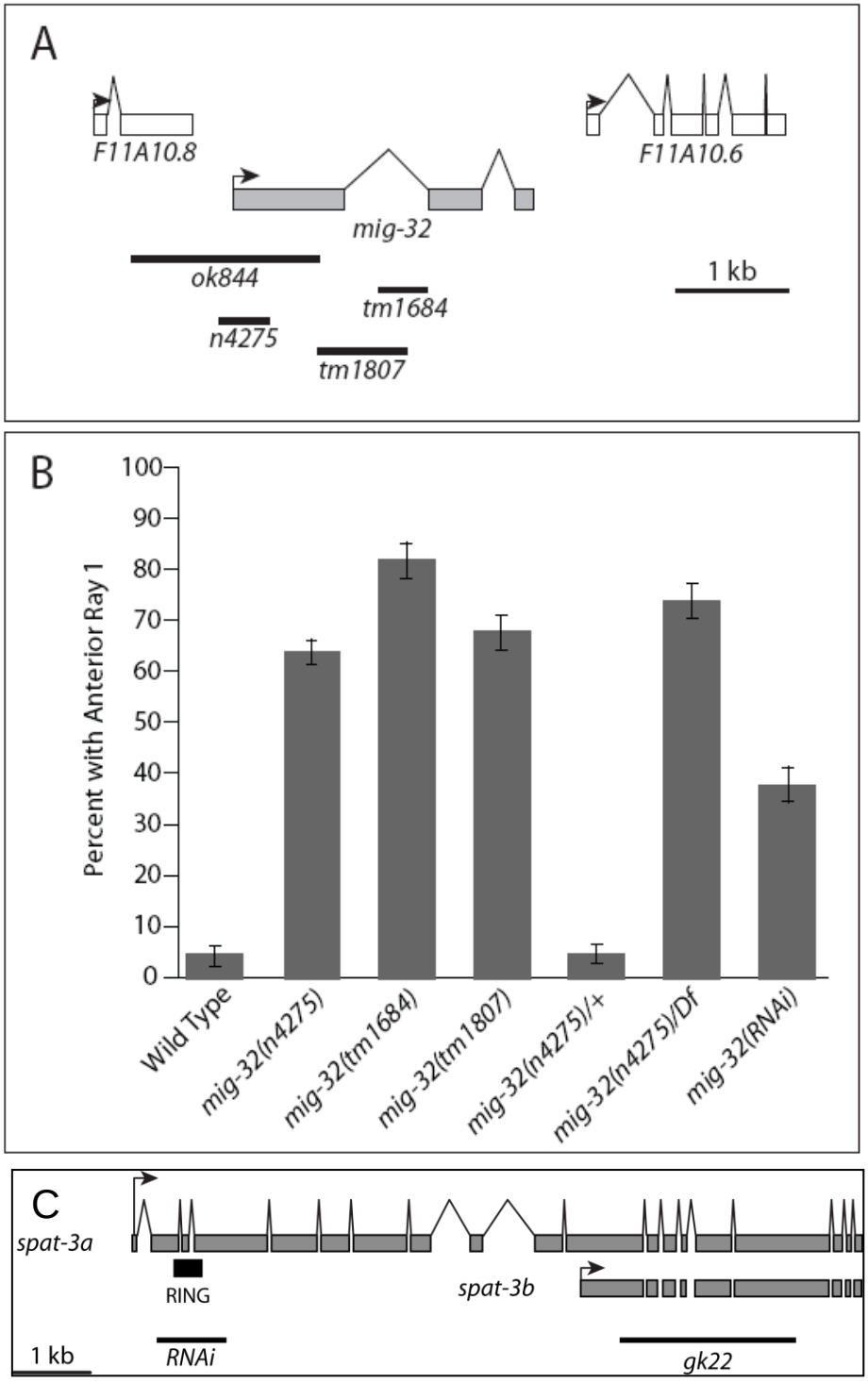
A
F11A10.8
mig-32
F11A10.6
ok844
tm1684
n4275
tm1807
1 kb
B
Percent with Anterior Ray 1
100
90
80
70
60
50
40
30
20
10
0
Wild Type
mig-32(n4275)
mig-32(tm1684)
mig-32(tm1807)
mig-32(n4275)/+
mig-32(n4275)/Df
mig-32(RNAi)
C
spat-3a
RING
spat-3b
1 kb
RNAi
gk22

Figure 2-4: Three deletion alleles of *mig-32* are strong loss of function or null.
(A) *mig-32* exons are indicated as shaded boxes, and exons of the 5' and 3' genes in the three-gene operon are indicated as unfilled boxes. Available mutations affecting *mig-32*, all of which are deletions, are indicated as solid lines. The *n4275* mutation deletes 460 nucleotides with a single nucleotide inserted at the deletion site, and removes the start codon and first 401 nucleotides of *mig-32*. The *tm1684* mutation deletes 465 nucleotides including intron sequences and the first seven nucleotides of exon 2. If transcribed and translated, this mutation is predicted to generate a protein that includes the first 333 amino acids of MIG-32, then one nonsense amino acid followed by a premature opal termination codon. The *tm1807* mutation deletes 791 nucleotides with two nucleotides inserted at the deletion site, and removes the last 219 nucleotides of exon 1. If transcribed and translated, this mutation is predicted to generate a protein that includes the first 260 amino acids of MIG-32, then four nonsense amino acids followed by a premature opal termination codon. The *ok844* allele deletes 1674 nucleotides with a two-nucleotide insertion at the deletion site. The mutation affects *F11A10.8* and *mig-32* coding sequences. (B) Quantification of defective male tails in *mig-32* mutants (see Figure 2-6). (C) The *spat-3* gene encodes two proteins using alternative promoters. *spat-3a* is longer and encodes a RING domain protein. There is one deletion allele available affecting both transcripts (*gk22*). I generated an RNAi clone that targets the RING domain of *spat-3a*.

2.3.2. *mig-32* is required for ubiquitylation of histone H2A

PRC1 contains three RING proteins, Ring1A, Ring1B, and BMI-1; of these, MIG-32 is most closely related to BMI-1 and, aside from the presence of a RING domain, has little sequence similarity to Ring1B (Figure 8 and data not shown). The defined biochemical function of PRC1 is ubiquitylation of histone H2A at position 119. In PRC1, the Ring1B protein serves as the E3 to catalyze H2A ubiquitylation (Wang et al., 2004a). Other core components, especially including BMI-1, stimulate the catalytic activity of Ring1B (Cao et al., 2005; Li et al., 2006; Wei et al., 2006) perhaps by promoting folding and stability of Ring1B (Ben-Saadon et al., 2006). I therefore asked whether H2A ubiquitylation was abnormal in *mig-32* mutants. I analyzed histone modification using western blots of acid-extracted histones from wild-type and *mig-32* mutant *C. elegans*. Using an H2A-specific antibody with extracts from wild-type animals I detected H2A and a rare, higher

molecular weight band that migrated at the size expected for ubiquitin-modified H2A; this band was not detected in extracts from *mig-32* mutant animals (Figure 2-4A and 10B). Using an antibody that detects ubiquitin with histone extracts from wild-type animals, I detected two bands that correspond to the predicted molecular weights of H2A and H2B, both of which are modified by ubiquitylation (Osley, 2006). H2A, the smaller of these bands, is not detected in extracts from *mig-32* mutants (Figure 2-4). These data suggest that MIG-32 is required for ubiquitylation of Histone H2A, the defining biochemical function of PRC1.

2.3.3. *mig-32* is broadly expressed, localized to nuclei and concentrated within nucleoli.

in situ hybridization using a *mig-32* cDNA suggested the gene is expressed prominently in the *C. elegans* germline (Y. Kohara, personal communication). I constructed a rescuing GFP reporter to determine the expression pattern in somatic cells (see Materials and Methods). The reporter construct contains 8 kb of genomic DNA including 2.6 kb of 5' sequence from the first gene in the operon, all of *mig-32*, and 2 kb of sequence 3' from the predicted termination codon of *mig-32*, including half of the 3'-most gene in the operon. Consistent with MIG-32 acting as a modifier of chromatin, the $P_{mig\text{-}32}$*mig-32:gfp* reporter is expressed broadly in most or all nuclei, beginning early in embryogenesis and continuing in larval development and into adulthood of both males and hermaphrodites (Figure 2-5 and data not shown). Expression is predominantly nuclear, with relatively

bright intranuclear areas of fluorescence that correspond with nucleoli evident as seen with Nomarski optics, particularly in some hypodermal cells where nucleoli are easily identified (Figure 2-5). Transfection of mammalian cells with a FLAG-epitope-tagged MIG-32 showed nuclear expression concentrated in a shell around nucleoli, suggesting that the interactions that determine subcellular localization may be evolutionarily conserved (Figure 2-5).

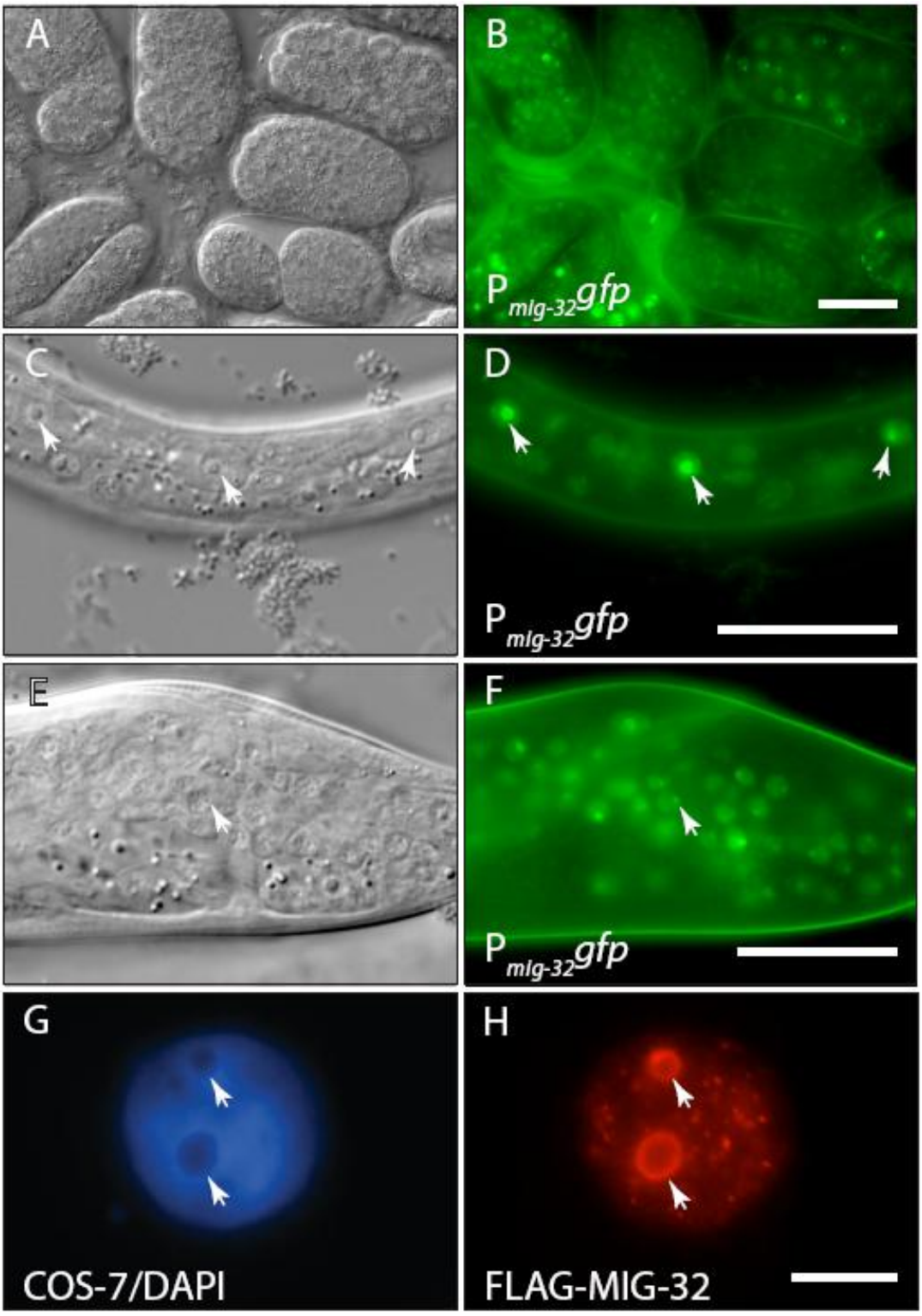
A
B
P mig-32 gfp
C
D
P mig-32 gfp
E
F
P mig-32 gfp
G
COS-7/DAPI
H
FLAG-MIG-32

Figure 2-5: *mig-32* is broadly expressed, localized to nuclei, and concentrated in nucleoli. Differential interference contrast (A,C, E) and epifluorescence (B, D, F) images of transgenic *C. elegans* are shown. (A,B) Mixed-stage embryos. (C,D) L1 stage larva showing the lateral hypodermal cells. Nucleoli within hypodermal nuclei are highlighted by arrowheads. (E,F) L4 stage male tail. Arrowhead highlights a nucleolus within a neuronal nucleus. (G, H) COS-7 cell transfected with FLAG epitope-tagged *C. elegans* MIG-32 (G) stained with DAPI to visualize DNA and (H) stained with anti-FLAG antibody. Arrowheads highlight nucleoli in the COS cell nucleus. Anterior is leftwards and ventral is downwards in images C-F. Scale bars are 10 microns.

I considered the possibility that localization of MIG-32 might depend upon *mes* gene activity. To test this, I examined the expression and localization of the $P_{mig\text{-}32}$*mig-32:gfp* reporter in *mes-2* mutants and observed that expression of the reporter is brighter in the *mes-2* mutant background but that the fusion protein remains localized to nuclei and nucleoli (data not shown).

2.3.4. *mig-32* may act with the Polycomb-group genes *mes-2, mes-3* and *mes-6* to position Ray 1 of the male tail

I observed that *mig-32* mutant males mate very poorly. Observation of the male tail using differential interference optics showed that Ray 1 is located abnormally anterior in *mig-32* mutants (Figure 2-6). The rays are positioned by their interactions with the hypodermis, which in part may be determined by the Rn.p (posterior daughter of any R blast cell) hypodermal cell generated by the cell lineages giving rise to each ray (Emmons, 2005). Several genetic pathways position Ray 1 appropriately in males. These include the *mes-2*, *mes-3* and *mes-6* genes, which encode *C. elegans* homologs of the PRC2 histone methyltransferase complex that initiates Polycomb complex-mediated

chromatin modification and transcriptional repression (Bender et al., 2004; Ross and Zarkower, 2003). I constructed double mutants between *mig-32* and putative null alleles of each of the *mes* genes. Strikingly, the Ray 1 position defects of these double mutants were not enhanced (Figure 2-6), suggesting that *mig-32* acts in the same genetic pathway as the *mes* genes to position Ray 1.

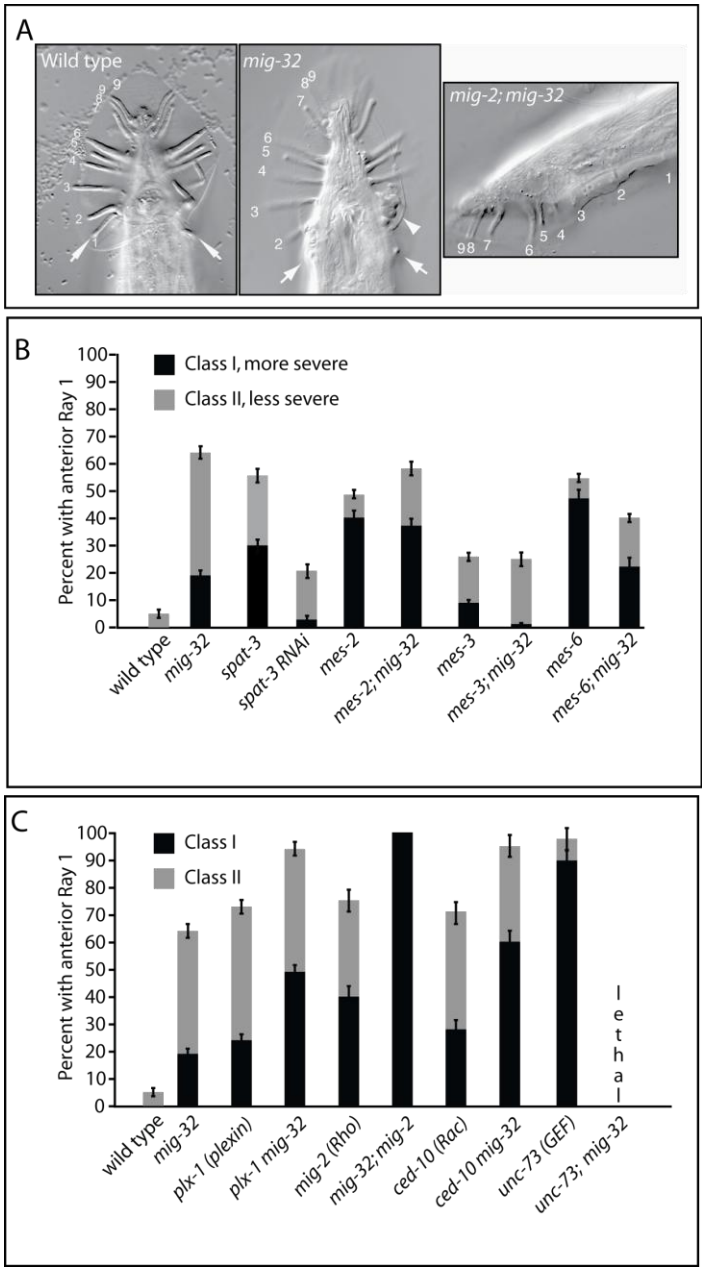

Figure 2-6: *mig-32* acts parallel to most known pathways that position Ray 1 with the exception of the *mes* genes

(A) Ventral views of the tails of male wild type and *mig-32* mutants and a lateral view of a *mig-2; mig-32* mutant male. The nine bilateral rays are numbered as indicated. Arrows indicate Ray 1 pairs in the wild-type and *mig-32* mutant; an arrowhead indicates crumpled Rays 2 and 3 in the *mig-32* mutant. (B) Graph representing the percentage of animals with anterior Ray 1 in wild-type and mutant animals. The severity of the Ray 1 migration defect is categorized as Class I, in which the ray is located anterior and outside the normal position of the cuticular fan, or Class II, in which the ray is anterior but present within the fan (Fujii et al., 2002; Ginzburg et al., 2002). (C) Graph representing the percentage of animals with anterior Ray 1 in wild type and mutant animals of the indicated genotypes, scored as in B. In building double mutants with the partial loss-of-function allele *unc-73(e936)* I were able to generate individual animals with the predicted correct genotype but these animals never had sufficient progeny to maintain or score the strain.

Several additional pathways position Ray 1, including signaling by semaphorins and a Plexin receptor (Fujii et al., 2002; Ginzburg et al., 2002), acting through the *unc-73* guanine nucleotide exchange factor and the *ced-10/Rac mig-2/Rho* GTPases (Dalpe et al., 2004). I constructed double mutants between *mig-32* and each of these genes and examined the position of Ray 1 in the tails of male animals. In each case I identified significantly enhanced defects in the position of Ray 1 (Figure 2-6), suggesting that *mig-32* acts parallel to these pathways to position Ray 1.

2.3.5. H2AK119-Ubiquityl mark is not maintained in L4 and adult stages *in C. elegans*

Ray 1 data suggest that *mig-32* might function in the same pathway with *mes* genes to determine the position of Ray 1. These data fit perfectly with the classical model of PRC1 and PRC2 functioning together to regulate target genes. However, *mes* gene mutants display a very significant defect that *mig-32* mutants do not have. *mes* mutants are sterile due to germline degeneration as a result of inefficient X-chromosome inactivation during germline development. *mig-32* mutants have a slight reduction in brood size but do not display any sterility. This difference in phenotypes might be due to *mig-32* independent functions of *mes* genes during germline development. I hypothesized that *mes* genes might not require *mig-32* for germline maintenance or *mig-32* might be redundant with other factors; these other factors could ubiquitylate H2A in a manner redundant with *mig-32* or could act redundantly through a distinct mechanism. To test this idea I

analyzed the levels of H2A ubiquitylation at different stages of worm development by western blots of histones extracted from synchronized L1s, L4s, and young adults. Remarkably, H2AK119-ubiquityl and H2BK123-ubiquityl marks are lost in L4 and young adult worms compared to L1 worms that had strong signal. This suggests that ubiquitylation of H2A is not required during germline development, and that another repressive mechanism acts with the *mes* genes to ensure fertility (Figure 2-7).

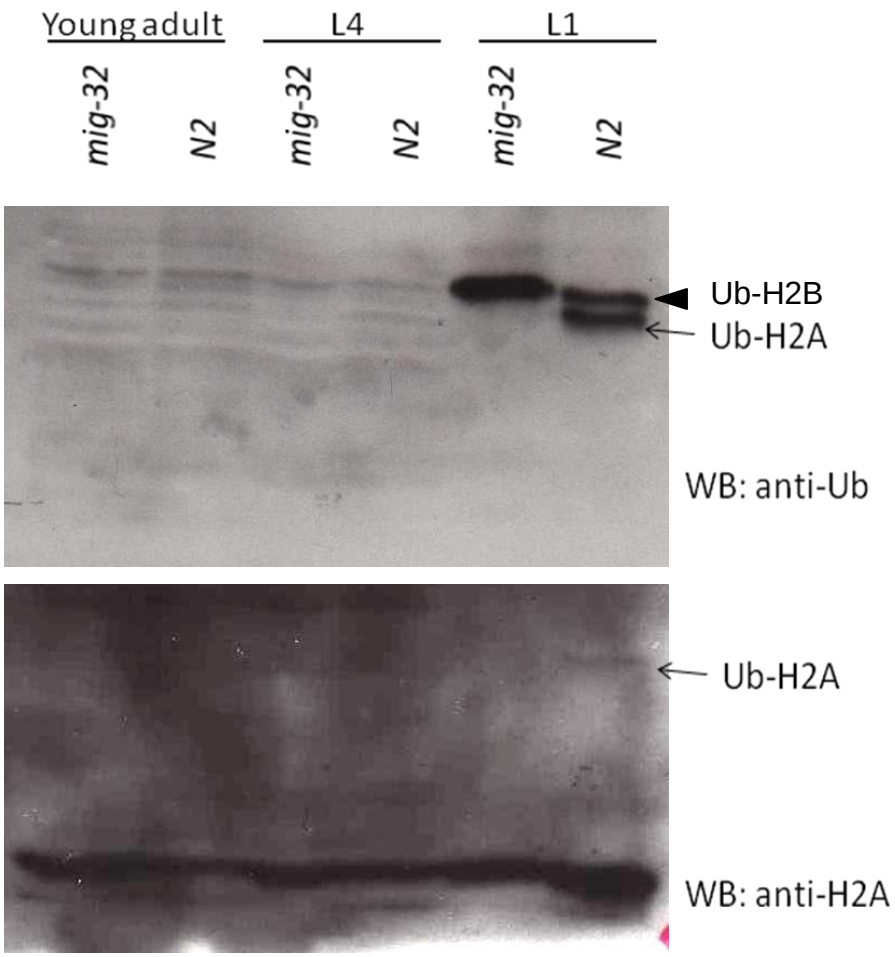

Figure 2-7: Ubiquitylation of H2A is not required during germline development. Staged worms were analyzed for Ubiquitylation of Histone H2A using western blots of extracted histones. Western blot with anti-Ubiquitin antibody shows that Ub-H2A is not present in L4 and young adult N2 worms compared to strong signal in L1 worms. The same membrane was stripped and probed with anti-H2A antibody as a loading control.

2.3.6. *mig-32* is required for some neuronal migrations and for guidance of some neuronal processes

I observed that *mig-32* mutants were variably egg-laying defective, with some animals in a population carrying more eggs than wild-type animals. In staged adults the wild-type strain N2 carried an average of 17.5 ± 5 eggs, compared with 28.8 ± 11 eggs in *mig-32* mutants (n=55 animals for each genotype, P<0.0001, unpaired two-tailed *t*-test). Egg-laying requires a vulva through which the eggs are laid, muscles to expel the eggs, and neurons to control the vulval muscles (Trent et al., 1983). I found that the two HSN neurons, which are essential for normal egg-laying (Trent et al., 1983), are often abnormal in *mig-32* mutants (Figures 2-8 and 2-9). During embryogenesis the HSN neurons migrate from the tail to the midbody (Sulston et al., 1983). Using the $P_{nlp\text{-}1}$*gfp* reporter to identify the HSN neurons (Li et al., 1999), the HSNs of *mig-32(n4275)* mutants fail to reach the midbody in 41 percent of mutants; by comparison, all HSNs migrated to their normal position in otherwise wild-type animals carrying the $P_{nlp\text{-}1}$*gfp* reporter (Figure 2-9). The axons extended by the HSN neurons were also abnormal. In wild type animals, each HSN extends an axon from the vulval region ventrally to the ventral nerve cord; the axons then turn anterior and extend to the head. 56 percent of the HSN axons of *mig-32* mutants failed to reach the head; by comparison, all HSN axons extended to the head of otherwise wild-type animals carrying the $P_{nlp\text{-}1}$*gfp* reporter (Figures 2-9). *mig-32* mutants carrying any of the three deletion alleles have

quantitatively and qualitatively similar defects in the HSN neurons (Figures 2-9). All HSNs of *mig-32* mutants expressed the P_{nlp-1}*gfp* reporter, suggesting that the HSN neurons correctly establish their identity and that the defects in HSN migration result from a requirement for *mig-32* in other processes important for migration and axon extension. The defects in HSN migration and axon extension likely account for the variable defects in egg-laying I observed in *mig-32* mutants; such variability has been associated with other mutants with defects in HSN migration (Desai et al., 1988).

Using *gfp* reporters, I surveyed *mig-32* mutants for defects in neuronal migration and processes extended by other neurons. The P_{unc-47}*gfp* reporter is expressed in the VD and DD motor neurons of the ventral nerve cord (McIntire et al., 1997). In otherwise wild-type animals carrying the P_{unc-47}*gfp* reporter the VD and DD neurons extend commissures from the ventral nerve cord laterally along the body wall to the dorsal nerve cord. In wild-type animals all but one pair of commissures track along the right side of the animal; only four percent of otherwise wild-type animals carrying the P_{unc-47}*gfp* reporter had more than one pair of commissures on the wrong side (Figure 2-8 and Table 2-2). In contrast, 63 percent of *mig-32* mutants had more than two left-sided commissures, with some animals having as many as five commissures on the wrong side (Figure 2-8 and Table 2-2). The number and positions of VD and DD neurons, the total number of commissures and the expression of P_{unc-47}*gfp* were normal in *mig-32* mutants (data not shown).

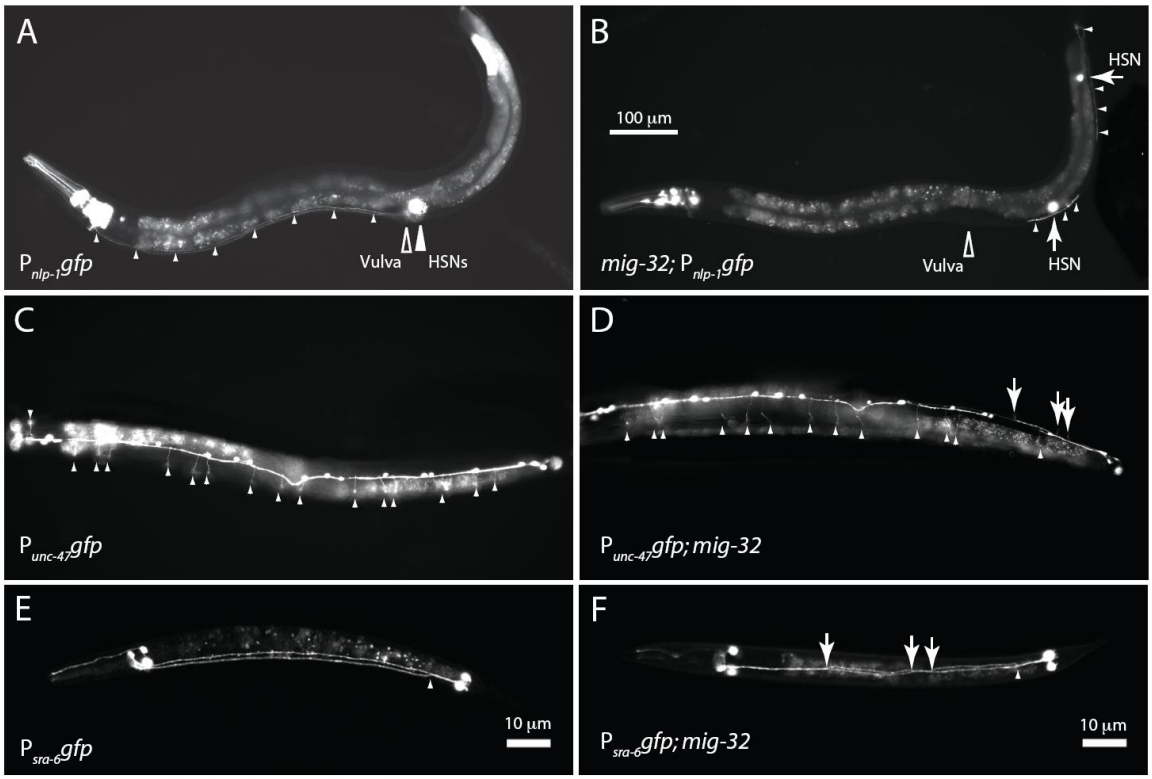

Figure 2-8: *mig-32* mutants have defects in neuronal migration and process extension. Images of otherwise wild type and *mig-32* mutant animals carrying *gfp* reporters are shown. (A) A wild type animal expressing $P_{nlp\text{-}1}gfp$ in the HSN neurons. HSN cell bodies are indicated with a large, filled arrowhead. A large, open arrowhead indicates the position of the vulva. Small, filled arrowheads highlight the axons of the two HSN neurons, which proceed along the ventral body wall to the head. (B) A *mig-32* mutant expressing $P_{nlp\text{-}1}gfp$ in the HSN neurons. Large, filled arrows indicate the HSN cell bodies and small arrowheads highlight the HSN axons. (C) Ventral view of a wild type animal expressing $P_{unc\text{-}47}gfp$ in the VD neurons. Small, filled arrowheads indicate lateral commissures. (D) Ventral view of a *mig-32* mutant expressing $P_{unc\text{-}47}gfp$ in the VD neurons. Small, filled arrowheads indicate lateral commissures. Large arrows indicate three commissures on the wrong side. (E) A wild type animal expressing $P_{sra\text{-}6}gfp$ in the PVQL and PVQR neurons. A small, filled arrowhead indicates the normal separation of the PVQ axons into the right and left sides of the ventral nerve cord. (F) A *mig-32* mutant expressing $P_{sra\text{-}6}gfp$ in the PVQ neurons. Three large arrows indicate inappropriate crossing by the PVQ neurons. Anterior is leftwards in all images. Scale bar in B applies to images in A, B, C and D, all of which are adult animals. Scale bars in E and F are shown, and L1 stage larvae are pictured. Ventral is downwards in images in A and B, up in C and D, and slightly rotated in E and F.

I also identified defects in midline crossing by the PVQR and PVQL neurons. The PVQ neurons are located in the lumbar ganglion, and each extends an axon anteriorly to the head. Initially, both axons extend along the right side of the hypodermal ridge that divides the ventral nerve cord. The PVQL axon then crosses the midline to the left side and proceeds to the head (White, 1986). Using the $P_{sra\text{-}6}$*gfp* reporter, which is expressed in the PVQ neurons (Troemel et al., 1995), I observed that the PVQ axons of *mig-32* mutants do not respect the midline boundary and cross inappropriately (Figure 2-8 and Table 2-2). 26 percent of the PVQ axons of *mig-32* mutants crossed the midline inappropriately, compared with 8 percent of otherwise PVQ axons of the wild-type animals carrying the $P_{sra\text{-}6}$*gfp* reporter. All PVQ neurons of *mig-32* mutants expressed $P_{sra\text{-}6}$*gfp* at levels similar to wild-type animals.

Some neurons and axons of *mig-32* mutants migrate and extend processes normally, while others are slightly abnormal. The CAN neurons originate in the head and migrate posteriorly to a position adjacent to the vulva. Using a $P_{ceh\text{-}23}$*gfp* reporter, 50 of 50 CAN neurons of *mig-32* mutants migrated appropriately and extended axons as in the wild type (data not shown). Several of the mechanosensory neurons migrate along the anterior-posterior body axis during development (Hamelin et al., 1992). The Q cells migrate anteriorly and divide, with the QR cell (right-sided Q cell) generating the AVM mechanosensory neuron and QL (left-sided Q cell) the PVM neuron. The ALM neurons

migrate posteriorly from the head. Using the $P_{mec\text{-}7}$*gfp* reporter to label the mechanosensory neurons and their axons, I found that the ALM neurons of *mig-32* mutants were slightly defective in posterior migration. Of 150 ALM neurons observed in *mig-32* mutants, 15 ALMs did not complete their migrations (Figures 2-9B). The processes of the ALM neurons were similar in *mig-32* and wild-type animals (data not shown). The PLM neurons do not migrate, but their posterior processes were often foreshortened in *mig-32* mutants. Of 100 PLM neurons of *mig-32* mutants, the posterior process terminated prematurely in 55 percent of animals, extending less than half the normal distance. In contrast, the posterior processes of the PLM neurons terminated prematurely in only 6 percent of 100 wild-type animals. The locations of the AVM and PVM neurons and the morphology of their processes were similar comparing 75 *mig-32* mutants with 50 wild-type animals (data not shown).

Genotype	Cell process	Percent of animals with a defect	n
$P_{nlp-1}gfp$	HSN axon	0	50
mig-32(n4275), $P_{nlp-1}gfp$	HSN axon	56	49
mig-32(tm1684), $P_{nlp-1}gfp$	HSN axon	46	46
mig-32(tm1807), $P_{nlp-1}gfp$	HSN axon	56	88
$P_{sra-6}gfp$	PVQ axons	8	50
mig-32; $P_{sra-6}gfp$	PVQ axons	26	87
$P_{unc-47}gfp$	VD commissures	4	25
mig-32; $P_{unc-47}gfp$	VD commissures	63	100

Table 2-2: *mig-32* mutants have defects in neuronal migration and process extension
The percent of animals with a defect in specific neuronal processes is shown. For the HSN axons, animals were scored as defective if the axon failed to reach the head; in general, axons that reached the head followed a normal path from the HSN ventrally into the ventral nerve cord then turned anterior to the head. HSN neurons that failed to migrate to the midbody often had more severe defects in axon pathfinding, with axons that tracked posterior rather than anterior. For the PVQ axons, defective axons included those that crossed the midline inappropriately compared to wild-type animals. For the VD commissures, defective commissures included those that tracked on the wrong side of the body wall. *mig-32* mutants had between zero and five commissures on the wrong side, with more posterior VD neurons being more likely to have defective commissures.

Migration of the distal tip cells, which are somatic cells that lead the anterior and posterior arms of the proliferating germ line along the body wall, appeared normal comparing 23 *mig-32* mutants with 18 wild-type animals (data not shown).

In summary, *mig-32* is required for normal migration of the HSN neurons and for extension of some neuronal processes. It participates in ensuring that VD neuronal commissures extend along the correct side of the animal, and that the PVQ axons do not cross the midline inappropriately. The defects I observed in *mig-32* mutants are unlikely to be a result of markedly altered neuronal differentiation because expression of all of the *gfp* reporters used for these experiments were expressed in the expected patterns in *mig-32* mutants (a list of reporters used is found in Materials and Methods).

2.3.7. *mig-32* acts parallel to most known pathways that act in HSN migration

Several genetic pathways have been identified that ensure correct migration of the HSN neurons from the tail to the vulva. To determine whether *mig-32* acts within one of these pathways I constructed double mutants between *mig-32* and other genes that regulate HSN migration including *mig-1*, a Wnt receptor and *Frizzled* homolog (Pan et al., 2006), *mig-10*, a cytoplasmic protein that mediates attractive and repulsive guidance signals by *unc-6*/Netrin and *slt-1* (Chang et al., 2006; Quinn et al., 2006) respectively, and *slt-1* (Hao et al., 2001). *mig-10* and *mig-1* are involved in antero-posterior (A-P) migration and process extension of HSN neurons. In each case, the double mutants with *mig-32* had significantly enhanced defects in HSN migration assayed with the $P_{nlp\text{-}1}$*gfp* reporter (Figures 2-9A). *slt-1* was reported to be required for dorso-ventral (D-V) guidance of AVM axons that have a similar anatomy to HSN axons (Hao et al., 2001). Single *slt-1* mutants look grossly normal for both A-P and D-V migration and axon guidance of HSNs. However, the *mig-32; slt-1* double mutant has increased D-V axon guidance defects in 30 percent of the HSNs tested compared to less than 10 percent in single mutants (data not shown). Antero-posterior migration and axon guidance of HSNs are similar in *mig-32; slt-1* and single *mig-32* mutants, suggesting that *slt-1* does not have a role in A-P migration and axon guidance. I could not generate homozygous double mutants of *mig-32* and *unc-6/NETRIN* or *unc-40/DCC*, suggesting that they also function

in parallel pathways, at least for viability (data not shown). In summary, *mig-32* acts genetically parallel these pathways to promote HSN migration and axon guidance.

A

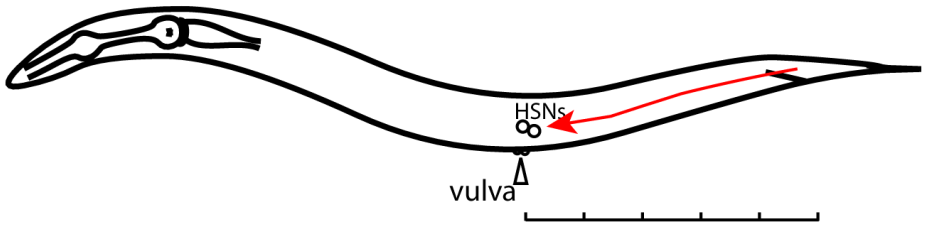

Genotype	Percent of HSN axons defective	Percent of HSNs at these positions					n
wild type	0		100				50
mig-32(n4275)	56		59	18	6	4	12	49
mig-32(tm1684)	46		59	31	4	6		46
mig-32(tm1807)	56		51	21	10	8	10	88
spat-3(gk22)	31		64	15	9	4	8	75
spat-3(RNAi)	26		84	6	7	2	1	150
mig-1(e1787)	63		50	38	8	4		50
mig-1(1787); mig-32(n4275)	66		16	30	22	14	18	50
mig-10(ct41)	38		10	42	26	14	8	50
mig-10(ct41); mig-32(n4275)	82		2	9	16	29	44	45
slt-1(eh15)	2	9	90	1				92
mig-32(n4275); slt-1(eh15)	46	2	54	27	6	8	2	99

B

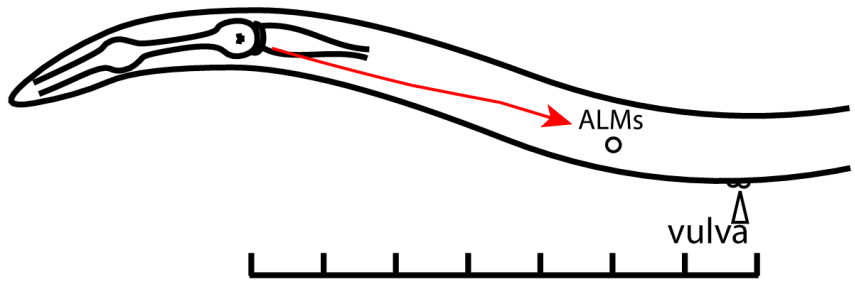

Genotype	Percent of ALMs at these positions						n
wild type				2	48	50	50
mig-32(n4275)	3	5	2	12	71	10	150

Figure 2-9: *mig-32* acts in parallel to most known pathways that regulate HSN migration. (A) Schematic diagram and graph depicting the migration path and final positions of the HSN neurons in otherwise wild-type and *mig-32* mutant transgenic animals. The migration path of the HSNs during embryogenesis from the tail to a position adjacent to the future vulva in the midbody is shown with a red arrow. All animals were transgenic for the $P_{nlp\text{-}1}$*gfp* reporter, which is expressed in the HSNs (Li et al., 1999). The final positions of the HSNs in adults were measured as a fraction of the expected migration from the tail (see Materials and Methods).
The shaded boxes indicate the percentage of animals with HSNs in specific regions, with the percentage shown in the box. For example, in *mig-32* mutants 59percent of animals have HSNs at the normal position, with the remaining animals having a distribution of HSNs between the posterior and vulva. The percentage of HSN axons that failed to reach the head is shown. n, number of HSNs assayed. (B) Schematic diagram and graph depicting the migration path and final positions of the ALM neurons in otherwise wild type and *mig-32* mutant transgenic animals. The migration path of the ALMs from the head to a position anterior to the vulva is shown with a red arrow. All animals were transgenic for the $P_{mec\text{-}7}$*gfp* reporter, which is expressed in the ALMs (Hamelin et al., 1992). The final positions of the ALMs in adults were measured as a fraction of the expected migration from the tail (see Materials and Methods). The shaded boxes indicate the percentage of animals with ALMs in specific regions, with the percentage shown in the box. n, number of ALMs.

CHAPTER 3

Mechanisms of *mig-32* function

3.1 Introduction

Genetic and biochemical experiments in chapter 2 revealed that *mig-32* might be a component of a PRC1-like complex in *C. elegans.* To understand better how *mig-32* functions, I sought interacting partners and genetic interactions with antagonistic pathways such as *Trithorax*. To find interacting partners I followed two approaches. In the first approach I used genetic and biochemical experiments to test if some *C. elegans* genes that are similar to fly and vertebrate PRC1 components might be involved in the PRC1-like complex in *C. elegans*. This approach identified the RING domain protein SPAT-3A as a homolog of RING1B. RING1B is the E3 ligase that directly catalyzes H2A ubiquitlylation in the PRC1 core complex, which also includes BMI-1. Our data suggest that MIG-32 and SPAT-3A are core components of a PRC1-like complex.

3.2. Results

3.2.1. SPAT-3A has a RING domain similar to that of RING1A/B E3 Ligase

RING1A and RING1B are the catalytic components of PRC1 complex that ubquitylates H2AK119. Using the BLAST algorithm to search for RING1B homologs, the best candidate in *C. elegans* is SPAT-3A, as shown in Figure 2-2C. SPAT-3A is the larger protein encoded by the *spat-3* gene, which has two alternative promoters (Figure 2-3C). Amino acids 162-228 of the *spat-3a* gene encode a RING domain very weakly similar to that of RING1A/B. The remainder of SPAT-3A has no obvious similarities to other proteins. SPAT-3 was initially identified as a suppressor of *par-2* embryonic lethal mutations, although the mechanism of suppression is unkonwn (Labbe et al., 2006). I hypothesized that SPAT-3A might be the E3 ligase component of the PRC1-like complex in *C .elegans,* and might act together with MIG-32.

3.2.2. *spat-3* is required for ubiquitylation of H2AK119 in *C. elegans*

Partial cDNA data together with gene prediction tools suggest that the *spat-3* gene encodes two proteins using alternative promoters. The SPAT-3A protein is encoded by 19 exons and is predicted to have 2,471 amino acid residues (Wormbase). Currently there is one mutant allele of *spat-3* available, and it is a 2318 base pair deletion that affects both SPAT-3A and SPAT-3B. If transcribed and translated, the *spat-3(gk22)* could result in a truncated protein composed of the first 1,619 amino acids of the wild type protein

and 58 nonsense amino acids followed by an opal termination codon. The RING domain, which is at the extreme N-terminus of the protein, is not affected by the deletion. Because *gk22* does not affect most of the protein it might be a partial loss of function allele. To determine whether the phenotype of *spat-3(gk22)* mutants is due to loss of SPAT-3A function, as predicted if SPAT-3A and MIG-32 act as part of a PRC1-like complex, I generated an RNAi clone targeting the RING domain of SPAT-3A as shown in Figure 2-3C.

To test the idea that SPAT-3A might be the E3 Ligase component of a PRC1-like complex in *C. elegans*, I analyzed histone modification using western blots of acid-extracted histones from wild-type and *spat-3* mutant *C. elegans*. Similar to *mig-32(n4275)* mutants, *spat-3(gk22)* mutants had reduced ubiquitylation of Histone H2AK119 (Figure 2-4). An anti-H2A western blot showed that ubiquityl-H2AK119 is not completely lost in *spat-3(gk22)* mutants, but greatly reduced. These data are consistent with *spat-3(gk22)* being a partial loss of function allele.

3.2.3. *spat-3* mutants have defects in migration and process extension of specific neurons similar to *mig-32* mutants.

If SPAT-3A is a part of a PRC1-like complex with MIG-32, I would expect to see very similar defects in *spat-3* and *mig-32* mutant worms. I analyzed HSN neurons of hermaphrodites and Ray 1 of male tails in *spat-3* mutants. I used the $P_{nlp\text{-}1}gfp$ reporter to

analyze HSN neurons, as I did for *mig-32* mutants. In *spat-3* mutants 36 percent of the HSNs were retarded compared to 0 percent in wild type and 44 percent in *mig-32* mutant worms. In addition, process extension of 31 percent of the HSNs was defective in *spat-3* mutants compared to 0 percent in wild type and 56 percent in *mig-32* mutant worms (Figure 2-9A). Like *mig-32* mutants, the male tails of *spat-3* mutants are also defective in the position of Ray 1. *spat-3* mutants have 57 ± 6 percent of Ray 1s anterior compared to 64 ± 5 percent in *mig-32* mutant worms and 5 ± 3 percent in wild type (Figure 2-6B). Knock down of *spat-3* using RNAi phenocopied the HSN and Ray 1 defects (Figures 2-6B and 2-9A). Together with the abnormalities in HSN migration, these data greatly strengthen the idea that MIG-32 and SPAT-3 function in a PRC1-like complex in *C. elegans*.

3.2.4. *cec-1*, which encodes a chromodomain, and *lin-61*, which encodes a MBT repeat protein, are not required for ubiquitylation of H2AK119 in *C. elegans*

Similar to the strategy I used for *spat-3*, I picked the best hits for PRC1 components of flies in a BLAST search in the *C. elegans* genome. The *cec-1* gene encodes a protein with a chromodomain that is similar to the one in fly Pc protein (Agostoni et al., 1996), and *lin-61* gene encodes a protein with MBT repeats that are similar to fly SCM (Harrison et al., 2007). I tested if *lin-61* and *cec-1* are required for ubiquitylation of H2A in *C. elegans* by western blots of histone extracts from

lin-61(n3809) and *cec-1(ok1005)* mutant worms. Anti-Ubiquitin and anti-H2A blots showed that loss of neither *lin-61* nor *cec-1* affected the ubiquitylation of H2AK119 (Figure 3-1).

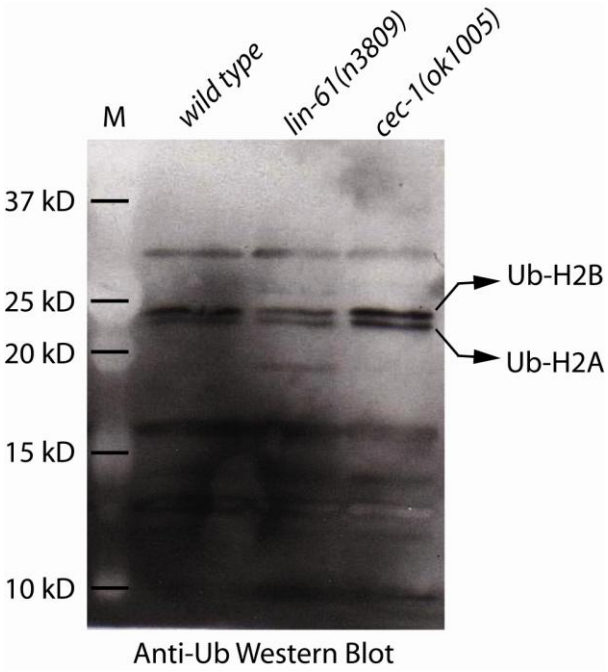

Figure 3-1: *lin-61* and *cec-1* are not required for ubiquitylation of H2A. Western blot analysis of acid-extracted histones from wild-type, *lin-61*, and *cec-1* mutant *C. elegans*. The filter was probed with anti-ubiquitin antibody. Arrows indicate ubiquitylated H2A and H2B.

3.2.5. Interaction of *mig-32* with Trithorax gene *lin-59*

Polycomb and Trithorax genes antagonize each other in regulation of target genes including *Hox* genes (Klymenko and Muller, 2004; Poux et al., 2002). Trithorax genes maintain an activated state of gene expression, in contrast to Polycomb genes, which maintain a repressed state. The interaction between Trithorax and Polycomb proteins on target genes is not necessarily mutually exclusive, suggesting that they might bind a

target gene together, but that the final outcome is dependent on the presence of other factors that cooperate with Polycomb or Trithorax proteins. The main components of the Trithorax complex in flies and human are Trithorax (TRX) and Mixed Lineage Leukemia (MLL) respectively. TRX and MLL have SET domains, the catalytic domain that has methyltransferase activity, and they specifically methylate histone H3 Lysine 4 (H3K4). This mark is associated with activated transcriptional states of genes.

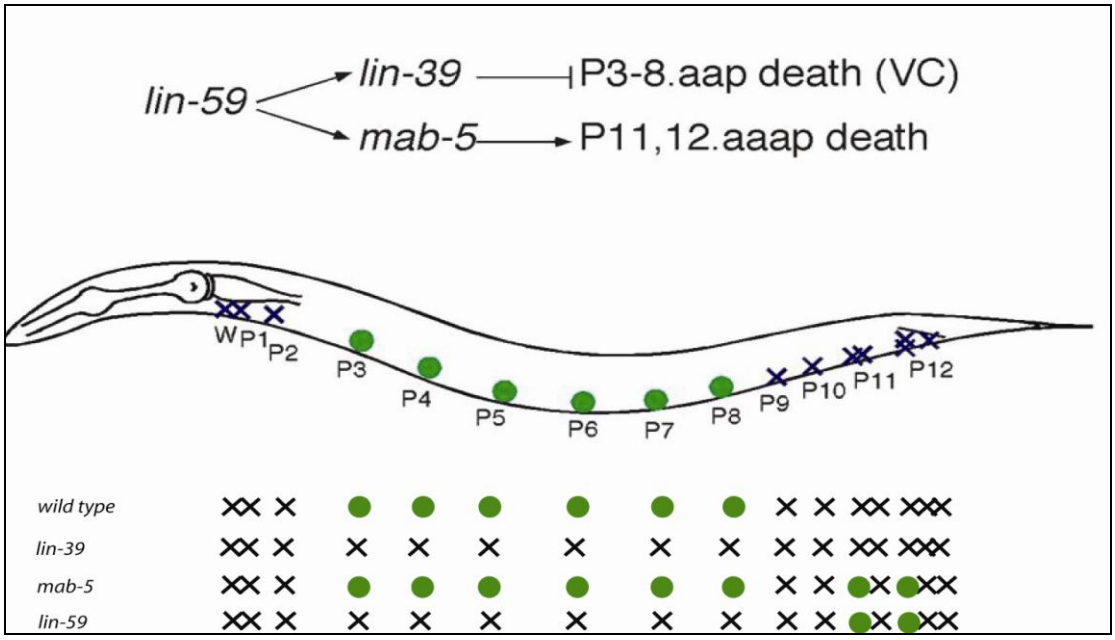

Figure 3-2: The *lin-59* gene regulates cell death in the VNC.
Schematic representation of VC neurons (green spots) and their anterior and posterior lineal equivalents in the VNC is shown. In wild type worms, P3-P8.aap cells survive and generate VC neurons. Anterior and posterior lineal equivalents of VC neurons die of programmed cell death (W, P1, P2, P9-P12.aap cells) as marked by crosses. In the posterior VNC, there are three extra cell deaths in the P11 and P12 lineages. *In lin-39* mutants, VC neurons die of ectopic *egl-1* expression. In *mab-5* mutants, P11.aaap and P12.aaap cells survive because of loss of *egl-1* expression. In *lin-59* mutants, VC cells die and P11.aaap and P12.aaap cells survive, combining defects of *lin-39* and *mab-5*, respectively.

The *lin-59* gene encodes a SET domain protein that is similar to ASH1, which is a component of the Trithorax complex in flies and human. *lin-59* null mutants are larval lethal, and weak mutants have defects associated with *Hox* gene downregulation (Chamberlin and Thomas, 2000). More specifically, the survival of VC motor neurons, and the death of some posterior cells are dependent on *lin-59*. VC neurons are the Pn.aap daughters of postembryonic P blast cells from P3 to P8 in the mid-ventral nerve cord (VNC). Anterior and posterior lineal equivalents of VC neurons die of programmed cell death (Figure 3-2). In *lin-59* partial loss-of-function mutants, VC neurons die. This effect of *lin-59* on VC neurons was shown to be through maintaining transcription of the *Hox* gene *lin-39* (Potts et al., 2008).

3.2.6. *mig-32* mutation does not suppress cell death defects of *lin-59* mutants.

I hypothesized that if MIG-32 functions in a PRC1-like complex, mutations of *mig-32* might suppress defects in *lin-59* mutants. To test this idea I generated double mutants of *mig-32* and partial loss of function mutations of *lin-59*. To analyze the cell death defects I used a *ced-1(n1735)* mutant background. *ced-1* is a gene required for engulfment of cell corpses by neighbor cells as a final step of programmed cell death. *ced-1* mutations allow us to see dead cell corpses as they are not engulfed and have a button-like appearance under DIC optics as seen in Figure 3-3. Using the *ced-1(n1735)* background I analyzed cell death defects in VNC. Table 3-1 shows the number of corpses in the VNC of late L2

animals in single and double mutants of *mig-32* and *lin-59*. Table 3-1 shows that the number of extra cell corpses in the midbody of *lin-59 and mig-32* double mutants is decreased compared to *lin-59* single mutants. Interestingly, in contrast to antagonism in the midbody, *mig-32* and *lin-59* synergize to decrease corpse number in the posterior VNC. However, the morphology of the corpses in the double mutants was not normal, that it was hard to distinguish and score the number of corpses (data not shown). These data suggest two possible explanations. First, *lin-39* and *mig-32* could antagonize each other to regulate death/survival of the VC neurons. Alternatively, *mig-32* might be involved in corpse engulfment or another pathway that interferes with the corpse visibility. To distinguish these two possibilities I did two tests.

First I tested if expression of a gfp reporter for the cell death gene *egl-1* is abnormal in *mig-32* mutants. *egl-1* is the key activator of all programmed cell death that occurs in somatic cells of *C. elegans.* Expression of *egl-1* determines if a cell is going to die or survive (Conradt and Horvitz, 1998). A gfp reporter generated in our lab, driven by the *egl-1* promoter, allows us to see all cells destined to die, so long as their death is prevented, for example through a mutation in a gene essential for cell death such as *ced-4*. To distinguish if the effect of *mig-32* mutations in the *ced-1* background was through the cell death pathway or something else that affects corpse appearance, I generated *ced-4(n1162)*; *mig-32(n4275)* double mutants carrying a $P_{egl\text{-}1}gfp$ reporter and asked if the number of cells activating the $P_{egl\text{-}1}gfp$ reporter in the posterior VNC is any different from the *ced-4(n1162)* background. Double mutants looked like single

ced-4(n1162) mutants, suggesting that in *mig-32* mutants the cell death pathway is activated normally in the posterior VNC (data not shown).

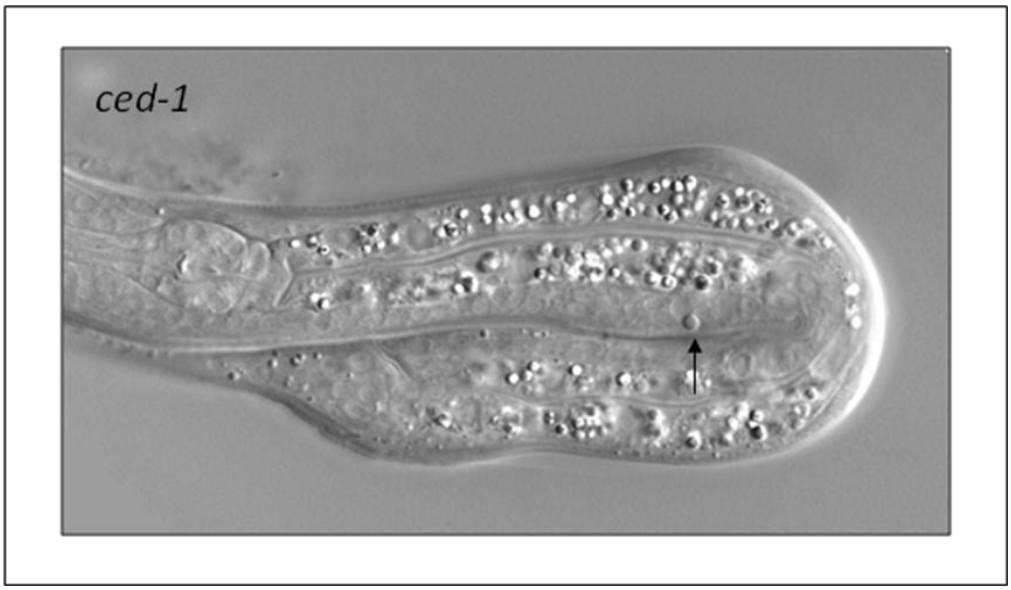

Figure 3-3: *ced-1(n1735)* mutant worms maintain cell corpses longer before they are engulfed by neighbor cells.
An L2 *ced-1* mutant worm displays a cell corpse in the ventral nerve cord as shown by an arrow.

Genotype	Number of corpses		
	Anterior	Midbody	Posterior
+	2.5 ± 0.1	0.0 ± 0.0	6.2 ± 0.2
lin-59(n3168)	2.9 ± 0.1	1.7 ± 0.2	4.4 ± 0.1
lin-59(n3192)	2.5 ± 0.1	1.4 ± 0.2	4.4 ± 0.2
lin-59(RNAi)	2.6 ± 0.1	2.8 ± 0.2	3.4 ± 0.3
mig-32(n4275)	1.5 ± 0.1	0.0 ± 0.0	4.3 ± 0.2
lin-59(n3168); mig-32(n4275)	2.3 ± 0.1	0.1 ± 0.0	3.5 ± 0.2
lin-59(n3192); mig-32(n4275)	1.7 ± 0.1	0.2 ± 0.1	3.4 ± 0.2
lin-39(n1760); mig-32(n4275)	2.2 ± 0.1	3.7 ± 0.2	5.2 ± 0.2
lin-39(n1760)	2.9 ± 0.1	4.2 ± 0.1	5.7 ± 0.1

Table 3-1: *mig-32* mutation decreases number of cell corpses in *lin-59* mutants

As a second approach to distinguish if *mig-32* is involved in the cell death pathway, I used the $P_{lin\text{-}11}gfp$ reporter to analyze the interaction between *mig-32* and *lin-59*. $P_{lin\text{-}11}gfp$ is expressed in six VC neurons (Cameron et al., 2002). In wild type worms there are six green cells in mid-VNC. In *lin-59(n3168)* weak mutants, the number of gfp-expressing cells is decreased due to ectopic cell death in VC neurons. In *lin-59(n3168); mig-32(n4275)* double mutants, the number of gfp-expressing cells is similar to *lin-59(n3168*) single mutants, indicating that the *mig-32* mutation cannot suppress *lin-59* defects in a $P_{lin\text{-}11}gfp$ reporter background (data not shown).

In conclusion, *mig-32* may not antagonize *lin-59* to regulate death/survival of VNC neurons but instead might be involved in a process that interferes with corpse visibility. This argument is also supported by another experiment we did to rescue the

null *lin-59(n3425)* allele with the *mig-32(n4275)* mutation, in which *mig-32(n4275)* mutation did not suppress lethality of *lin-59(n3425)* mutation in double mutants.

3.2.7. *mig-32* does not repress posterior *Hox* genes *egl-5* and *mab-5*

The classical description of a *Polycomb* gene involves repression of *Hox* genes during development (Lewis, 1978). There are six *Hox* genes in *C. elegans*. These are *ceh-13, lin-39, mab-5, egl-5, nob-1, nob-2* in order of expression domains anterior to posterior. *mab-5* and *egl-5* are expressed in the posterior part of the body (Costa et al., 1988; Ferreira et al., 1999). It was reported before that three *C. elegans*-specific Polycomb-like genes, *sop-2, sor-1,* and *sor-3,* were required to restrict expression of these two *Hox* genes to posterior regions. In *sop-2, sor-1,* and *sor-3* mutants expression domains *of egl-5* and *mab-5* transcriptional gfp reporters were expanded to far anterior regions of the body (Wang et al., 2004a; Yang et al., 2007; Zhang et al., 2003; Zhang et al., 2004). *sop-2, sor-1,* and *sor-3* mutants also displayed anterior-to-posterior transformations in cell fates, a typical defect seen in Polycomb mutants in flies and vertebrates as a result of ectopic expression of certain *Hox* genes. I thought that as a Polycomb gene *mig-32* might repress the expression of certain hox genes. I analyzed the expression patterns of $P_{egl\text{-}5}$*gfp* and $P_{mab\text{-}5}$*gfp* reporters in *mig-32* mutants compared to wild type worms. I could not see any global expansion in expression domains of either reporter in *mig-32* mutants.

In addition, to test if there are any anterior-to-posterior transformations in *mig-32* mutants I used $P_{pkd\text{-}2}$*gfp* reporter, which marks RnB type neurons of male tail rays. Each

ray is composed of two neurons (RnA, RnB), and a structural cell, which are descendants of postembryonic blast cells V5, V6, and T. *mab-5* and *egl-5* expression is required for normal fates of these cells in the sensory rays (Chow and Emmons, 1994). V1-V4 lineages, on the other hand, generate bilateral seam cells. $P_{pkd\text{-}2}$*gfp* is only expressed in sensory rays but not in V1-V4 seam cells (Barr and Sternberg, 1999). Expansion of *egl-5* and *mab-5* expression domains to V1-V4 seam cells transforms them to sensory ray cells, and they start to express $P_{pkd\text{-}2}$*gfp*. I tested if *mig-32* mutants display anterior expansion of the *pkd-2* expression domain, an indication of transformation of seam cells into sensory rays. I observed that there is not any difference between *mig-32* and wild type worms. This suggests that the fates of the anterior seam cells are normal.

As another test for a role of *mig-32* in regulating *Hox* genes in the male tail, I generated double mutants of *mig-32* and *pal-l*. *pal-1* is the worm homolog of Caudal, and it is required for the expression of *Hox* genes *egl-5* and *mab-5* in V5 and V6 lineages and thus for the normal fates of the sensory rays 1-6 (Ferreira et al., 1999; Hunter et al., 1999; Waring and Kenyon, 1991). *pal-1* null mutants do not have the corresponding ray structures as a result of posterior-to-anterior transformation due to loss of *egl-5* and *mab-5* expression. I thought if *mig-32* is a repressor of *mab-5* and *egl-5*, *mig-32* mutation should suppress *pal-1* defects in the male tail. To test this idea, I compared the male tails of *pal-1(e2091); mig-32(n4275)* doubles to *pal-1(e2091)* singles and saw no significant difference (data not shown). Together with the *mab-5* and *egl-5* reporters these data

suggest that *mig-32* does not regulate the expression of posterior *Hox* genes *mab-5* and *egl-5* or it is redundant with other factors.

3.2.8. Interaction of *mig-32* with Synthetic Multi-Vulva (SynMuv) genes

Development of the vulva is one of the processes that has been studied extensively in *C. elegans*. It is composed of 22 cells generated through a four-stage process induced by an intricate pattern of signaling pathways. In the first stage six vulval precursor cells (VPC) are generated from posterior daughters of the P3-P8 blast cells (Pn.p). These six cells retain their VPC identity and do not fuse with hyp7, a large syncytium that comprises most of the hypodermis of the worm. This retention is accomplished by the *Hox* gene *lin-39*, which represses genes involved in membrane fusion. In the second stage VPC5, VPC6, and VPC7 are formally committed to vulval cell fate by the action of an EGF-like ligand LIN-3 (Hill and Sternberg, 1992). In the third stage, depending on the strength of the LIN-3 signal, VPC6 adopts a so-called 1° cell fate and VPC5 and VPC7 adopt 2° cell fates. An intricate pattern of interactions of at least three pathways, Ras–MAPK, Notch, and Wnt, maintains this pattern of fates and leads to generation of a total of 22 cells (Felix, 2005; Sternberg, 2005; Sundaram, 2005). The final stage involves the morphogenesis of the organ, which is not well understood yet.

Screens in the Horvitz lab for mutants that have defects in vulval development identified two main groups of mutants. The first group of mutations caused too many VPCs induced and the second group had too few, which led to Multi-Vulva (Muv) and

Vulvaless (Vul) phenotypes, respectively. The Muv phenotype is a result of ectopic induction of vulval fate in Pnp cells other than P6p. An interesting subset of the Muv group of genes was identified and called Synthetic Multi-Vulva (SynMuv) genes. The SynMuv phenotype required mutations in two genes instead of one. This requirement for mutations in two genes means that the phenotype in the double mutants is "synthetic" and needs a genetic synergy (Fay and Yochem, 2007). SynMuv genes are classified into 3 classes, Class A, Class B, and Class C. Single or double mutants of any two genes in the same class do not have a Muv phenotype, but combinations of mutations from two different class have the Muv phenotype (Figure 3-4). SynMuv genes are listed in Table 7. Class B genes are mostly involved in pRb-like pathway in *C. elegans*, which represses the Ras-MAPK pathway. Retiniblastoma protein (pRb) and it relatives are negative regulators of cell proliferation in mammals. Their activity is regulated by cyclin dependent kinases during cell cycle progression. pRb forms complexes with E2F transcription factors to inhibit E2F-dependent transcriptional activity and progression of cell cycle (Fay and Yochem, 2007; Frolov and Dyson, 2004; Harbour and Dean, 2000; Korenjak et al., 2004).

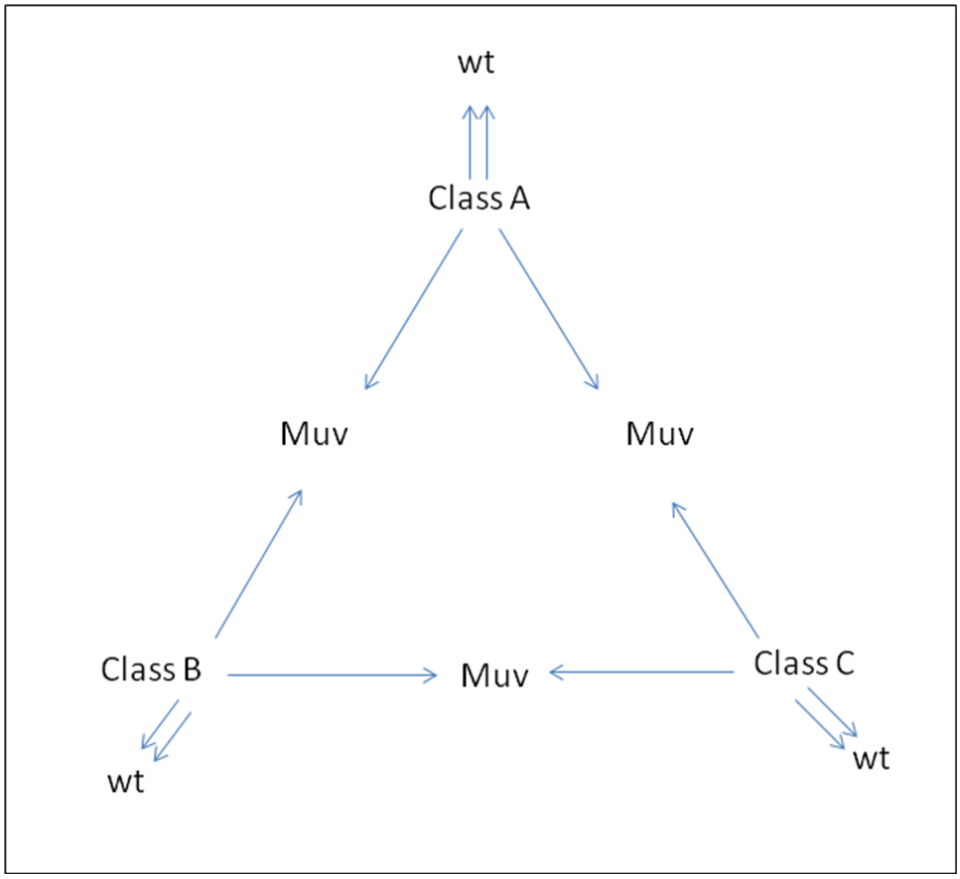

Figure 3-4: Interaction between SynMuv gene classes.
There are three classes of SynMuv genes. Single or a double mutants of genes in one class have wild type phenotype. However, combinations of double mutants from different classes synergize and generate the SynMuv phenotype.

Gene	Description
Class A	
lin-8	Novel
lin-15a	Novel
lin-38	Novel
lin-56	Novel
smo-1	SUMO, ubiquitin-related peptide
uba-2	E1B, SUMO activating enzyme
Class B	
dpl-1	DP family of transcription factors
efl-1	E2F family of transcription factors
gei-4	Coiled-coil and Q/N-rich domains
hda-1	HDAC
hpl-2	Heterochromatin protein 1 (HP1), CHROMO domain
let-418	Mi-2/CHD3, DNA helicase
lin-9	Novel
lin-13	C2H2 zinc finger, LXCXE motif
lin15b	Novel
lin-35	Similar to human pRb, p107, p130
lin-36	Novel
lin-37	Novel
lin-52	Novel
lin-53	Similar to human Rb associated protein 48, RbAP48
lin-54	Cysteine-rich,
lin-61	MBT repeats, similar to human L(3)MBT
lin-65	Novel
mep-1	C2H2 zinc finger and Q/N-rich domains
met-2	Predicted histone H3 lysine-9 methyltransferase
tam-1	RING finger and B-box domains
tra-4	C2H2 zinc finger domains
ubc-9	E2, SUMO conjugating enzyme
E01A2.4	Similar to human NFκB activating protein
W01G7.3	Similar to human RNA polymerase II subunit J
Class C	
epc-1	Similar to enhancer or Polycomb-like, HAT-associated
mys-1	MYST Histone acetyltransferase, CHROMO domain
ssl-1	SWI/SNF ATPase homolog
trr-1	Similar to mammalian TRRAP, HAT-associated

Table 3-2: SynMuv genes

3.2.9. *mig-32* modifies *lin-15(n765ts)* allele at permissive temperature

Our interest in SynMuv genes started when I tried to generate a double mutant of *mig-32* with *lin-15(n765ts)* allele as a co-injection marker. The *lin-15(n765ts)* allele is a special one that has a normal phenotype at 15ºC, but a Muv phenotype at elevated temperatures over 20ºC. Analysis of the *lin-15* locus identified two genes expressed from an operon; *lin-15a* and *lin-15b. lin-15a* and *lin-15b* are SynMuv genes in classes A and B, respectively. The vulva of *lin-15(n765ts)* is morphologically normal when mutants are raised at 15ºC but is Muv when they are raised at 22.5ºC.

Interestingly, double mutants of *mig-32(n4275); lin-15(n765ts)* had a Muv phenotype at permissive temperature (15ºC). *mig-32* RNAi on *lin-15(n765ts)* worms phenocopied the double mutants (Figure 3-5). These results suggested that *mig-32* might be a SynMuv gene.

3.2.12. *mig-32* is not a Syn-Muv gene but it modifies the *lin-15(ts)* allele at 15ºC

To test the idea that *mig-32* might be a Syn-Muv gene I generated double mutants of *mig-32* with some of the Class A and Class B SynMuv genes. However none of the double mutants displayed the SynMuv phenotype at either 20ºC or 25ºC (data not shown). The genes tested include the Class A genes, *lin15A,* and *lin-8*, and the Class B genes, *lin-9*, *lin-35, dpl-1*, *lin-15b*, *lin-53*, *lin-61*, and *tam-1*. These data suggest that *mig-32* might not be a classical SynMuv gene, but rather that it modifies the *lin-15* gene

function at permissive temperature. In addition, it indicates that *mig-32* is involved in vulval development.

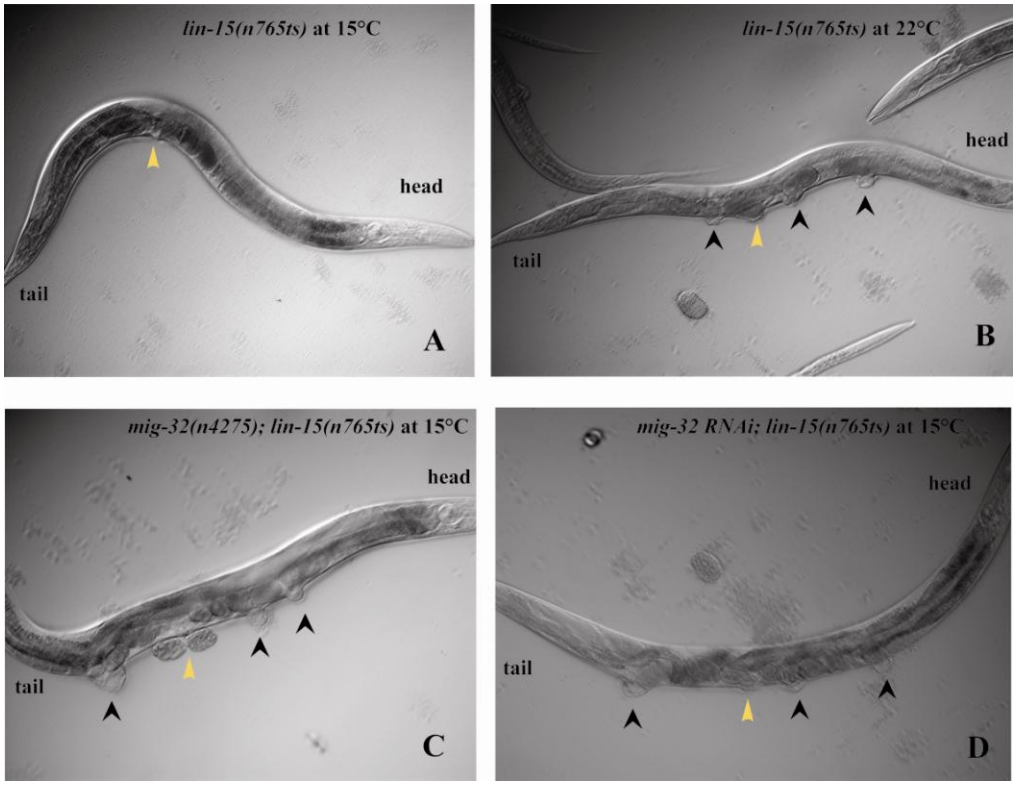

Figure 3-5: Genetic interaction between *mig-32* and *lin-15.*
(A) *lin-15(n765ts)* mutants have normal vulval development at 15ºC. (B) *lin-15(n765ts)* mutants have multiple vulvae (Muv) at 22ºC. (C) *mig-32(n4275); lin-15(n765ts)* double mutants are Muv at 15ºC. (D) *mig-32* RNAi on *lin-15(n765ts)* worms phenocopies double mutants at 15ºC. Yellow arrowheads mark the normal vulva position.

3.2.13. An RNAi screen to find interacting partners of MIG-32

I thought that the modifier effect of *mig-32* on *lin-15(n765ts)* worms at permissive temperature might provide an efficient assay to screen for possible partners of MIG-32 using RNAi. Using a candidate gene approach I generated a list of *C. elegans* genes that are homologs of vertebrate and fly genes that encode proteins identified to be involved in:

1) Repressive complexes,
2) Interactions with vertebrate and fly PRC1 RING proteins
3) Chromatin modification

The list of the genes tested is in Table 3-3. I fed the *lin-15(n765ts)* worms at 15ºC with bacteria expressiong RNAi for each gene and analyzed if any RNAi caused a Muv phenotype similar to *mig-32* RNAi. I repeated the experiments three times. In these trials some genes behaved inconsistently and some consistently. Three of the genes tested caused a Muv phenotype in all three trials with a penetrance higher than 50 percent. These genes are *lin-61, hpl-2,* and *utx-1*. *lin-61* is a SynMuv Class B gene that encodes a protein with MBT repeats that are similar to fly PRC1 component SCM (Harrison et al., 2007). *hpl-2* is another SynMuv Class B gene and a homolog of a fly heterochromatin protein (Coustham et al., 2006; Couteau et al., 2002). *utx-1* encodes a histone demethylase specific to H3K27 (Agger et al., 2007). A fourth gene that I did not test in our screen is also a good candidate as an interacting partner of *mig-32, rbr-2*. *rbr-2* encodes another histone demethylase specific for H3K4 (Christensen et al., 2007). *rbr-2* RNAi was shown to enhance *lin-15(n765ts)* phenotype at permissive temperature

(Christensen et al., 2007). A mammalian homolog of RBR-2 was shown to interact with RING6A protein which is one of the homologs of MIG-32 in mammals (Lee et al., 2007).

Currently I have cloned cDNAs for *lin-61, hpl-2, utx-1 and rbr-2* in mammalian expression vectors but have not conducted further experiments.

			Experiment 1		Experiment 2		Experiment 3	
Mam/D.m.	**Protein Domain**	**CE Genes**	**percent Muv**	**n**	**percent Muv**	**n**	**percent Muv**	**n**
Titin	Fibronectin	*unc-22*	**19**	**82**	**6**	**255**	4	**100**
BMI-1	RING	*mig-32*	70	132	75	88	74	100
E(Z)	SET	*mes-2*	9	56	1	100	N/D	N/D
		mes-3	16	68	0	170	N/D	N/D
EED	SAM	*mes-6*	11	53	8	107	N/D	N/D
SMRTER		*gei-8*	14	65	0	81	N/D	N/D
dTAFII250		*taf-1*	32	55	0	23	N/D	N/D
dMi-2	PHD, Chromo	*chd-3*	49	79	29	115	37	100
SWI2		*C52B9.8*	26	79	48	133	23	100
dSin3A		*sin-3*	43	95	3	67	N/D	N/D
dSbf1(+PH-d)		*mtm-5*	61	77	16	113	N/D	N/D
dTAFII110		*taf-4*	58	55	N/D	N/D	N/D	N/D
SCM/dTAFII85	MBT	*lin-61*	90	70	100	114	99	100
CtBP1 & 2		*ctbp-1*	35	57	10	134	N/D	N/D
PC	Chromo	*hpl-2*	56	85	90	111	65	100
PC	Chromo	*cec-1*	35	65	18	122	N/D	N/D
dTAFII62		*taf-6.1*	19	53	25	194	N/D	N/D
REPTIN		*ruvb-1*	34	59	79	52	N/D	N/D
DTAFII30		*taf-11.1*	15	52	7	127	N/D	N/D
DTAFII30		*taf-11.2*	34	100	27	117	14	50
YAF2	Zn-finger	*tag-294*	30	60	13	115	N/D	N/D
Wdr5	WD40	*tag-125*	0	67	N/D	N/D	N/D	N/D
Wdr5	WD40	*K04G11.4*	48	102	35	92	N/D	N/D
JHDM1D	JmJC	*F29B9.2*	32	102	7	89	6	50
JHDM1D	JmJC	*F43G6.6*	27	76	N/D	N/D	8	50
FBXL10	JmJC	*T26A5.5*	20	78	N/D	N/D	4	50
Ankyrin-1	ankyrin	*B0350.2*	42	80	27	125	24	50
WHSC1		*mes-4*	8	60	1	82	N/D	N/D
TINMAN/Nkx2-5	homeobox	*ceh-22*	59	83	45	110	38	50
HP	Chromo	*hpl-1*	56	91	46	126	30	50
PKNOX1		*psa-3*	26	75	52	136	N/D	N/D
UTX-1	JmJC	*utx-1*	N/D	N/D	N/D	N/D	86	50
JDCP5	JmJC	*C06H2.3*	N/D	N/D	N/D	N/D	2	50
JMJD3	JmJC	*C29F7.6*	N/D	N/D	N/D	N/D	14	50
JMJD3	JmJC	*F23D12.5*	N/D	N/D	N/D	N/D	22	50
JMJD6	JmJC	*psr-1*	N/D	N/D	N/D	N/D	6	50
JMJD3	JmJC	*tag-279*	N/D	N/D	N/D	N/D	6	50
ARID4A	ARID	*Y108G3AL.7*	N/D	N/D	N/D	N/D	4	50
ARID3A	ARID	*cfi-1*	N/D	N/D	N/D	N/D	0	50

Table 3-3: RNAi screen for enhancers of *lin-15(n765ts)* at permissive temperature

CHAPTER 4

Discussion and conclusions

4.1 Discussion

In these chapters I report the consequences for *C. elegans* of loss of MIG-32, a protein most similar to BMI-1 and related proteins that are components of PRC1 and related Polycomb repression complexes. *mig-32* is broadly expressed in the germline and in somatic cells. *mig-32* mutants have defects in the anatomy of their nervous system, and *mig-32* mutations markedly enhance the phenotype of many mutants with defects in the nervous system. These observations suggest that *mig-32* participates in many processes and that some of these processes occur normally in *mig-32* mutants because of redundancy with other factors. Five of the six vertebrate homologs of MIG-32 have been identified in PRC1 related complexes, and *mig-32* mutants are defective in ubiquitylation of H2A, the defined biochemical function of PRC1. I therefore propose that MIG-32 is a component of a PRC1-like complex in *C. elegans.*

4.1.1. The relationship of MIG-32 to PcG complexes of *C. elegans*

There are at least two complexes in *C. elegans* that are functionally related to the *Drosophila* and mammalian Polycomb repression complexes. The MES-2/MES-3/MES-6 complex includes MES-2 and MES-6, which share sequence similarity and biochemical

function with their mammalian and *Drosophila* homologs, and MES-3, a novel protein (Xu et al., 2001a). Strong genetic and biochemical evidence indicate that this complex is functionally analogous to the PRC2 complex, which places the histone H3K27me3 mark characteristic of Polycomb repression (Bender et al., 2004; Fong et al., 2002; Holdeman et al., 1998; Xu et al., 2001a). *mes* mutants are sterile, likely as a consequence of inappropriate expression of genes normally silenced in the developing germ cells. If *mig-32* was part of a PRC1-like complex that recognizes the H3K27me3 mark placed by PRC2 to maintain repression, *mig-32* mutants might be expected to share the Mes phenotype of sterility. However, *mig-32* mutants are fertile. *mig-32* could be redundant with another protein or complex responsible for H2A ubiquitylation in the germline, or H2A ubiquitylation could be dispensable for the silencing function that is thought to be the essential role of the *mes* genes in ensuring germline integrity. I suggest that the latter case is more likely, because H2A-ubiquitylation is lost during germline development in wild type worms. More recently the *sop-2, sor-1* and *sor-3* genes have been proposed as components of a distinct Polycomb-like repressive mechanism in *C. elegans*. Mutations affecting these genes result in expanded domains of *Hox* gene expression (Wang et al., 2004a; Yang et al., 2007; Zhang et al., 2003; Zhang et al., 2004). All are essential genes, and mutants carrying partial loss-of-function alleles have severe defects not observed in *mes* null mutants, suggesting that the *sop* and *sor* genes have many important functions in somatic cells and do not simply maintain the pattern of gene expression established by the *mes* genes, which have comparatively subtle functions in somatic cells (Ross and

Zarkower, 2003). The pattern of nuclear fluorescence I observed for a rescuing MIG-32:GFP fusion protein suggests that MIG-32 does not colocalize with the SOP-2 and SOR-1 proteins (Saurin et al., 1998; Yang et al., 2007; Zhang et al., 2006). Given the numerous and severe defects of the *sop* and *sor* mutants and the comparatively limited defects of *mig-32* mutants, *mig-32* is unlikely to be an essential component of a putative SOP/SOR Polycomb-like complex. Instead, I propose that *mig-32* is a component of an as yet undefined complex that is functionally analogous to PRC1. The *C. elegans* genome encodes RING domain proteins that could be functional homologs of Ring1A and Ring1B and that could act as the E3 in a PRC1-like complex, or MIG-32 could serve this function itself. Our analysis of *spat-3* suggests that SPAT-3A interacts with MIG-32 in ubiquitylation of H2A. This idea is supported by our finding showing that the H2A ubiquityl mark is decreased in *spat-3* mutants. The mechanism through which MIG-32 promotes H2A ubiquitylation is still unclear at present and will require further study.

4.1.2. The roles of Polycomb complexes in nervous system development

The *mig-32* homolog BMI-1 has been intensively studied following its isolation as a target gene upregulated by proviral integration in Eμ-myc-driven lymphomas in mice (Haupt et al., 1991; van Lohuizen et al., 1991). In the mammalian nervous system BMI-1 is required for the self-renewal of neural stem cells (Molofsky et al., 2005; Molofsky et al., 2003), and epigenetic regulation of the cell cycle is a critical function of BMI-1 in the hematopoietic and nervous systems (Jacobs et al., 1999; Molofsky et al., 2005; Molofsky

et al., 2003). I have not noticed abnormalities in cell numbers in *mig-32* mutants that would suggest an essential role in the regulation of the cell cycle, but have not directly examined this possibility.

Expression of additional MIG-32 homologs in the mammalian nervous system has been reported (Gunster et al., 1997; Jacobs et al., 1999; Kim et al., 2005; Leung et al., 2004; Molofsky et al., 2003; Nunes et al., 2001; Schoorlemmer et al., 1997; Shakhova et al., 2005; van der Lugt et al., 1994), but with the exception of BMI-1 little is known about what these genes contribute to nervous system function. Our data suggest that epigenetic regulation of gene expression by the *mig-32* homologs will participate in neuronal migration and process extension, but the precise basis for the defects I observe in *mig-32* mutants is not yet clear. Specifically, does *mig-32* regulate transcription of individual gene targets that are critical regulators of individual cell migrations or process extensions, or does loss of *mig-32* result in a "noisy" pattern of gene expression to which some cells are more sensitive? Recent genomic screens in *Drosophila* and vertebrates have identified targets of Polycomb repression complexes (Boyer et al., 2006; Bracken et al., 2006; Lee et al., 2006; Negre et al., 2006; Schwartz et al., 2006; Tolhuis et al., 2006). Many of these biochemically-defined targets are involved in nervous system patterning, and our data raise the possibility that some of these targets are regulated in a functionally important way in the developing nervous system. Our observation that most cells appear to adopt fates similar to those of wild-type animals as suggested by normal expression of the cell type-specific *gfp* reporters used in this study suggests that *mig-32* is not critical

for establishing cell fates, but instead acts in a subtle manner to refine cellular phenotypes.

4.1.3. Defects in *Hox* gene expression are unlikely to be central for the *mig-32* mutant phenotype

Mutations affecting *Hox* genes result in abnormal neuronal migrations in *C. elegans* (Baum et al., 1999; Chalfie and Sulston, 1981; Chisholm, 1991; Clark et al., 1993; Harris et al., 1996; Kenyon, 1986; Salser and Kenyon, 1992; Wang et al., 1993) and given the classical role of Polycomb family members as repressors of *Hox* gene activity I asked whether abnormal *Hox* gene activity might underlie the defects in the nervous system I observed. However, our data suggest that regulation of *Hox* gene expression by *mig-32* may be subtle. In general, the migration and neuronal process extension defects of *mig-32* mutants have little in common with those observed in gain- or loss-of-function *Hox* mutants. In addition, the expression domains of the $P_{mab\text{-}5}$*gfp*, *Pegl-5gfp Hox* and $P_{pkd\text{-}2}$*gfp* reporters do not appear to be expanded in *mig-32* mutants, and *mig-32* mutations do not suppress *pal-1* mutations, which reduce *Hox* activity (unpublished observations). These data suggest that non-*Hox* targets of *mig-32* are more likely to be responsible for the defects I describe in *mig-32* mutants, and are consistent with the Polycomb targets of *Drosophila* and mammalian cells, the vast majority of which are not *Hox* genes. However, our data do not rule out a role for MIG-32 as a regulator of *Hox* gene activity,

and further work to define the genetic and biochemical properties of *mig-32* in germ line and somatic cells will allow comparison to the Polycomb complexes of other species.

4.2. Conclusions

In this thesis, I provide evidence for the presence of a PRC1-like complex in *C. elegans*. I identified a *C. elegans* gene, *mig-32*, which encodes a RING domain protein that is similar to mammalian PRC1 protein BMI-1. In mammals, BMI-1 is required for the stability and function of RING proteins, RING1A and RING1B. RING1A & B are the catalytic components of the PRC1 complex, which ubiquitylate Histone H2A Lysine 119 (H2AK119). The H2AK119-Ub mark is associated with silencing of target genes. *mig-32* null mutant worms displayed an apparently complete loss of the H2AK119-Ub mark, suggesting that it is required for all ubiquitylation of H2As in *C. elegans*. In addition to *mig-32*, I showed that *spat-3* encodes a RING protein similar to human RING1A & B, which is also involved in ubiquitylation of H2A in *C. elegans*. Mutants of *mig-32* and *spat-3* displayed similar defects in neuronal migration and axon guidance of specific neurons, strengthening the possibility that the protein products of the two genes function in the same protein complex. These data suggest that a PRC1-like complex with RING components is present in *C. elegans* at least from a biochemical perspective, but it is not clear yet how this complex functions. Other components of the complex and the target genes are still to be elucidated. Biochemical roles of each component are another

question to be answered. In addition, the target genes and the mechanism of regulation of these genes are not known.

The specific defects I described in *mig-32* mutants might be grouped into categories. First group involves defects in migration and process extension of specific neurons including HSNs, ray neurons, PVQs, D type motor neurons, ALMs, and PLMs. Double mutants of *mig-32* with genes involved in migration and axon guidance suggested that *mig-32* functions parallel to these genes (Figures 2-7 & 2-9). However it is still possible that some of these genes might be regulated by *mig-32.*

Additional defects are present in vulval development. These defects indicate that *mig-32* action is not restricted to neuronal tissues. Vulval development is a complex process that involves multiple steps of cell fate determination, cell divisions, migrations, and morphogenesis. It is not clear yet at what step is *mig-32* involved. As it causes ectopic vulva induction synergizing with *lin-15, mig-32* might be involved in repression of genes involved in vulval induction, such as *lin-3* and other Ras-pathway genes. The brood size of *mig-32* mutants are two-thirds of wild type worms indicating that *mig-32* might be involved in germline development. However it is also possible that the deletion alleles harbor background mutations that impair fertility.

In *mig-32* mutants many cell-specific reporters are expressed normally, indicating that most of these defects might not be because of a change in cell fates but some other aspects of each process such as migration or morphogenesis. However it is not clear how *mig-32* contributes to these processes. It is possible that *mig-32* regulates transcription of

individual gene targets that are critical regulators of individual cell migrations or process extensions. A second possibility is that loss of *mig-32* might result in a "noisy" pattern of gene expression to which some cells are more sensitive. Discovering the target genes might help us to understand how *mig-32* contributes to cell migration and process extension.

mig-32 does not display defects such as anterior-to-posterior transformations of body pattern similar to those of Polycomb gene mutants in flies and vertebrates. Consistent with this I observed that expression of two *C. elegans Hox* genes *mab-5* and *egl-5* is not affected in *mig-32* mutants, indicating that these genes might not be targets of *mig-32*. These data suggest that the PRC1-like complex in *C. elegans* might have conserved the biochemical function but diverged in the target genes regulated compared to flies and vertebrates.

Components of a PRC2-like complex were identified in *C. elegans*; such as *mes-2*, *mes*-3, and *mes-6* (Capowski et al., 1991). I showed that double mutants of *mig-32* and each of these *mes* genes did not enhance one specific defect, Ray 1 position, compared to single mutants. This suggests that they might function in the same pathway in determining the proper position of Ray 1 in male tail. This is also an indication of conserved relationship between PRC2 and PRC1 complexes in *C. elegans*. However, *mes* genes and *mig-32* mutants display other defects not related to one another. For example, *mes* mutants are maternal effect sterile but *mig-32* mutants are fertile although brood size is reduced. This might be due to two possible explanations. First, *mig-32* might be

redundant with other genes to interpret *mes* gene signals. Second, *mes* genes might function in germline maintenance independent of *mig-32*. The slightly reduced brood size of *mig-32* mutants suggests that the first explanation might be right. However, I also showed that the H2AK119-UB mark is undetectable in wild type worms at L4 and young adult stages indicating that this mark is not required for germline development. This indirectly supports the second explanation. In addition, *mes* mutants do not display the defects I observed in *mig-32* mutants in HSN and PVQ migration and process extension. All these data suggest that *mig-32* and *mes* genes function together or independent of each other in different processes in *C. elegans.* This relationship might be conserved in other organisms including humans.

In conclusion, our data show that a PRC1-like complex is present in *C. elegans*, and that MIG-32 and SPAT-3A are RING protein components of this complex required for H2A ubiquitylation with important roles during development of the nervous system. These data suggest a model in which MIG-32 and SPAT-3 with other components of the PRC1-like complex bind to target sites dependent or independent of the PRC2-like complex and recruit other factors by direct binding or indirectly by placing the H2AK119-Ub mark that could be recognized by other proteins. Target genes might be repressed or activated depending on the recruited factors. However our knowledge from fly and vertebrate studies suggests a repressive function more than an activating function. This model requires some questions to be answered. Below are the questions and the experiments I propose to answer some parts of these questions.

4.2.1. What are the other components of the PRC1-like complex in *C. elegans*?

Presence of RING components of a PRC1-like complex suggests that there might be also other components in *C. elegans*. In addition, there is not any report of involvement of fly and vertebrate RING protein components of PRC1 in target binding. This suggests that MIG-32 and SPAT-3 might not be enough to find the target sites but might need other components of the complex. To understand how a PRC1-like complex functions in *C. elegans* I should identify other components. To do this, two different approaches might be used. The first approach involves biochemical purification of the complex from worms. I generated transgenic worm strains carrying tagged versions of *mig-32* gene, including TAP-Tag, GFP, and Biotin tags. These strains might be used to purify the complex using specific affinity chromatography methods. The second approach might involve the expansion of the RNAi screen I already did for enhancers of the *lin-15(ts)* allele at 15ºC. I already screened a limited number of genes. I might expand it to all nuclear factors. As a second step for the screen I can test mutants of candidate genes for the presence of the H2AK119-Ub mark. However this step might miss the components that are not essential for ubiquitylation. Once some strong candidates are identified follow-up experiments should be done, including genetic analysis of the genes and their relationship to *mig-32*.

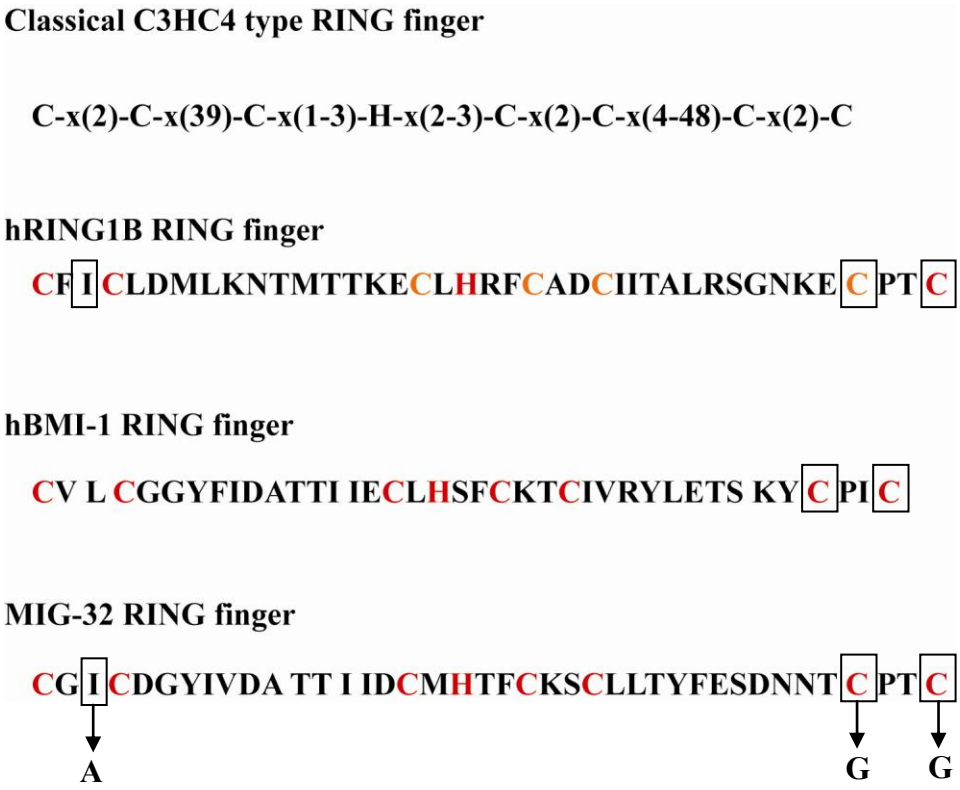

Figure 4-1: RING domain mutations of MIG-32.
hRING1B, hBMI-1, and C.e. MIG-32 have C3HC4 type RING finger domains. Isoleucine and csyteines of MIG-32 in boxes are mutated to alanine and glycines, respectively. Plasmid constructs composed of MIG-32 cDNA driven by *plx-1* promoter were used to mutate these residues. In one construct only I331A, and in the second construct C565G & C368G mutations, are present.

4.2.2. How does the PRC1-like complex ubiquitylate H2AK119?

I know that *mig-32* and *spat-3* are required for ubiquitylation of H2A, but it is not clear which one is the catalytic subunit. As RING proteins MIG-32 and SPAT-3A are candidates for the catalytic subunit. Although MIG-32 is most similar to BMI-1, which is not catalytic, and SPAT-3A is most similar to RING1A & B, which are the catalytic subunits of human PRC1, the RING domains of both proteins are also similar, indicating

that either MIG-32 or SPAT-3A might be the catalytic subunit. To test this I can do an in vitro ubiquitylation assay using recombinant purified MIG-32 or SPAT-3A to test if either of them is sufficient for ubiquitylation of H2A in vitro.

4.2.3. Is the H2AK119-Ub mark important for defects observed in *mig-32* mutants including neuronal migration and process extension?

Our data indicate that *mig-32* is required for ubiquitylation of H2A and migration and process extension of specific neurons. However, it is not clear if ubiquitylation of H2A is a part of the mechanism that regulates neuronal migration and process extension. To answer this question different mutant versions of *mig-32* cDNA might be introduced into *mig-32* mutant worms to test if the mutant constructs can rescue *mig-32* specific defects. I generated a construct that might be the backbone for our constructs in this assay. I cloned CFP-tagged *mig-32* cDNA downstream of a *Plexin-1 (plx-1)* promoter that is expressed in the male tail. As I mentioned in the Results section for Chapter 3, this construct can rescue the male tail Ray 1 defect to 90 percent wild type. I changed this construct using site-directed mutagenesis to generate mutant versions of *mig-32* (Figure 4-1). Modified constructs encode: full length MIG-32 with two cysteines of the RING domain changed into glycines, full length MIG-32 with the isoleucine right after the first cysteine of RING domain changed into an alanine, and a truncated MIG-32, which expresses the last 150 amino acids, including the RING domain. These constructs are being injected into *mig-32* mutant worms to test if they can rescue the Ray 1 defects in males. If

ubiquitylation of H2A is required for Ray 1 position, RING domain mutant constructs should not rescue the Ray 1 defect. The RING domains of MEL-18 and BMI-1 are required for interaction with RING1B and for H2A-Ubiquityl-transferase activity of RING1B in mammals (Buchwald et al., 2006; Cao et al., 2005; Elderkin et al., 2007; Li et al., 2006; Wei et al., 2006). If MIG-32 is a homolog of BMI-1 I expect that introduction of cysteine-defective MIG-32 into *mig-32* mutant worms should not rescue the H2AK119-Ub defect. In addition, if ubiquitylation of H2A by the PRC1-like complex is required for normal Ray 1 position, cysteine-defective MIG-32 is not expected to rescue Ray 1 defects in *mig-32* mutants. Our second MIG-32 construct with the isoleucine mutation may test whether MIG-32 is the E3-ligase in the complex. An isoleucine of BRCA-1 is required for interacting with ubiquitin-conjugating enzyme Ubc5C in mammals (Brzovic et al., 2003; Elderkin et al., 2007). If MIG-32 is the E3-ligase component of the complex, isoleucine mutant MIG-32 might not rescue either the H2AK119-Ub or Ray 1 position defects of *mig-32* mutants if Ray 1 position is regulated by ubiquitylation of H2A. Our last construct containing a C-terminal piece of MIG-32 with the RING domain, is to test if the RING domain itself is sufficient to rescue both the H2AK119-Ub and Ray 1 position defects. These constructs together will help us to learn if the RING domain of MIG-32 is essential and sufficient for H2AK119-Ubiquitylation and if ubiquitylation status of H2A correlates with Ray 1 position.

4.2.4. How does *mig-32* contribute to neuronal migration and process extension?

The defects in neuronal migration and process extension of *mig-32* mutants suggest that human PRC1 complex might also be involved in generation of the fine architecture of nervous system. However, there is not yet any information about how *mig-32* might be involved in this process. I propose that a PRC1-like complex involving MIG-32 and SPAT-3A might regulate transcription of genes that are involved in cell migration and process extension. To find the target genes, two approaches might be used. The first approach is to test candidate genes. Recent reports identified PRC1 target sites in flies and vertebrates using genome-wide approaches (Boyer et al., 2006; Bracken et al., 2006; Lee et al., 2006; Negre et al., 2006; Ringrose, 2007; Schwartz et al., 2006; Tolhuis et al., 2006). From these targets a list of genes involved in cell migration and axon guidance might be generated and transcription of the *C. elegans* homologs of these genes might be analyzed using real time PCR in *mig-32* mutants to see if any of them are affected. In addition, I can use the transgenic worms carrying the GFP-tagged MIG-32 in Chromatin Immunoprecipitation (ChIP) experiments to test if MIG-32 binds to promoters of the candidate genes. In the second approach I can use a ChIP on microarray assay to screen the entire *C. elegans* genome for possible MIG-32 targets. For this assay again I can use the transgenic worms that carry the GFP tagged MIG-32. After chromatin IP I can anneal the bound DNA pieces a microarray chip of tiled *C. elegans* genome to see

what regions of the *C. elegans* genome are occupied by MIG-32. Revealing the target genes might help us to understand how *mig-32* contributes to neuronal development. In broader perspective, this might provide information about how human PRC1 might be involved in development of the nervous system.

4.2.5. What is the role of *mig-32* in germline development?

The classical Polycomb model says that PRC1 functions downstream of PRC2 in flies and vertebrates. This model suggests that *C. elegans* PRC1-like complex might also function downstream of the PRC2-like complex, and my work provided evidence for this model in controlling neuronal migration. The *C. elegans* PRC2 complex involves MES-2, MES-3, and MES-6 as core components. The most prominent defect of *mes* gene mutants is the sterility due to degeneration of germline cells. I would expect that as a component of PRC1-like complex, *mig-32* mutants should display a phenotype similar to that of *mes* gene mutants. However this is not the case, and *mig-32* mutants are not sterile. It is possible that *mig-32* functions redundantly with other genes in germline maintenance. An RNAi screen for enhanced sterility in *mig-32* mutants might reveal such genes. It is expected that some nuclear factors should be involved in this process to interpret the PRC-2 signal. Thus, it might be proper to start with a library of nuclear genes.

BIBLIOGRAPHY

Agger, K., Cloos, P.A., Christensen, J., Pasini, D., Rose, S., Rappsilber, J., Issaeva, I., Canaani, E., Salcini, A.E., and Helin, K. (2007). UTX and JMJD3 are histone H3K27 demethylases involved in HOX gene regulation and development. Nature *449*, 731-734.

Agostoni, E., Albertson, D., Wittmann, C., Hill, F., Tobler, H., and Muller, F. (1996). cec-1, a soma-specific chromobox-containing gene in *C. elegans*. Dev Biol *178*, 316-326.

Akashi, K., He, X., Chen, J., Iwasaki, H., Niu, C., Steenhard, B., Zhang, J., Haug, J., and Li, L. (2003). Transcriptional accessibility for genes of multiple tissues and hematopoietic lineages is hierarchically controlled during early hematopoiesis. Blood *101*, 383-389.

Alkema, M.J., Jacobs, J., Voncken, J.W., Jenkins, N.A., Copeland, N.G., Satijn, D.P., Otte, A.P., Berns, A., and van Lohuizen, M. (1997). MPc2, a new murine homolog of the Drosophila Polycomb protein is a member of the mouse Polycomb transcriptional repressor complex. J Mol Biol *273*, 993-1003.

Altschul, S.F., Gish, W., Miller, W., Myers, E.W., and Lipman, D.J. (1990). Basic local alignment search tool. J Mol Biol *215*, 403-410.

Barr, M.M., and Sternberg, P.W. (1999). A polycystic kidney-disease gene homologue required for male mating behaviour in *C. elegans*. Nature *401*, 386-389.

Bateman, A., Birney, E., Cerruti, L., Durbin, R., Etwiller, L., Eddy, S.R., Griffiths-Jones, S., Howe, K.L., Marshall, M., and Sonnhammer, E.L. (2002). The Pfam protein families database. Nucleic Acids Res *30*, 276-280.

Belote, J.M., Hoffmann, F.M., McKeown, M., Chorsky, R.L., and Baker, B.S. (1990). Cytogenetic analysis of chromosome region 73AD of Drosophila melanogaster. Genetics *125*, 783-793.

Ben-Saadon, R., Zaaroor, D., Ziv, T., and Ciechanover, A. (2006). The Polycomb protein Ring1B generates self atypical mixed ubiquitin chains required for its in vitro histone H2A ligase activity. Mol Cell *24*, 701-711.

Bender, L.B., Cao, R., Zhang, Y., and Strome, S. (2004). The MES-2/MES-3/MES-6 complex and regulation of histone H3 methylation in *C. elegans*. Curr Biol *14*, 1639-1643.

Boyer, L.A., Plath, K., Zeitlinger, J., Brambrink, T., Medeiros, L.A., Lee, T.I., Levine, S.S., Wernig, M., Tajonar, A., Ray, M.K.*, et al.* (2006). Polycomb complexes repress developmental regulators in murine embryonic stem cells. Nature *441*, 349-353.

Bracken, A.P., Dietrich, N., Pasini, D., Hansen, K.H., and Helin, K. (2006). Genome-wide mapping of Polycomb target genes unravels their roles in cell fate transitions. Genes Dev *20*, 1123-1136.

Bracken, A.P., Kleine-Kohlbrecher, D., Dietrich, N., Pasini, D., Gargiulo, G., Beekman, C., Theilgaard-Monch, K., Minucci, S., Porse, B.T., Marine, J.C.*, et al.* (2007). The Polycomb group proteins bind throughout the INK4A-ARF locus and are disassociated in senescent cells. Genes Dev *21*, 525-530.

Brenner, S. (1974). The genetics of *Caenorhabditis elegans*. Genetics *77*, 71-94.

Brown, J.L., Fritsch, C., Mueller, J., and Kassis, J.A. (2003). The Drosophila pho-like gene encodes a YY1-related DNA binding protein that is redundant with pleiohomeotic in homeotic gene silencing. Development *130*, 285-294.

Brown, J.L., Grau, D.J., DeVido, S.K., and Kassis, J.A. (2005). An Sp1/KLF binding site is important for the activity of a Polycomb group response element from the Drosophila engrailed gene. Nucleic Acids Res *33*, 5181-5189.

Brown, J.L., Mucci, D., Whiteley, M., Dirksen, M.L., and Kassis, J.A. (1998). The Drosophila Polycomb group gene pleiohomeotic encodes a DNA binding protein with homology to the transcription factor YY1. Mol Cell *1*, 1057-1064.

Brzovic, P.S., Keeffe, J.R., Nishikawa, H., Miyamoto, K., Fox, D., 3rd, Fukuda, M., Ohta, T., and Klevit, R. (2003). Binding and recognition in the assembly of an active BRCA1/BARD1 ubiquitin-ligase complex. Proc Natl Acad Sci U S A *100*, 5646-5651.

Buchwald, G., van der Stoop, P., Weichenrieder, O., Perrakis, A., van Lohuizen, M., and Sixma, T.K. (2006). Structure and E3-ligase activity of the Ring-Ring complex of Polycomb proteins Bmi1 and Ring1b. Embo J *25*, 2465-2474.

Buszczak, M., and Spradling, A.C. (2006). Searching chromatin for stem cell identity. Cell *125*, 233-236.

Cameron, S., Clark, S.G., McDermott, J.B., Aamodt, E., and Horvitz, H.R. (2002). PAG-3, a Zn-finger transcription factor, determines neuroblast fate in *C. elegans*. Development *129*, 1763-1774.

Cao, R., Tsukada, Y., and Zhang, Y. (2005). Role of Bmi-1 and Ring1A in H2A ubiquitylation and *Hox* gene silencing. Mol Cell *20*, 845-854.

Cao, R., Wang, L., Wang, H., Xia, L., Erdjument-Bromage, H., Tempst, P., Jones, R.S., and Zhang, Y. (2002). Role of histone H3 lysine 27 methylation in Polycomb-group silencing. Science *298*, 1039-1043.

Capowski, E.E., Martin, P., Garvin, C., and Strome, S. (1991). Identification of grandchildless loci whose products are required for normal germ-line development in the nematode *Caenorhabditis elegans*. Genetics *129*, 1061-1072.

Chalfie, M., Sulston, J.E., White, J.G., Southgate, E., Thomson, J.N., and Brenner, S. (1985). The neural circuit for touch sensitivity in *Caenorhabditis elegans*. J Neurosci *5*, 956-964.

Chamberlin, H.M., and Thomas, J.H. (2000). The bromodomain protein LIN-49 and trithorax-related protein LIN-59 affect development and gene expression in *Caenorhabditis elegans*. Development *127*, 713-723.

Chan, C.S., Rastelli, L., and Pirrotta, V. (1994). A Polycomb response element in the Ubx gene that determines an epigenetically inherited state of repression. Embo J *13*, 2553-2564.

Chang, C., Adler, C.E., Krause, M., Clark, S.G., Gertler, F.B., Tessier-Lavigne, M., and Bargmann, C.I. (2006). MIG-10/lamellipodin and AGE-1/PI3K promote axon guidance and outgrowth in response to slit and netrin. Curr Biol *16*, 854-862.

Chow, K.L., and Emmons, S.W. (1994). HOM-C/*Hox* genes and four interacting loci determine the morphogenetic properties of single cells in the nematode male tail. Development *120*, 2579-2592.

Christensen, J., Agger, K., Cloos, P.A., Pasini, D., Rose, S., Sennels, L., Rappsilber, J., Hansen, K.H., Salcini, A.E., and Helin, K. (2007). RBP2 belongs to a family of demethylases, specific for tri-and dimethylated lysine 4 on histone 3. Cell *128*, 1063-1076.

Conradt, B., and Horvitz, H.R. (1998). The *C. elegans* protein EGL-1 is required for programmed cell death and interacts with the Bcl-2-like protein CED-9. Cell *93*, 519-529.

Costa, M., Weir, M., Coulson, A., Sulston, J., and Kenyon, C. (1988). Posterior pattern formation in *C. elegans* involves position-specific expression of a gene containing a homeobox. Cell *55*, 747-756.

Coustham, V., Bedet, C., Monier, K., Schott, S., Karali, M., and Palladino, F. (2006). The *C. elegans* HP1 homologue HPL-2 and the LIN-13 zinc finger protein form a complex implicated in vulval development. Dev Biol *297*, 308-322.

Couteau, F., Guerry, F., Muller, F., and Palladino, F. (2002). A heterochromatin protein 1 homologue in *Caenorhabditis elegans* acts in germline and vulval development. EMBO Rep *3*, 235-241.

Czermin, B., Melfi, R., McCabe, D., Seitz, V., Imhof, A., and Pirrotta, V. (2002). Drosophila enhancer of Zeste/ESC complexes have a histone H3 methyltransferase activity that marks chromosomal Polycomb sites. Cell *111*, 185-196.

Davis, J.A., and Reed, R.R. (1996). Role of Olf-1 and Pax-6 transcription factors in neurodevelopment. J Neurosci *16*, 5082-5094.

Delaval, K., and Feil, R. (2004). Epigenetic regulation of mammalian genomic imprinting. Curr Opin Genet Dev *14*, 188-195.

Desai, C., Garriga, G., McIntire, S.L., and Horvitz, H.R. (1988). A genetic pathway for the development of the *Caenorhabditis elegans* HSN motor neurons. Nature *336*, 638-646.

Dias, S., Silva, H., Jr., Cumano, A., and Vieira, P. (2005). Interleukin-7 is necessary to maintain the B cell potential in common lymphoid progenitors. J Exp Med *201*, 971-979.

Dubois, L., and Vincent, A. (2001). The COE--Collier/Olf1/EBF--transcription factors: structural conservation and diversity of developmental functions. Mech Dev *108*, 3-12.

Durbin, R. (1987). Studies on the development and organization of the nervous system of *Caenorhabditis elegans*. *Vol. Ph.D. Cambridge University, Cambridge, UK.*

Elderkin, S., Maertens, G.N., Endoh, M., Mallery, D.L., Morrice, N., Koseki, H., Peters, G., Brockdorff, N., and Hiom, K. (2007). A phosphorylated form of Mel-18 targets the Ring1B histone H2A ubiquitin ligase to chromatin. Mol Cell *28*, 107-120.

Emmons, S.W. (2005). Male development. WormBook, 1-22.

Fauvarque, M.O., and Dura, J.M. (1993). polyhomeotic regulatory sequences induce developmental regulator-dependent variegation and targeted P-element insertions in Drosophila. Genes Dev *7*, 1508-1520.

Fay, D.S., and Yochem, J. (2007). The SynMuv genes of *Caenorhabditis elegans* in vulval development and beyond. Dev Biol *306*, 1-9.

Felix, M.A. (2005). An inversion in the wiring of an intercellular signal: evolution of Wnt signaling in the nematode vulva. Bioessays *27*, 765-769.

Ferreira, H.B., Zhang, Y., Zhao, C., and Emmons, S.W. (1999). Patterning of *Caenorhabditis elegans* posterior structures by the Abdominal-B homolog, egl-5. Dev Biol *207*, 215-228.

Fong, Y., Bender, L., Wang, W., and Strome, S. (2002). Regulation of the different chromatin states of autosomes and X chromosomes in the germ line of *C. elegans*. Science *296*, 2235-2238.

Francis, N.J., Kingston, R.E., and Woodcock, C.L. (2004). Chromatin compaction by a Polycomb group protein complex. Science *306*, 1574-1577.

Fritsch, C., Brown, J.L., Kassis, J.A., and Muller, J. (1999). The DNA-binding Polycomb group protein pleiohomeotic mediates silencing of a Drosophila homeotic gene. Development *126*, 3905-3913.

Frolov, M.V., and Dyson, N.J. (2004). Molecular mechanisms of E2F-dependent activation and pRB-mediated repression. J Cell Sci *117*, 2173-2181.

Fujii, T., Nakao, F., Shibata, Y., Shioi, G., Kodama, E., Fujisawa, H., and Takagi, S. (2002). *Caenorhabditis elegans* PlexinA, PLX-1, interacts with transmembrane semaphorins and regulates epidermal morphogenesis. Development *129*, 2053-2063.

Garcia-Dominguez, M., Poquet, C., Garel, S., and Charnay, P. (2003). Ebf gene function is required for coupling neuronal differentiation and cell cycle exit. Development *130*, 6013-6025.

Garel, S., Garcia-Dominguez, M., and Charnay, P. (2000). Control of the migratory pathway of facial branchiomotor neurones. Development *127*, 5297-5307.

Garel, S., Marin, F., Grosschedl, R., and Charnay, P. (1999). Ebf1 controls early cell differentiation in the embryonic striatum. Development *126*, 5285-5294.

Garel, S., Marin, F., Mattei, M.G., Vesque, C., Vincent, A., and Charnay, P. (1997). Family of Ebf/Olf-1-related genes potentially involved in neuronal differentiation and regional specification in the central nervous system. Dev Dyn *210*, 191-205.

Garel, S., Yun, K., Grosschedl, R., and Rubenstein, J.L. (2002). The early topography of thalamocortical projections is shifted in Ebf1 and Dlx1/2 mutant mice. Development *129*, 5621-5634.

Ginzburg, V.E., Roy, P.J., and Culotti, J.G. (2002). Semaphorin 1a and semaphorin 1b are required for correct epidermal cell positioning and adhesion during morphogenesis in *C. elegans*. Development *129*, 2065-2078.

Guitton, A.E., and Berger, F. (2005). Control of reproduction by Polycomb Group complexes in animals and plants. Int J Dev Biol *49*, 707-716.

Hagman, J., Belanger, C., Travis, A., Turck, C.W., and Grosschedl, R. (1993). Cloning and functional characterization of early B-cell factor, a regulator of lymphocyte-specific gene expression. Genes Dev *7*, 760-773.

Hagman, J., Gutch, M.J., Lin, H., and Grosschedl, R. (1995). EBF contains a novel zinc coordination motif and multiple dimerization and transcriptional activation domains. Embo J *14*, 2907-2916.

Hamelin, M., Scott, I.M., Way, J.C., and Culotti, J.G. (1992). The mec-7 beta-tubulin gene of *Caenorhabditis elegans* is expressed primarily in the touch receptor neurons. Embo J *11*, 2885-2893.

Hao, J.C., Yu, T.W., Fujisawa, K., Culotti, J.G., Gengyo-Ando, K., Mitani, S., Moulder, G., Barstead, R., Tessier-Lavigne, M., and Bargmann, C.I. (2001). *C. elegans* slit acts in midline, dorsal-ventral, and anterior-posterior guidance via the SAX-3/Robo receptor. Neuron *32*, 25-38.

Harbour, J.W., and Dean, D.C. (2000). The Rb/E2F pathway: expanding roles and emerging paradigms. Genes Dev *14*, 2393-2409.

Harrison, M.M., Lu, X., and Horvitz, H.R. (2007). LIN-61, one of two *Caenorhabditis elegans* malignant-brain-tumor-repeat-containing proteins, acts with the DRM and

NuRD-like protein complexes in vulval development but not in certain other biological processes. Genetics *176*, 255-271.

Heard, E. (2005). Delving into the diversity of facultative heterochromatin: the epigenetics of the inactive X chromosome. Curr Opin Genet Dev *15*, 482-489.

Hill, R.J., and Sternberg, P.W. (1992). The gene lin-3 encodes an inductive signal for vulval development in *C. elegans*. Nature *358*, 470-476.

Hock, H., Hamblen, M.J., Rooke, H.M., Traver, D., Bronson, R.T., Cameron, S., and Orkin, S.H. (2003). Intrinsic requirement for zinc finger transcription factor Gfi-1 in neutrophil differentiation. Immunity *18*, 109-120.

Hodgson, J.W., Argiropoulos, B., and Brock, H.W. (2001). Site-specific recognition of a 70-base-pair element containing d(GA)(n) repeats mediates bithoraxoid Polycomb group response element-dependent silencing. Mol Cell Biol *21*, 4528-4543.

Holdeman, R., Nehrt, S., and Strome, S. (1998). MES-2, a maternal protein essential for viability of the germline in *Caenorhabditis elegans*, is homologous to a Drosophila Polycomb group protein. Development *125*, 2457-2467.

Horard, B., Tatout, C., Poux, S., and Pirrotta, V. (2000). Structure of a Polycomb response element and in vitro binding of Polycomb group complexes containing GAGA factor. Mol Cell Biol *20*, 3187-3197.

Hunter, C.P., Harris, J.M., Maloof, J.N., and Kenyon, C. (1999). *Hox* gene expression in a single *Caenorhabditis elegans* cell is regulated by a caudal homolog and intercellular signals that inhibit wnt signaling. Development *126*, 805-814.

Irminger-Finger, I., and Nothiger, R. (1995). The Drosophila melanogaster gene lethal(3)73Ah encodes a ring finger protein homologous to the oncoproteins MEL-18 and BMI-1. Gene *163*, 203-208.

Jia, Y., Xie, G., McDermott, J.B., and Aamodt, E. (1997). The *C. elegans* gene pag-3 is homologous to the zinc finger proto-oncogene gfi-1. Development *124*, 2063-2073.

Kahn, T.G., Schwartz, Y.B., Dellino, G.I., and Pirrotta, V. (2006). Polycomb complexes and the propagation of the methylation mark at the Drosophila ubx gene. J Biol Chem *281*, 29064-29075.

Kassis, J.A. (1994). Unusual properties of regulatory DNA from the Drosophila engrailed gene: three "pairing-sensitive" sites within a 1.6-kb region. Genetics *136*, 1025-1038.

Kennison, J.A., and Tamkun, J.W. (1988). Dosage-dependent modifiers of Polycomb and antennapedia mutations in Drosophila. Proc Natl Acad Sci U S A *85*, 8136-8140.

Kim, K., Colosimo, M.E., Yeung, H., and Sengupta, P. (2005). The UNC-3 Olf/EBF protein represses alternate neuronal programs to specify chemosensory neuron identity. Dev Biol *286*, 136-148.

King, I.F., Francis, N.J., and Kingston, R.E. (2002). Native and recombinant Polycomb group complexes establish a selective block to template accessibility to repress transcription in vitro. Mol Cell Biol *22*, 7919-7928.

Klymenko, T., and Muller, J. (2004). The histone methyltransferases Trithorax and Ash1 prevent transcriptional silencing by Polycomb group proteins. EMBO Rep *5*, 373-377.

Klymenko, T., Papp, B., Fischle, W., Kocher, T., Schelder, M., Fritsch, C., Wild, B., Wilm, M., and Muller, J. (2006). A Polycomb group protein complex with sequence-specific DNA-binding and selective methyl-lysine-binding activities. Genes Dev *20*, 1110-1122.

Korenjak, M., Taylor-Harding, B., Binne, U.K., Satterlee, J.S., Stevaux, O., Aasland, R., White-Cooper, H., Dyson, N., and Brehm, A. (2004). Native E2F/RBF complexes contain Myb-interacting proteins and repress transcription of developmentally controlled E2F target genes. Cell *119*, 181-193.

Krivtsov, A.V., Twomey, D., Feng, Z., Stubbs, M.C., Wang, Y., Faber, J., Levine, J.E., Wang, J., Hahn, W.C., Gilliland, D.G.*, et al.* (2006). Transformation from committed progenitor to leukaemia stem cell initiated by MLL-AF9. Nature *442*, 818-822.

Kuzmichev, A., Jenuwein, T., Tempst, P., and Reinberg, D. (2004). Different EZH2-containing complexes target methylation of histone H1 or nucleosomal histone H3. Mol Cell *14*, 183-193.

Kuzmichev, A., Margueron, R., Vaquero, A., Preissner, T.S., Scher, M., Kirmizis, A., Ouyang, X., Brockdorff, N., Abate-Shen, C., Farnham, P.*, et al.* (2005). Composition and histone substrates of Polycomb repressive group complexes change during cellular differentiation. Proc Natl Acad Sci U S A *102*, 1859-1864.

Kuzmichev, A., Nishioka, K., Erdjument-Bromage, H., Tempst, P., and Reinberg, D. (2002). Histone methyltransferase activity associated with a human multiprotein complex containing the Enhancer of Zeste protein. Genes Dev *16*, 2893-2905.

Labbe, J.C., Pacquelet, A., Marty, T., and Gotta, M. (2006). A genomewide screen for suppressors of par-2 uncovers potential regulators of PAR protein-dependent cell polarity in *Caenorhabditis elegans*. Genetics *174*, 285-295.

Lee, M.G., Norman, J., Shilatifard, A., and Shiekhattar, R. (2007). Physical and functional association of a trimethyl H3K4 demethylase and Ring6a/MBLR, a Polycomb-like protein. Cell *128*, 877-887.

Lee, T.I., Jenner, R.G., Boyer, L.A., Guenther, M.G., Levine, S.S., Kumar, R.M., Chevalier, B., Johnstone, S.E., Cole, M.F., Isono, K.*, et al.* (2006). Control of developmental regulators by Polycomb in human embryonic stem cells. Cell *125*, 301-313.

Levine, S.S., Weiss, A., Erdjument-Bromage, H., Shao, Z., Tempst, P., and Kingston, R.E. (2002). The core of the Polycomb repressive complex is compositionally and functionally conserved in flies and humans. Mol Cell Biol *22*, 6070-6078.

Lewis, E.B. (1978). A gene complex controlling segmentation in Drosophila. Nature *276*, 565-570.

Li, C., Nelson, L.S., Kim, K., Nathoo, A., and Hart, A.C. (1999). Neuropeptide gene families in the nematode *Caenorhabditis elegans*. Ann N Y Acad Sci *897*, 239-252.

Li, Z., Cao, R., Wang, M., Myers, M.P., Zhang, Y., and Xu, R.M. (2006). Structure of a Bmi-1-Ring1B Polycomb group ubiquitin ligase complex. J Biol Chem *281*, 20643-20649.

Lickteig, K.M., Duerr, J.S., Frisby, D.L., Hall, D.H., Rand, J.B., and Miller, D.M., 3rd (2001). Regulation of neurotransmitter vesicles by the homeodomain protein UNC-4 and its transcriptional corepressor UNC-37/groucho in *Caenorhabditis elegans* cholinergic motor neurons. J Neurosci *21*, 2001-2014.

Martinez, A.M., and Cavalli, G. (2006). The role of Polycomb group proteins in cell cycle regulation during development. Cell Cycle *5*, 1189-1197.

McIntire, S.L., Reimer, R.J., Schuske, K., Edwards, R.H., and Jorgensen, E.M. (1997). Identification and characterization of the vesicular GABA transporter. Nature *389*, 870-876.

Miller, D.M., 3rd, and Niemeyer, C.J. (1995). Expression of the unc-4 homeoprotein in *Caenorhabditis elegans* motor neurons specifies presynaptic input. Development *121*, 2877-2886.

Muller, J., Hart, C.M., Francis, N.J., Vargas, M.L., Sengupta, A., Wild, B., Miller, E.L., O'Connor, M.B., Kingston, R.E., and Simon, J.A. (2002). Histone methyltransferase activity of a Drosophila Polycomb group repressor complex. Cell *111*, 197-208.

Negre, N., Hennetin, J., Sun, L.V., Lavrov, S., Bellis, M., White, K.P., and Cavalli, G. (2006). Chromosomal distribution of PcG proteins during Drosophila development. PLoS Biol *4*, e170.

Nusslein-Volhard, C., Kluding, H., and Jurgens, G. (1985). Genes affecting the segmental subdivision of the Drosophila embryo. Cold Spring Harb Symp Quant Biol *50*, 145-154.

O'Carroll, D., Erhardt, S., Pagani, M., Barton, S.C., Surani, M.A., and Jenuwein, T. (2001). The Polycomb-group gene Ezh2 is required for early mouse development. Mol Cell Biol *21*, 4330-4336.

Pan, C.L., Howell, J.E., Clark, S.G., Hilliard, M., Cordes, S., Bargmann, C.I., and Garriga, G. (2006). Multiple Wnts and frizzled receptors regulate anteriorly directed cell and growth cone migrations in *Caenorhabditis elegans*. Dev Cell *10*, 367-377.

Papp, B., and Muller, J. (2006). Histone trimethylation and the maintenance of transcriptional ON and OFF states by trxG and PcG proteins. Genes Dev *20*, 2041-2054.

Pflugrad, A., Meir, J.Y., Barnes, T.M., and Miller, D.M., 3rd (1997). The Groucho-like transcription factor UNC-37 functions with the neural specificity gene unc-4 to govern motor neuron identity in *C. elegans*. Development *124*, 1699-1709.

Pires-daSilva, A., and Sommer, R.J. (2003). Finally, worm Polycomb-like genes meet *Hox* regulation. Dev Cell *4*, 770-772.

Polo, S.E., and Almouzni, G. (2006). Chromatin assembly: a basic recipe with various flavours. Curr Opin Genet Dev *16*, 104-111.

Potts, M., Wang, D., and Cameron, S. (2008). Trithorax, *Hox*, and TALE-class homeodomain proteins promote cell survival through repression of the BH3-only gene *egl-1*. *submitted*.

Poux, S., Horard, B., Sigrist, C.J., and Pirrotta, V. (2002). The Drosophila trithorax protein is a coactivator required to prevent re-establishment of Polycomb silencing. Development *129*, 2483-2493.

Poux, S., Melfi, R., and Pirrotta, V. (2001). Establishment of Polycomb silencing requires a transient interaction between PC and ESC. Genes Dev *15*, 2509-2514.

Prasad, B., Karakuzu, O., Reed, R.R., and Cameron, S. (2008). *unc-3*-dependent repression of specific motor neuron fates in *Caenorhabditis elegans*. Dev Biol *323*, 207-215.

Prasad, B.C., Ye, B., Zackhary, R., Schrader, K., Seydoux, G., and Reed, R.R. (1998). *unc-3*, a gene required for axonal guidance in *Caenorhabditis elegans*, encodes a member of the O/E family of transcription factors. Development *125*, 1561-1568.

Puschendorf, M., Terranova, R., Boutsma, E., Mao, X., Isono, K., Brykczynska, U., Kolb, C., Otte, A.P., Koseki, H., Orkin, S.H.*, et al.* (2008). PRC1 and Suv39h specify parental asymmetry at constitutive heterochromatin in early mouse embryos. Nat Genet *40*, 411-420.

Quinn, C.C., Pfeil, D.S., Chen, E., Stovall, E.L., Harden, M.V., Gavin, M.K., Forrester, W.C., Ryder, E.F., Soto, M.C., and Wadsworth, W.G. (2006). UNC-6/netrin and SLT-1/slit guidance cues orient axon outgrowth mediated by MIG-10/RIAM/lamellipodin. Curr Biol *16*, 845-853.

Rastelli, L., Chan, C.S., and Pirrotta, V. (1993). Related chromosome binding sites for zeste, suppressors of zeste and Polycomb group proteins in Drosophila and their dependence on Enhancer of zeste function. Embo J *12*, 1513-1522.

Ringrose, L. (2007). Polycomb comes of age: genome-wide profiling of target sites. Curr Opin Cell Biol *19*, 290-297.

Ringrose, L., Ehret, H., and Paro, R. (2004). Distinct contributions of histone H3 lysine 9 and 27 methylation to locus-specific stability of Polycomb complexes. Mol Cell *16*, 641-653.

Ringrose, L., and Paro, R. (2004). Epigenetic regulation of cellular memory by the Polycomb and Trithorax group proteins. Annu Rev Genet *38*, 413-443.

Ross, J.M., and Zarkower, D. (2003). Polycomb group regulation of *Hox* gene expression in *C. elegans*. Dev Cell *4*, 891-901.

Sanchez, C., Sanchez, I., Demmers, J.A., Rodriguez, P., Strouboulis, J., and Vidal, M. (2007). Proteomics analysis of Ring1B/Rnf2 interactors identifies a novel complex with the Fbxl10/Jhdm1B histone demethylase and the Bcl6 interacting corepressor. Mol Cell Proteomics *6*, 820-834.

Satijn, D.P., Hamer, K.M., den Blaauwen, J., and Otte, A.P. (2001). The Polycomb group protein EED interacts with YY1, and both proteins induce neural tissue in Xenopus embryos. Mol Cell Biol *21*, 1360-1369.

Saurin, A.J., Shao, Z., Erdjument-Bromage, H., Tempst, P., and Kingston, R.E. (2001). A Drosophila Polycomb group complex includes Zeste and dTAFII proteins. Nature *412*, 655-660.

Schinkmann, K., and Li, C. (1992). Localization of FMRFamide-like peptides in *Caenorhabditis elegans*. J Comp Neurol *316*, 251-260.

Schubert, D., Clarenz, O., and Goodrich, J. (2005). Epigenetic control of plant development by Polycomb-group proteins. Curr Opin Plant Biol *8*, 553-561.

Schuettengruber, B., Chourrout, D., Vervoort, M., Leblanc, B., and Cavalli, G. (2007). Genome regulation by Polycomb and trithorax proteins. Cell *128*, 735-745.

Schwartz, Y.B., Kahn, T.G., Nix, D.A., Li, X.Y., Bourgon, R., Biggin, M., and Pirrotta, V. (2006). Genome-wide analysis of Polycomb targets in Drosophila melanogaster. Nat Genet *38*, 700-705.

Schwartz, Y.B., and Pirrotta, V. (2007). Polycomb silencing mechanisms and the management of genomic programmes. Nat Rev Genet *8*, 9-22.

Shao, Z., Raible, F., Mollaaghababa, R., Guyon, J.R., Wu, C.T., Bender, W., and Kingston, R.E. (1999). Stabilization of chromatin structure by PRC1, a Polycomb complex. Cell *98*, 37-46.

Simon, J., Chiang, A., and Bender, W. (1992). Ten different Polycomb group genes are required for spatial control of the abdA and AbdB homeotic products. Development *114*, 493-505.

Sparmann, A., and van Lohuizen, M. (2006). Polycomb silencers control cell fate, development and cancer. Nat Rev Cancer *6*, 846-856.

Spieth, J., Brooke, G., Kuersten, S., Lea, K., and Blumenthal, T. (1993). Operons in *C. elegans*: polycistronic mRNA precursors are processed by trans-splicing of SL2 to downstream coding regions. Cell *73*, 521-532.

Springer, N.M., Danilevskaya, O.N., Hermon, P., Helentjaris, T.G., Phillips, R.L., Kaeppler, H.F., and Kaeppler, S.M. (2002). Sequence relationships, conserved domains, and expression patterns for maize homologs of the Polycomb group genes E(z), esc, and E(Pc). Plant Physiol *128*, 1332-1345.

Sternberg, P.W. (2005). Vulval development. WormBook, 1-28.

Sternberg, P.W., and Horvitz, H.R. (1984). The genetic control of cell lineage during nematode development. Annu Rev Genet *18*, 489-524.

Stiernagel, T. (1999). Maintenance of *C. elegans*, . *In C. elegans : A Practical Approach, I. A. Hope, ed. (New York: Oxford University Press)*, 51-67.

Sulston, J.E. (1976). Post-embryonic development in the ventral cord of *Caenorhabditis elegans*. Philos Trans R Soc Lond B Biol Sci *275*, 287-297.

Sulston, J.E., and Horvitz, H.R. (1977). Post-embryonic cell lineages of the nematode, *Caenorhabditis elegans*. Dev Biol *56*, 110-156.

Sulston, J.E., Schierenberg, E., White, J.G., and Thomson, J.N. (1983). The embryonic cell lineage of the nematode *Caenorhabditis elegans*. Dev Biol *100*, 64-119.

Sundaram, M.V. (2005). The love-hate relationship between Ras and Notch. Genes Dev *19*, 1825-1839.

Taylor-Harding, B., Binne, U.K., Korenjak, M., Brehm, A., and Dyson, N.J. (2004). p55, the Drosophila ortholog of RbAp46/RbAp48, is required for the repression of dE2F2/RBF-regulated genes. Mol Cell Biol *24*, 9124-9136.

Tie, F., Prasad-Sinha, J., Birve, A., Rasmuson-Lestander, A., and Harte, P.J. (2003). A 1-megadalton ESC/E(Z) complex from Drosophila that contains Polycomblike and RPD3. Mol Cell Biol *23*, 3352-3362.

Timmons, L., Court, D.L., and Fire, A. (2001). Ingestion of bacterially expressed dsRNAs can produce specific and potent genetic interference in *Caenorhabditis elegans*. Gene *263*, 103-112.

Tolhuis, B., de Wit, E., Muijrers, I., Teunissen, H., Talhout, W., van Steensel, B., and van Lohuizen, M. (2006). Genome-wide profiling of PRC1 and PRC2 Polycomb chromatin binding in Drosophila melanogaster. Nat Genet *38*, 694-699.

Trent, C., Tsuing, N., and Horvitz, H.R. (1983). Egg-laying defective mutants of the nematode *Caenorhabditis elegans*. Genetics *104*, 619-647.

Trimarchi, J.M., Fairchild, B., Wen, J., and Lees, J.A. (2001). The E2F6 transcription factor is a component of the mammalian Bmi1-containing Polycomb complex. Proc Natl Acad Sci U S A *98*, 1519-1524.

Troemel, E.R., Chou, J.H., Dwyer, N.D., Colbert, H.A., and Bargmann, C.I. (1995). Divergent seven transmembrane receptors are candidate chemosensory receptors in *C. elegans*. Cell *83*, 207-218.

Tsai, R.Y., and Reed, R.R. (1998). Identification of DNA recognition sequences and protein interaction domains of the multiple-Zn-finger protein Roaz. Mol Cell Biol *18*, 6447-6456.

Wang, H., Wang, L., Erdjument-Bromage, H., Vidal, M., Tempst, P., Jones, R.S., and Zhang, Y. (2004a). Role of histone H2A ubiquitination in Polycomb silencing. Nature *431*, 873-878.

Wang, L., Brown, J.L., Cao, R., Zhang, Y., Kassis, J.A., and Jones, R.S. (2004b). Hierarchical recruitment of Polycomb group silencing complexes. Mol Cell *14*, 637-646.

Wang, M.M., and Reed, R.R. (1993). Molecular cloning of the olfactory neuronal transcription factor Olf-1 by genetic selection in yeast. Nature *364*, 121-126.

Wang, S., Robertson, G.P., and Zhu, J. (2004c). A novel human homologue of Drosophila Polycomblike gene is up-regulated in multiple cancers. Gene *343*, 69-78.

Wang, S.S., Betz, A.G., and Reed, R.R. (2002). Cloning of a novel Olf-1/EBF-like gene, O/E-4, by degenerate oligo-based direct selection. Mol Cell Neurosci *20*, 404-414.

Wang, S.S., Lewcock, J.W., Feinstein, P., Mombaerts, P., and Reed, R.R. (2004d). Genetic disruptions of O/E2 and O/E3 genes reveal involvement in olfactory receptor neuron projection. Development *131*, 1377-1388.

Wang, S.S., Tsai, R.Y., and Reed, R.R. (1997). The characterization of the Olf-1/EBF-like HLH transcription factor family: implications in olfactory gene regulation and neuronal development. J Neurosci *17*, 4149-4158.

Waring, D.A., and Kenyon, C. (1991). Regulation of cellular responsiveness to inductive signals in the developing *C. elegans* nervous system. Nature *350*, 712-715.

Wei, J., Zhai, L., Xu, J., and Wang, H. (2006). Role of Bmi1 in H2A ubiquitylation and *Hox* gene silencing. J Biol Chem *281*, 22537-22544.

White, J.G., Southgate, E., Thomson, J.N., and Brenner, S. (1976). The structure of the ventral nerve cord of *Caenorhabditis elegans*. Philos Trans R Soc Lond B Biol Sci *275*, 327-348.

White, J.G., Southgate, E., Thomson, J.N., and Brenner, S. (1986). The structure of the nervous system of the nematode *Caenorhabditis elegans*. Philos Trans R Soc Lond B Biol Sci, 1-340.

Wightman, B., Baran, R., and Garriga, G. (1997). Genes that guide growth cones along the *C. elegans* ventral nerve cord. Development *124*, 2571-2580.

Winnier, A.R., Meir, J.Y., Ross, J.M., Tavernarakis, N., Driscoll, M., Ishihara, T., Katsura, I., and Miller, D.M., 3rd (1999). UNC-4/UNC-37-dependent repression of motor neuron-specific genes controls synaptic choice in *Caenorhabditis elegans*. Genes Dev *13*, 2774-2786.

Xu, L., Fong, Y., and Strome, S. (2001). The *Caenorhabditis elegans* maternal-effect sterile proteins, MES-2, MES-3, and MES-6, are associated in a complex in embryos. Proc Natl Acad Sci U S A *98*, 5061-5066.

Zahn, T.R., Macmorris, M.A., Dong, W., Day, R., and Hutton, J.C. (2001). IDA-1, a *Caenorhabditis elegans* homolog of the diabetic autoantigens IA-2 and phogrin, is expressed in peptidergic neurons in the worm. J Comp Neurol *429*, 127-143.

Zhu, P., Zhou, W., Wang, J., Puc, J., Ohgi, K.A., Erdjument-Bromage, H., Tempst, P., Glass, C.K., and Rosenfeld, M.G. (2007). A histone H2A deubiquitinase complex coordinating histone acetylation and H1 dissociation in transcriptional regulation. Mol Cell *27*, 609-621.